PACIFIC EARTHQUAKE ENGINEERING RESEARCH CENTER

F-Rec Framework: Novel Framework for Probabilistic Evaluation of Functional Recovery of Building Systems

Vesna Terzic

Peny K. Villanueva

Daniel Saldana

Dong Y. Yoo

Department of Civil Engineering and Construction Engineering Management

California State University Long Beach

PEER Report No. 2021/06

Pacific Earthquake Engineering Research Center
Headquarters at the University of California, Berkeley
September 2021

PEER 2021/06
September 2021

F-Rec Framework: Novel Framework for Probabilistic Evaluation of Functional Recovery of Building Systems

Vesna Terzic

Peny K. Villanueva

Daniel Saldana

Dong Y. Yoo

Department of Civil Engineering and Construction Engineering Management
California State University Long Beach

PEER Report 2021/06
Pacific Earthquake Engineering Research Center
Headquarters at the University of California, Berkeley

September 2021

ABSTRACT

Earthquakes are one of the most destructive natural disasters with potentially devastating consequences on communities and the supporting infrastructure. To mitigate the effects of earthquakes on communities and infrastructure, the recovery process of building systems should be considered during the design of the building as it is essential for continued operation. This study presents a novel, probabilistic, building-level framework for modeling and evaluating the entire recovery process (F-Rec Framework), including a building's post-earthquake functionality along with duration and path of functional recovery. The proposed framework considers all structural and nonstructural building components/systems. It consists of three novel and integrated methods for evaluation building's post-earthquake functionality, mobilization time, and repair time. The framework—in line with the probabilistic performance-based earthquake engineering methodology—uses FEMA P-58 damage/performance assessment results to evaluate the recovery process. With its modular structure, this framework is extendable and lends itself to the additional of new components.

The method for evaluating a building's post-earthquake functionality utilizes FEMA P-58 damage assessment results in conjunction with fault trees of complex building systems to provide a probabilistic estimate about the percent of the inaccessible functional area within a building and to identify building components that impair its functionality. To facilitate functionality analysis, the research proposes a fault tree for a complex building system and introduces user-defined probabilistic limit state functions of individual building components that define the damage thresholds for partial (local) and full loss of the building functionality.

A comprehensive, probabilistic repair time method is developed in collaboration with general contractors to realistically reflect current construction practices. The method utilizes the critical path method (CPM) to calculate the total duration of repair project, where repair and resources are scheduled based on the sporadic spatial distribution of damage accounting for surge in construction demand and labor congestion. It consists of two components: (1) the repair scheduling method; which can accommodate any repair sequencing and considers realistic labor allocations; and (2) the resource scheduling method; which provides an efficient way of reducing workers during labor congestions while minimizing its prolonging effect on the project duration.

The mobilization time method proposes new algorithm for evaluation of mobilization time (time between the closure of a facility and the beginning of repairs) that is based on published research and data collected by interviewing general contractors, building inspectors, structural engineers, and facility managers. The unique feature of the method is its capability to derive different building limits states (i.e., the repairability limit state, detailed inspection limit state, and functionality limit state) and to use them to determine mobilization activities on a project and associated mobilization times.

The distinguishing feature of the framework is its capability of generating the recovery curve and isolating the main contributors to the interrupted building operation and recovery process. This is demonstrated in the case study of an existing 13-story office building. Importantly,

the outcomes of the study showcase how these unique recovery-based results can be effectively used as a guide for the development of earthquake mitigation strategies and design/retrofit solutions to improve seismic performance.

ACKNOWLEDGMENTS

This work was supported by the National Science Foundation through Award CMMI-1563428 and Pacific Earthquake Engineering Research (PEER) Center through Project 2002-NCEEVT. This support, as well as significant input provided by Professor Stephen A. Mahin and building contractors, engineers, inspectors, and facility managers, including Bob Berenguer, John F. Rochford, Fred Wallitsch, Richard Cavecche, Gene Calkin, Jesse Karns, Lance Kenyon, David Bonowitz, Joshua Cichuniec, and Predrag Nikolic, is gratefully acknowledged. Any opinions, findings, and conclusions expressed herein are those of the authors and do not necessarily reflect those of the sponsors or the Regents of the University of California.

CONTENTS

LIST OF TABLES

LIST OF FIGURES

1 Introduction

1.1 BACKGROUND

Major earthquakes are capable of severely damaging infrastructure, which in turn may result in significant economic losses and major social disruption. As evidenced by M8.8 27 February 2010 Maule, Chile, earthquake, a great number of buildings experienced considerable damage that resulted in building closures, causing significant indirect losses (lost product and income) [Miranda et al. 2012; EERI 2010]. Toyoda [2008] demonstrated that the 1995 Kobe, Japan, earthquake contributed significant direct loss (cost of repairs) and indirect loss to the total capital loss of the stricken area. Furthermore, his research showed that lost productivity or income in terms of estimated indirect losses continued to rise for more than 10 years post-event. The resilience of built environment in the aftermath of major earthquakes can be improved by implementing enhanced seismic design criteria that consider a building's post-earthquake functionality and recovery time. A case study by Terzic and Mahin [2017] demonstrates how building systems essential for providing continued functionality of a community can be protected through improved seismic design.

The performance-based earthquake engineering (PBEE) methodology developed by the Pacific Earthquake Engineering Research Center (PEER) provides a probabilistic framework for performance assessment and design of buildings utilizing performance objectives meaningful to decision-makers, stakeholders, and insurers (e.g., repair cost, recovery time, and return on investment). Recently, Federal Emergency Management Agency's (FEMA) P-58 initiative [FEMA 2012; 2018a; and 2018b] adopted the PBEE methodology for general use by developing a comprehensive library of peer-reviewed fragility curves and associated consequence functions that consider more than 700 structural and nonstructural building components.

The first step in this methodology is selection of ground-motion records representative of excitations expected at the site. Typically, ground motions are selected to represent different levels of earthquake hazard, ranging from low to high. For each hazard level, the selected ground-motion records are used in conjunction with dynamic analysis software and appropriately selected numerical models to simulate the range of structural responses. Furthermore, engineering demand parameters (EDPs) are selected for all components of the system and related by components' fragility curves (cumulative exceedance probability distributions of corresponding EDPs) to their damage measures/states (DMs) (e.g., local beam flange buckling, broken windows, etc.) to evaluate the level of damage a building might have sustained given the magnitude of the earthquake. These DMs are used in conjunction with components' consequence functions to estimate the corresponding earthquake losses or damage consequences (e.g., the repair cost and time required for various components, etc.). Finally, the component losses are used to evaluate the total earthquake losses (e.g., total repair cost). These earthquake losses are known as decision variables (DVs) that provide valuable information for stakeholders, upon which informed design decisions can be made.

The primary DVs considered in FEMA P-58 focus on total repair costs and a crude estimate of the total repair time. Although the methodology represents a significant step forward towards quantifying earthquake-induced losses, it lacks models for evaluating a building's functional recovery process that is necessary for probabilistic estimation of associated indirect losses and system resiliency. Moreover, a probabilistic building-level model for evaluating recovery process is essential for assessing the effect of individual buildings on community resilience [Cimellaro et al. 2010; Gordin 2010; Burton et al. 2015; Terzic et al. 2015; Mieler et al. 2018; and Sun et al. 2019].

The functional recovery process of a building is schematically presented in Figure 1.1, which is based on a recovery curve established by Cimellaro et al. [2010]. As a result of earthquake damage, at time T_1, a building's functionality might be reduced or fully lost. Repair of damaged components restores functionality to a desired level so that the building can operate or function in the same, close to, or better than the original state (time T_3 in Figure 1.1). The recovery time (i.e., downtime) is defined as the period necessary to restore the functionality of a structure to the desired level, and the recovery path is the path that a particular building takes to repair earthquake induced damage. The recovery time is naturally derived from the mobilization time and repair time; see Figure 1.1. Mobilization time precedes repair time and includes the time required for building inspection, site preparation, moving of occupants and building contents, providing engineering services, obtaining permits, securing financing, and acquiring essential material coupled with construction services (defined by Comerio [2006]). Repair time is the time required to perform the actual repairs of a structure. Since recovery time is associated with the time to restore functionality, actual mobilization and repair times must be used in conjunction with different building limit states, including functionality limit state (FLS), detailed inspection limit state (DILS), and repairability limit state (RLS), (defined by Burton et al. [2015]), to project them into their recovery time contributions. Therefore, the functional recovery process can be fully determined through evaluation of different building limit states, and associated recovery time and recovery path.

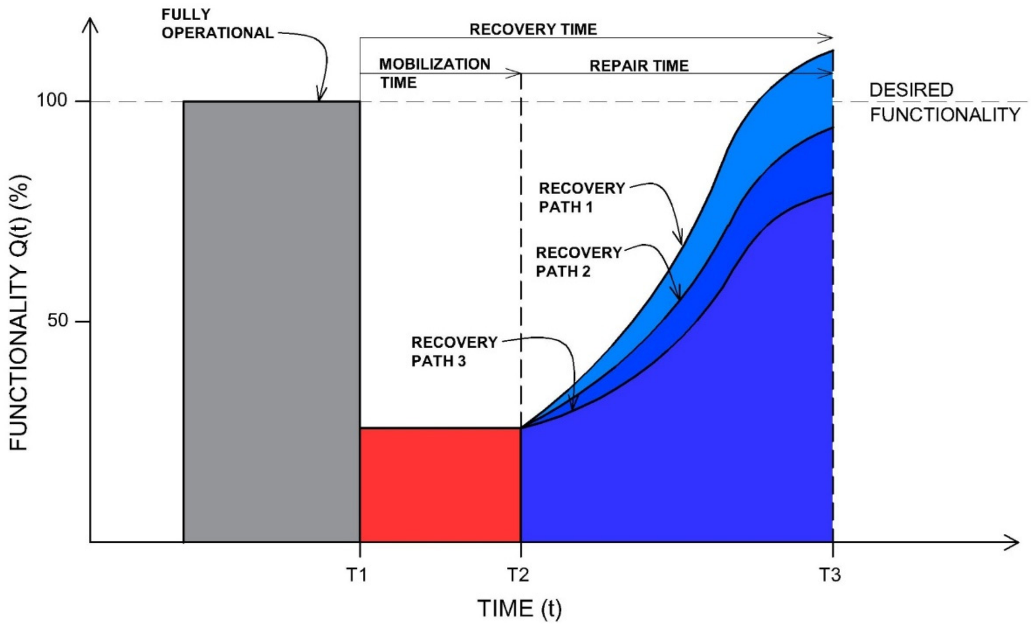

Figure 1.1 Schematic representation of the recovery curve for a building system after an earthquake (after Terzic et al. [2021]).

In 2013, Arup developed the Resilience-based Earthquake Design Initiative (REDi™) rating system that complements FEMA P-58 methodology by utilizing downtime as one of the performance metrics in its "resilience-based earthquake design." While the REDi™ downtime model was a step forward in performance assessment, it is based on many crude assumptions, which may cause inaccurate predictions of downtime. For example:

- Limit state functions are not explicitly considered;
- Repair time utilizes a fixed repair schedule (see also Mason et. al. [2000] and FEMA 2012]) and a predetermined workforce irrespective of the amount and severity of damage (see also FEMA [2012]); and
- Mobilization time is based on the damage state of the most severely damaged component in a building, irrespective of the number of components with such damage.

Lack of accuracy of the REDi™ model is illustrated by the case study by Haselton et al. [2019] that presents REDi™ downtime estimates for different designs of a 40-story tall building. The study considers code-based design and alternate designs that include several significant improvements of nonstructural and structural components. As shown by Haselton et al. [2019], when the initial code-compliant building design was improved by increasing the strengths of the lateral load-resisting system and equipment anchorage by 50%, and by reducing the design interstory drift ratio from 2% to 1%, the median downtime at a DBE level (according to REDi™ model) was only slightly reduced, from about 22 months to 17 months; this seems unreasonable.

In 2015, Burton et al. [2015] proposed a framework for incorporating PBEE in the assessment of seismic resilience of residential communities, where the functional recovery of individual single-family residential buildings was evaluated by incorporating limit states defined by SPUR [Poland et al. 2009]. The study established general definitions for limit states necessary for evaluation of functional recovery and has provided their formulation for simple single-family residential buildings. For complex building systems, Porter and Ramer [2012] and Jacques et al. [2014] have demonstrated that fault-tree analysis (FTA) can be effective in evaluating the risk of losing functionality. In these studies, FTA is used to relate the functionality of complex building systems to the state of the subsystems and its components. Jacques et al. [2014] applied the FTA method to deterministically assess the "reduction in functionality" and "complete loss of functionality" of critical hospital services due to earthquake damage. To validate the fault-tree model, they used field data from the 2011 Christchurch earthquake and reported a mixed level of success in capturing all parameters of functionality that occurred post-event. While the method successfully estimated the functionality of most hospital services, it failed to accurately estimate the functionality of few services due to the lack of a dynamic aspect in the fault-tree structure. Porter and Ramer [2012] applied FTA to a computer data center to characterize the risk of losing functionality due to earthquake damage. The example analysis by Porter and Ramer [2012] was validated by several means: a red-team exercise, comparison with generic judgment-based standards, comparison with the actual earthquake performance history of the facilities, and comparison with their own judgment and that of the facility operators; reasonable agreement between analysis and observations was reported.

1.2 NEW FRAMEWORK FOR MODELING FUNCTIONAL RECOVERY

The research presented herein proposes F-Rec Framework, a comprehensive probabilistic framework for modeling the entire functional recovery process of a building system [Terzic et al. 2021]. The framework supports detailed evaluation of seismic performance of buildings considering all structural and nonstructural building components/systems, and calculation of performance metrics relevant for the assessment of the recovery process, including a building's post-earthquake functionality along with the duration and path of functional recovery; see Figure 1.1. As shown in Figure 1.2, the F-Rec framework is in line with the probabilistic PBEE framework and complements FEMA P-58 [FEMA, 2018a] performance assessment methodology. The framework consists of three novel and integrated methods for evaluating a building post event:

1. Post-earthquake functionality [Terzic and Villanueva 2021];
2. Repair time [Terzic et al. 2016; Yoo 2016]; and
3. Mobilization time [Terzic et al. 2021].

The main inputs for the recovery analysis of a building are generated through FEMA P-58 performance assessment analysis (either with PACT [FEMA 2018b] or the NHERI-SimCenter/PBE [2019] tool) and include detailed information about damage states of all building components and corresponding repair times. All components of the framework are founded on information collected from interviews with general contractors, building inspectors, structural engineers, and facility managers who were actively involved in the recovery of Los Angeles following the 1994 Northridge earthquake.

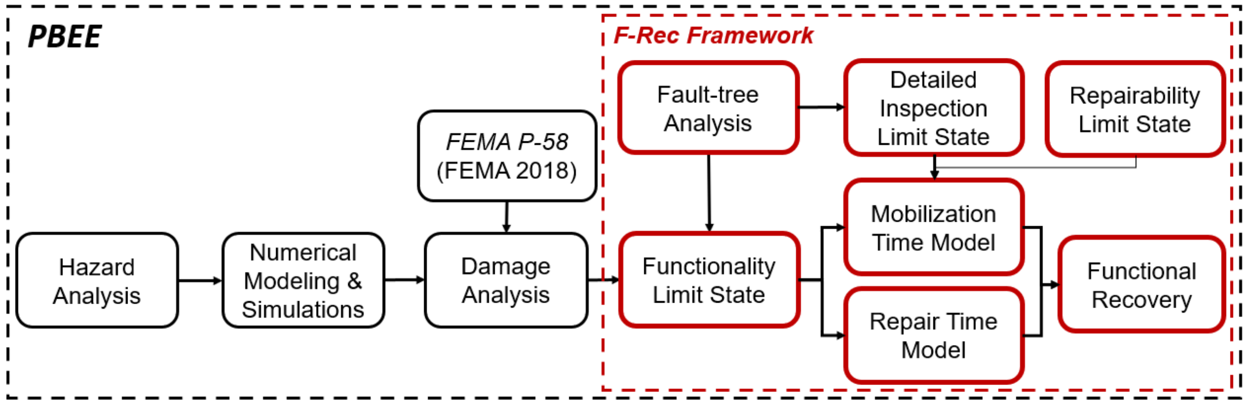

Figure 1.2 **F-Rec Framework for modeling functional recovery in conjunction with PBEE/FEMA P-58 methodology. The components of the recovery framework are shown in red (after Terzic et al. [2021]).**

Terzic and Villanueva's [2021] method for evaluating a building's post-earthquake functionality utilizes FEMA P-58 damage assessment results in conjunction with fault trees of complex building systems to: (1) generate FLS (probability that "x" percent loss in building functionality will be reached, where "x" is any number between 0 and 100); (2) provide a probabilistic estimate about the percent of the inaccessible functional area within a building; and (3) identify building components that impair its functionality.

To facilitate the functionality analysis, the research proposes a fault tree for a complex building system, which is derived from author's interviews with facility managers and published work [Porter and Ramer 2012; Jacques et al 2014; Johnson et al. 1999; Pate-Cornell 1984; Vesely et al. 1981; and Prassinos et al. 1986]. The primary user-defined inputs are probabilistic limit state functions of individual building components, which define the damage thresholds for partial (local) and full loss of the building functionality (introduced by Terzic and Villanueva [2021]). The method is presented in detail in Section 2.1.

A comprehensive, probabilistic repair time method proposed by Terzic et al. [2016] and Yoo [2016] was developed in collaboration with general contractors to realistically reflect current construction practices accounting for differences between new construction and repairing earthquake-induced damage. The repair time method utilizes the critical path method (CPM), which is widely used in the construction industry, to calculate the total duration of repair project, where repair and resources are scheduled based on the sporadic spatial distribution of damage while accounting for a surge in construction demand and labor congestion. It consists of two methods: (1) the repair scheduling method; and (2) the resource scheduling method. The repair scheduling method accommodates any repair sequencing and considers realistic labor allocations. In contrast, resource scheduling provides an efficient way of reducing workers during labor congestions while minimizing its prolonging effect on the project duration. Importantly, the repair time method can be used in two ways: (1) to find the total repair time associated with all damaged components (stand-alone); and (2) to find the repair time and repair path associated with damaged components that impair building operation and therefore affect the recovery process. The method is presented in detail in Section 2.2.

Terzic et al.'s [2021] method for evaluating mobilization time (time between the closure of a facility and the beginning of repairs) is developed utilizing mobilization activities defined by Comerio [2006], information about post-earthquake inspection strategies presented in FEMA 352 [FEMA 2000], and data collected by interviewing general contractors, building inspectors, structural engineers, and facility managers. The method first uses FEMA P-58 damage assessment results to evaluate building's repairability state (yes or no) and detailed inspection state (yes or no) [per Terzic et al. [2021]). Next, this information is used together with the building's functionality state (full, partial, no loss), considering the types of damaged components that impair functionality (e.g., equipment, nonstructural, and/or structural) and functionality tag of building components (full, partial, or no loss) to identify mobilization activities on a project and associated mobilization times. Finally, these mobilization times are used within Terzic et al [2021] mobilization time algorithm to evaluate the total mobilization time for all realizations of Monte Carlo simulation process. To provide realistic estimates of mobilization time with this method, median estimates of mobilization activity times must be acquired from the building developers and their teams. The method is presented in detail in Section 2.3.

The main distinguishable features of the F-Rec framework are as follows:

1. The post-earthquake functionality limit state (FLS) is explicitly evaluated, providing a probabilistic estimate of the percent of the functional area within the building;
2. Recovery time and path (like the one schematically presented in Figure 1.1) are evaluated using novel repair time and mobilization time methods that only consider components whose extent of damage is sufficiently large to impair functionality;
3. Repair time method utilizes the CPM, where repair and resources are scheduled based on the sporadic spatial distribution of damage while accounting for surge in construction demand and labor congestion;
4. Mobilization time method proposes new algorithm for evaluation of mobilization time; it also derives different building limits states (i.e., repairability limit state, detailed inspection limit state, and functionality limit state) and utilizes them to determine mobilization activities on a project and associated mobilization times;
5. The framework identifies damaged systems/components that reduce functionality and highlights all repair and mobilization activities that dominate the recovery process; and
6. The framework has modular structure allowing for effortless extension and additions of new features along with rapid evaluation through use of workflows between different components of the framework.

The F-Rec framework overcomes many deficiencies of the currently available building-level recovery (and/or repair time) models that do not explicitly consider different building limit states and are based on fixed repair schedules [Mason et. al. 2000; FEMA 2018a; and Arup 2013] and a predetermined workforce, irrespective of the amount and severity of damage [FEMA 2018a; Arup, 2013]. To highlight the differences between widely used REDi™ model and the F-Rec framework introduced herein, Table 1.1 compares two frameworks considering all PBEE components.

The F-Rec framework can efficiently support functionality-based seismic design initiative of NIST/FEMA [2021] and can be used in either the probabilistic performance-based seismic design of new buildings or for the evaluation and retrofit of existing buildings. The flexibility and robustness of the framework are demonstrated in Chapter 3 of this report, with detailed evaluation of functional recovery of an existing 13-story office building located in a region of high seismicity (described by Garza et al. [2018]). Its recovery-based results are used to showcase how they can guide the retrofit measures for improved seismic performance.

Table 1.1 Comparison between REDi™ and F-Rec Framework.

Framework	Functionality limit state	Repair time model			Mobilizaton time model	
		Repair schedule	Labor allocation	Repair activities	Based on	Detailed inspection limit state
REDi™	Not explicitly considerd	Fixed	Based on floor area	Grouped by subsystem type (structural, electrical, etc.)	Damage state of the most severely damaged component in a building	Not explicitly considered
F-Rec	Explicitly considered	Flexible (uses critical path method)	Based on amount and severity of damage	Each component is individually considered	Damage state of all building components in aggregate	Explicitly considered

1.3 ORGANIZATION OF REPORT

This publication compiles components of the new recovery framework, previously published individually [Terzic et al. 2016; Yoo 2016; Terzic and Villanueva 2021; and Terzic et al. 2021], into an overarching and detailed report.

Chapter 2 presents the F-Rec framework, including a detailed description of all of its constituents: (1) the probabilistic method for post-earthquake functionality; Section 2.1; (2) the repair time model; see Section 2.2; and (3) the mobilization time model; see Section 2.3.

Chapter 3 demonstrates the proposed framework on a case study of an existing 13-story building (described in Section 3.1). Since the proposed framework is in line with the PBEE, this section presents all types of modeling/analysis necessary for recovery evaluation of the building, including: ground-motion selection, structural modeling and analysis (Section 3.2), performance modeling per FEMA P-58 (Section 3.3), recovery modeling with the proposed framework (Section 3.4), and evaluation of functional recovery with the emphasis on how the recovery-based results can be used to guide retrofit solutions for improved seismic performance (Section 3.5).

Chapter 4 provides summary of the presented research and offers numerous opportunities for the application of the F-Rec framework.

2 F-Rec Framework for Modeling Functional Recovery

A new framework for modeling the functional recovery of a building system, F-Rec Framework, is introduced in Section 1.2 and depicted in Figure 1.2. It is in line with the probabilistic PBEE framework and complements FEMA P-58 [FEMA 2018a] performance assessment methodology. The framework supports detailed evaluation of seismic performance of buildings considering all structural and nonstructural building components/systems, and calculation of performance metrics relevant for the assessment of the recovery process including building's post-earthquake functionality along with the duration and path of functional recovery (as shown in Figure 1.1). It consists of three comprehensive and integrated methods for evaluating building's (1) post-earthquake functionality [Terzic and Villanueva 2021]; (2) repair time [Terzic et al. 2016; Yoo 2016]; and (3) mobilization time [Terzic et al. 2021]. These methods are next described in detail.

2.1 PROBABILISTIC METHOD FOR POST-EARTHQUAKE FUNCTIONALITY

Terzic and Villanueva's [2021] method for evaluating a building's post-earthquake functionality relies on generating functionality limit state (FLS) for a particular earthquake scenario as a probability that "x" percent loss in building functionality will be reached (where "x" is any number between 0 and 100). Within the context of this research, the functionality loss represents a percent of the inaccessible functional area within a building. The proposed method uses FEMA P-58 damage assessment results in conjunction with a fault tree of a complex building system to generate a building's functionality limit state and to identify components that impair its functionality. The primary user-defined inputs are probabilistic limit state functions of individual building components (introduced by Terzic and Villanueva [2021]), which define the damage thresholds for partial (local) and full loss of the building functionality. The proposed method is created with the following goals in mind:

1. Flexibility; branches in the fault trees can be easily turned ON and OFF;
2. Robustness; the method has a modular structure allowing for effortless expansion by adding new features; and

3. Speed of evaluation; workflows between structural analysis, damage analysis, and post-earthquake functionality analysis can be created to allow rapid evaluation of building's functionality.

The method presented herein is applicable to the cases when a building is owned by a single entity, however, the method is highly robust and flexible, and can be extended to include cases when the building is owned by multiple entities.

2.1.1 Generic Fault Tree of a Complex Building System

To facilitate the development of the building-level probabilistic FLS for a particular seismic hazard, Terzic and Villanueva [2021] propose a fault tree for a complex building system. The fault tree is derived from authors' interviews with facility managers and published work [Porter and Ramer 2012; Jacques et al. 2014; Johnson et al. 1999; Pate-Cornell 1984; Vesely et al. 1981; and Prassinos et al. 1986]. A generic fault tree that relates the functionality of a complex building system to the state of its subsystems is shown in Figure 2.1. The top event is associated with the percent loss of building functionality, and lower events represent the percent loss of function of its subsystems. Note that the term "Fails" in the figure means either full or partial loss in building functionality, where damage can fully or partially (locally) impair a building function. Lower events are represented by subsystems critical for maintaining the basic building function and include the core building systems (electrical power system, HVAC system, piping system, vertical transportation system, architectural systems, and structural system), as well as the lifeline and other systems (e.g., utility systems, critical building equipment, staff, and supplies). Each subsystem is related to the top event through an "or" gate, indicating that the reduced functionality of any of the lower events reduces the functionality of the top event. Furthermore, each subsystem has its own fault tree that relates the functionality of the subsystem to the damage state of its components; these fault trees are presented in Section 2.1.3. Note: the great majority of residential and office multi-story buildings mostly comprise these core subsystems, providing the broad application for the main developments presented in this research. While the presented study does not provide detailed information on building-specific and lifeline systems, these can be adopted from other studies (e.g., Porter and Ramer [2012] and Jacques et al. [2014]) and accounted for by adding additional branches to the fault tree presented in Figure 2.1. Additionally, each of the subsystems presented in Figure 2.1, can be turned off from the fault tree if not applicable to the building of interest.

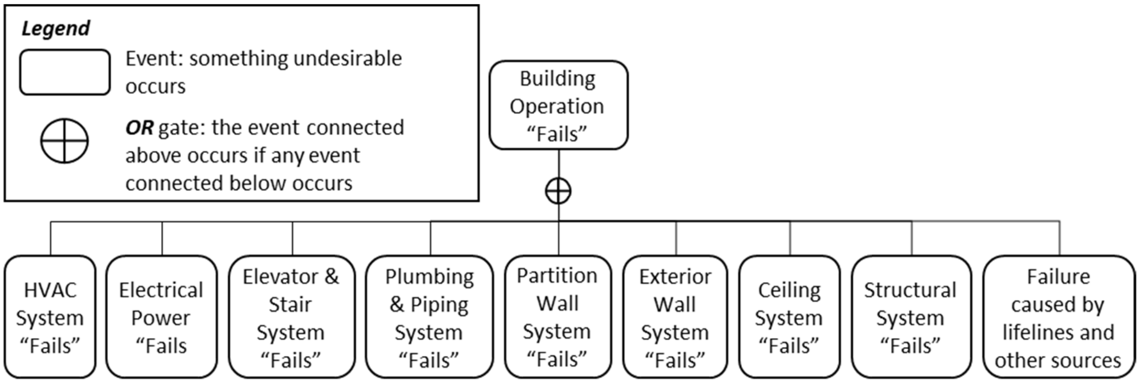

Figure 2.1 Generic fault tree for a complex building system (after Terzic and Villanueva [2021]).

2.1.2 Step-by-Step Procedure for Establishing Functionality Limit State

In line with FEMA P-58 methodology, the proposed method utilizes information on damage states of all building components generated through the Monte Carlo process, which evaluates building performance for a large number (hundreds to thousands) of realizations to explore the effect of uncertainty on the predicted outcome. Each realization of the Monte Carlo simulation process represents one possible damage state of the building, and the loss of functionality for the entire building (assuming that the building is owned by a single entity) is expressed by one of the three outcomes:

1. 0% loss of functionality; when all building subsystems are fully functional;
2. X% (partial) loss of functionality ($0 < X < 100$); when a function of some subsystems is compromised. Partial loss of functionality applies to cases when damage to the subsystems is localized, restricting access to the areas in the building affected by the damage while the rest of the building remains open and functional; and
3. 100% loss of functionality; when any of the critical subsystems fail.

The functionality outcomes from all realizations are ordered from smallest to largest to construct a post-earthquake functionality limit state, which is expressed as a probability that "x" percent loss in functionality will be reached. The high-level procedure for the development of this limit state is described next and is supplemented by the low-level procedures pertinent to specificities of the core-building subsystems; see Section 2.1.3.

To derive the functionality limit state for the building system, first, the functionality of all subsystems is evaluated at every floor of the building utilizing their fault trees, where each subsystem consists of components whose damage can reduce the subsystem's capacity to function; their fault trees are provided in Section 2.1.3. Loss in functionality from all subsystems is then utilized to calculate the loss in functionality of the entire building system (per the method described in this section). Figure 2.2 provides a flowchart that illustrates the process for evaluating the loss in building's functionality for every realization of the FEMA P-58 performance assessment simulation. The process initiates by the acquisition of data from existing FEMA P-58 performance model and analysis results, it is followed by user-defined inputs (i.e., LSFs), and is finalized with the calculation of the loss in system functionality. The entire process is next described in detail.

Step 1: **Acquire data from FEMA P-58 performance model and isolate components that can impair functionality**. The first step of the proposed method is acquiring fragility IDs from an existing the FEMA P-58 performance model and identifying those building components that can impair the functionality of their subsystems. Furthermore, damage states of each selected fragility are evaluated to recognize those that can influence functionality. For example, lower damage states of many building components are associated with minor or cosmetic damage that does not impact functionality; as such, these damage states are not considered in functionality calculations.

Step 2: **Group fragility IDs by component type and calculate group quantities**. Components that can impair functionality are grouped by component type. In the FEMA P-58 performance model, multiple fragility IDs of the same component type can occur. For example, several fragilities representing moment connections of different sizes and joint types (e.g., beams on two sides of the joint or beam from one side only) may be present in the performance model of the building. For the purpose of evaluating post-earthquake functionality, they will be grouped together and assigned to a component type; for example, the "moment connections" component type. Note that the grouping of fragility IDs should apply only to those component types where grouped fragilities have similar implications on the loss in functionality of the subsystem. Moreover, each component type might have multiple groups; for each floor and for the entire building (referred to as component groups). Finally, the total quantities (i.e., number of units) of a component type will be calculated for all of its groups as applicable (per floor and for the entire building) utilizing information extracted from the FEMA P-58 performance model.

Step 3: **Set user-defined inputs.** To calculate the functionality limit state of a subsystem, each component of a subsystem is defined with the limit state functions (LSFs) that define the extent of component damage to trigger either partial (local) or full interruption of subsystem function. Given that many of building subsystems can preserve its full function with some damage to its components, LSFs for partial interruption of function are very important as they set the threshold for the acceptable extent of the damage. Additionally, each LSF should receive a tag that specifies whether the functionality is impaired immediately or only during the actual repair. This information is used to properly evaluate the consequences of the incurred damage. For example, if the incurred damage of a component type only impairs functionality during the actual repair, it will not have an effect on the post-earthquake building functionality but will have an effect on the recovery process as a whole.

Limit state functions are lognormal distributions, defined by their medians and dispersions, for every damage state of a component type that can impair functionality (provided by a user and unique to a project). Furthermore, if a component is located only at one level of the building (e.g., a cooling tower located at the roof level), its LSFs are defined as ratios of damaged components with respect to its total quantity, triggering partial and/or full interruption of the subsystem function. For components distributed throughout the building (e.g., shear tabs located at every floor), two types of LSFs must be defined:

- *Floor-based LSFs*: expressed with ratios of damaged components within a floor along with a number of floors with such damage necessary to trigger full and partial loss of subsystem function; see example provided in Table 2.1; and
- *Building-based LSFs*: expressed as ratios of damaged components within the entire building to trigger partial and/or full loss of subsystem function; see example provided in Table 2.1.

These two types of LSFs for the distributed components allow consideration of the effects of their local (floor-based) and overall (building-based) damage on functionality. They are used one at a time to evaluate the functionality of a subsystem, where the highest loss in functionality between the two results is the final result of the subsystem. Please note that for taller buildings, a certain extent of component damage must be exceeded across several floors to compromise its functionality. Thus, floor-based LSFs are defined with two parameters: a damage ratio threshold for a floor and a number of floors where damage needs to exceed the threshold to compromise building functionality. Table 2.1 shows an example of user-defined inputs for LSFs for a building component located on every floor. Note: the example presented below only serves for illustrative purposes where medians and dispersions of LSFs may not be realistic.

Table 2.1 Limit state functions for the component damage states as defined in FEMA P-58 (after Terzic and Villanueva [2021]).

<table>
<tr><th rowspan="4">Component type</th><th rowspan="4">DS#</th><th rowspan="4">DS description</th><th colspan="6">Median ratios of damaged component that trigger interruption of function and their dispersions</th></tr>
<tr><th colspan="2">Building-based LSFs</th><th colspan="4">Floor-based LSFs</th></tr>
<tr><th rowspan="2">Partial loss LSF</th><th rowspan="2">Full loss LSF</th><th colspan="2">Partial loss</th><th colspan="2">Full loss</th></tr>
<tr><th>LSF</th><th>No. of stories</th><th>LSF</th><th>No. of stories</th></tr>
<tr><td rowspan="2">Shear tabs</td><td>2</td><td>Partial tearing of shear tab and possibility of bolt shear failure (6-bolt or deeper connections)</td><td>*0.1 (M)
0.3 (D)</td><td>0.2 (M)
0.3 (D)</td><td>*0.15 (M)
0.3 (D)</td><td>5</td><td>0.3 (M)
0.3 (D)</td><td>3</td></tr>
<tr><td>3</td><td>Complete separation of shear tab, close to complete loss of vertical load resistance</td><td>0.05 (M)
0.3 (D)</td><td>0.1 (M)
0.3 (D)</td><td>0.075 (M)
0.3 (D)</td><td>5</td><td>0.15 (M)
0.3 (D)</td><td>3</td></tr>
</table>

DS: damage state; M: median; D: dispersion; and LSF: limit state function.

*Functionality affected only during actual repair.

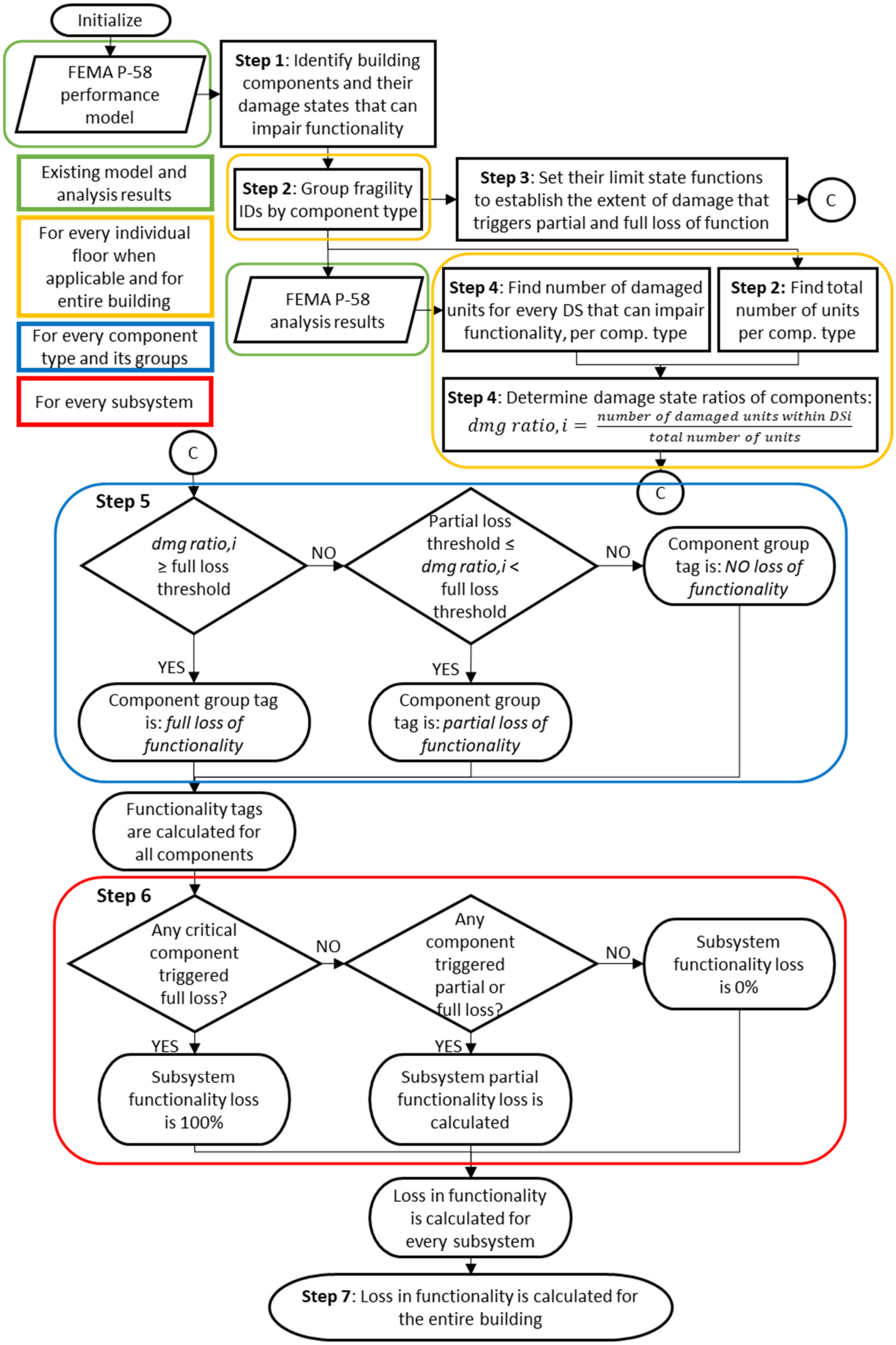

Figure 2.2 Flowchart for evaluating the loss in functionality for one realization for the entire building (after Terzic and Villanueva [2021]).

Step 4: **Acquire the number of damaged units from FEMA P-58 analysis results.** Next, FEMA P-58 analysis results are utilized to extract the number of damaged units (i.e., quantity) for each damage state that can impair functionality, and their quantities are aggregated per component type. This information is then used to find the ratios of damaged components (designated as the *dmg* ratio in Figure 2.2) for every damage state of interest. These damage state ratios are calculated by dividing the number of damaged units in the damage state of interest by the total number of units in the group. Multiple damage state ratios are obtained for each damage state of a component type; one for the entire building and one for every individual floor when applicable.

In some cases there may be a need for introducing an aggregate damage ratio that is a weighted combination of considered damage ratios for a component type. Consider the example of shear tabs presented in Table 2.1. It is clear that the full loss of functionality will be triggered if more than 10% of the shear tabs in the building have experienced the full tearing (DS3); but it may also be reasonable to trigger the full loss of functionality if 8% of shear tabs have full tearing (DS3) and 15% of shear tabs have partial tearing (DS2).

To capture such cases, an aggregate damage ratio (ADR) can be defined as $\mathrm{ADR} = \sum_i^n W_i DR_i$, where i is the damage state number, W_i is the weight assigned to damage state i (user-defined input, where $\sum_i^n W_i = 1$), and DR_i is the ratio of units in damage state i. In cases when an aggregate damage ratio is used, the weights associated with different damage states along with the corresponding LSF shall be defined in Step 3, along with all other user defined parameters. For example, if a user assigns weights of 0.4 for DS2 and 0.6 for DS3 of shear tabs, and defines full-loss LSF with a median of 0.1, then for a case of 15% shear tabs in DS2 and 8% of shear tabs in DS3 the ADR = (0.4 × 0.15) + (0.6 × 0.08) = 0.108, which exceeds the median limit state threshold of 0.1, and may therefore result in the full loss of functionality.

Step 5: **Calculate functionality tags for all component types.** To initiate the calculation of the post-earthquake functionality of the building, functionality tags are established for all component types. Then, based on the amount and severity of damage, three tags can be assigned: (1) no loss in functionality; (2) partial loss in functionality; and (3) full loss in functionality.

To assign the tag to a component type, damage state ratios of its groups (per floor and for the building) are used together with LSFs of associated damage states to determine if the component group has the potential to trigger reduction of subsystem functionality. To keep the method probabilistic, a random number generator is used to determine if the functionality limit state threshold for a component is exceeded for the considered realization. For each group, the damage state ratio of a component type is compared with the threshold for triggering the full loss of functionality. If the threshold is exceeded, the group receives a 'full loss of functionality' tag. Otherwise, the damage state ratio of a component type is compared with the threshold for triggering partial loss of functionality. The resulting group tag, in this case, can either be "partial loss" (if the threshold is exceeded) or "no loss in function" (if the threshold is not exceeded). This information is next used to generate two functionality tags: building-based and floor-based.

While the building-based functionality tag of the considered component type directly corresponds to its group that represents the entire building, the floor-based tag is calculated using tags of individual floors in conjunction with the number of damaged floors required to trigger the reduction of functionality. If the number of floors with "full loss of functionality" tag for floors exceeds the threshold, the floor-based tag is "full loss of functionality." Otherwise, the number of floors with an aggregate of full and partial loss of functionality tags is compared with the threshold. The resulting floor-based tag will be either "partial loss of functionality" if the threshold is exceeded or "no loss of functionality" if it is not. Finally, the building-based tag and the floor-based tag are compared, and the tag representing the higher loss of functionality is assigned to the considered component type.

Step 6: **Calculate the loss of functionality for every subsystem.** With functionality tags assigned to all component types, the calculation of the functionality loss of a subsystem is performed next. This calculation process is unique for each subsystem and is based on the logic of the subsystem's fault tree. While the fault trees for all subsystems and calculation of partial loss in their functionality is presented in detail in Section 2.1.3, the general procedure is presented here.

In general, if any critical component of a subsystem (those connected to the upper event in the fault tree with an "or" gate) receives a "full loss of functionality" tag, the subsystem's functionality loss is 100%. Otherwise, the subsystem fault tree logic is used to calculate the loss of functionality if one of the following two outcomes is realized: (1) the highest tag among subsystem components is "partial loss of functionality," or (2) there is at least one component connected to the upper event with an "and" gate that receives "full loss of functionality" tag. Finally, if all component types within a subsystem receive "no loss of functionality" tag, the subsystem's functionality loss is 0%.

When a subsystem causes partial loss of building functionality for a considered realization, an analysis is conducted for each floor to calculate the percent area of the floor with compromised/lost function. The subsystem loss of function for the entire building is then calculated as the weighted average loss in functionality from all floors. Next, the loss in functionality of a subsystem calculated for all realizations is used to develop a functionality limit state for the subsystem.

Step 7: **Calculate the loss of functionality for the entire building system and create a functionality limit state**. With a loss in functionality evaluated for each subsystem at every floor of the building, the calculation of the loss of functionality for the entire building system is performed next. The loss of building functionality is expressed with one of the three outcomes: (1) no loss of functionality if all building subsystems are fully functional; (2) partial loss of functionality when the function of some of the subsystems is compromised; and (3) full (100%) loss of functionality if any of the critical subsystems fail.

When partial loss of functionality is observed, two models are considered: (1) the common area model, which assumes that damage to different subsystems affects the same area within a floor; and (2) the complementary area model, which assumes that damage to different subsystems affects different floor areas that do not overlap. These assumptions are necessary as the FEMA P-58 procedure does not provide information about the location of damaged components within a floor. While neither model is accurate, they bound the estimate of the partial loss of building functionality. In the case of the common area model, the maximum loss in functionality from all subsystems at one floor is announced the loss in functionality for that floor. The complementary model, however, calculates the loss of floor functionality as the sum of functionality losses from all subsystems at the floor and is not to exceed 100%. The loss of functionality for the entire building system is then calculated as the average loss in functionality among all floors considering both, common, and complementary area models. Finally, the functionality outcomes from all realizations of the Monte Carlo simulation process are ordered from smallest to largest to construct post-earthquake functionality limit state, which is expressed as a probability that "x" percent loss in building functionality will be reached. If excessive, the partial functionality outcomes for a building can also be used to trigger the full loss of functionality (e.g., loss of building function of 80% may result in the full building closure).

2.1.3 Building Subsystems Fault Trees

Each of the core building subsystems has its own fault tree that relates the functionality of a subsystem to the damage states of its components. Note that while a complete procedure for calculating loss in functionality of a subsystem is presented in Section 2.1.2, this section presents fault tree logics for *all* core building subsystem and provides a method that shall be used to calculate the partial loss of functionality if one of the following two outcomes is realized: (1) the highest tag among subsystem components is "partial loss of functionality"; or (2) there is at least one component connected to the upper event with an "and" gate that is tagged as "full loss of functionality."

When evaluating the functionality of building subsystems, it is important to account for interdependencies among different subsystems. For example, the functionality of the HVAC system depends on an available electrical power supply and functional motor control centers, which distribute power to the HVAC equipment. Furthermore, electrical power available for HVAC components depends on the functionality of the elevator system as the total power has to be shared between the elevators and HVAC equipment. To account for interdependencies among subsystems, the fault trees of core building subsystems are next presented in the order in which they have to be evaluated to properly account for the interdependencies.

Structural System. Figure 2.3 shows the fault tree for a structural system. For this tree, branches include structural component groups that can affect reduction or loss of building functionality (e.g., moment connections of the steel moment frame can be assigned to Group 1), as well as consideration of excessive residual drifts and collapse. Given that different buildings comprise of different component types that provide resistance to gravity and lateral loads, they may have a different number of groups/branches in the tree.

If any of the structural component groups triggers full loss of function, which is directly related to the trigger of unsafe placard due to structural damage, the subsystem will have a full loss of function. If partial loss of functionality is triggered for one or more component groups, the percent loss in functionality is then approximated as the sum of ratios of damaged components among component groups. For example, if at a considered floor, 20% of moment connections and 15% of shear tabs trigger partial loss of functionality, loss in functionality for the subsystem at that floor is 35% (20% + 15%). This method assumes that damage to different component groups affects different areas of the building, possibly overestimating the affected area that loses functionality, thus representing an upper bound for the loss in function of the structural subsystem. More accurate methods for evaluation of the partial functionality loss as a result of damage to different components of the structural system should be further investigated.

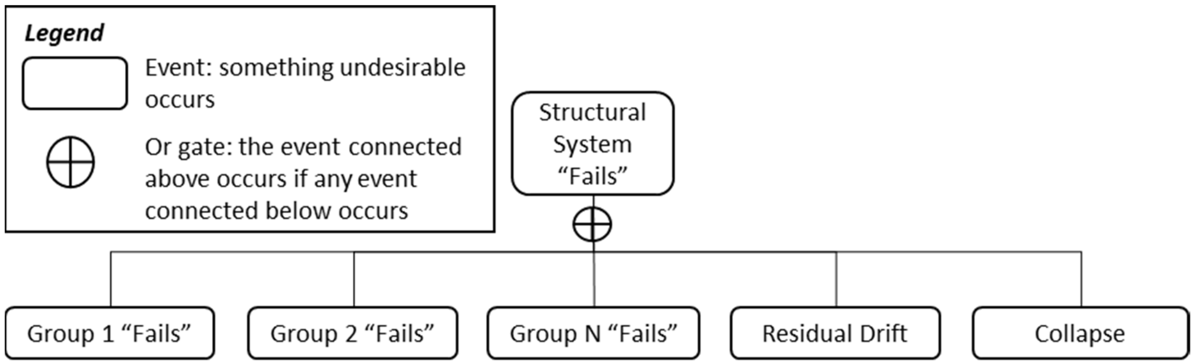

Figure 2.3 Fault tree for a structural system (after Terzic and Villanueva [2021]).

Electrical Power System. The fault tree for the system that provides the electrical power consists of the components presented in Figure 2.4. The purpose of the power system is to distribute and control power throughout the building. The power system in a building depends on utilities or backup systems to supply electricity and components necessary for the power distribution (e.g., low voltage switchgear, distribution panels, etc.). Although every multi-story building has low voltage switchgear and power distribution panels, backup system, transformers, and control panels may not be present and in such a case should be turned off from the fault tree.

If all components of the power distribution system fail, the entire power system fails. Otherwise, if the power supply system is functional but the functionality of some components of the power distribution system is compromised, the power system may have partial functionality. In this case, the remaining functionality depends on the configuration of the building distribution system and must be modeled accounting for its specificities. For example, if switchgear is located at every floor of a 10-story building and are dysfunctional only at one floor—assuming no damage to other components of the power distribution system—10% of the power will be lost. However, if switchgear is located at every other floor, thus distributing power over two floors, failure at one floor results in a 20% loss in power for the building.

The backup power system typically provides power from a centralized location and is more likely to be present in buildings with critical functions, e.g., IT buildings (critical for communications) and hospitals [Joshua Cichuniec, Personal Communication, January 22, 2019]. The capacity of power supplied to the building would depend on the type of generators in the building that often provide only a partial supply of power. For power to be generated, all components of the system must function, including generators, batteries, battery racks, and power control systems. In case of failure of any of the subsystem components, the functionality is fully compromised.

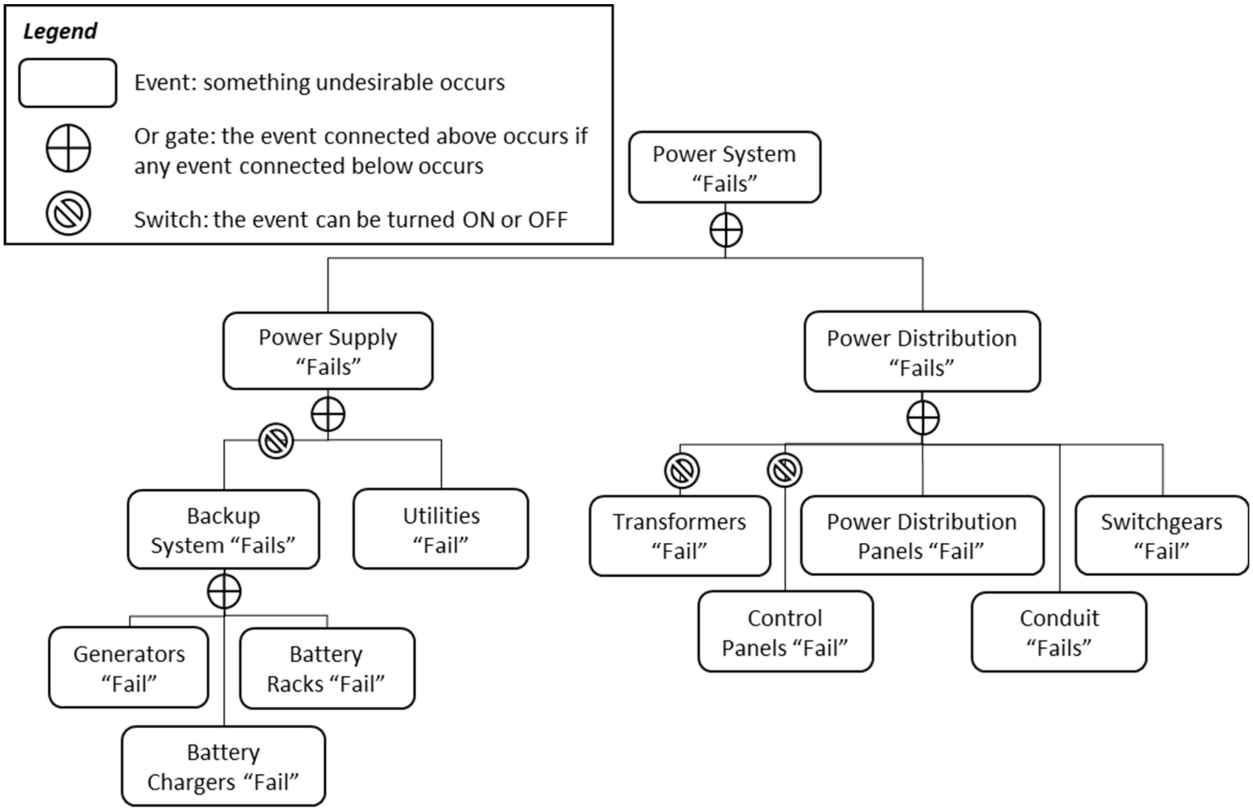

Figure 2.4 Electrical power system fault tree (after Terzic and Villanueva [2021]).

Stair and Elevator Systems. The fault trees for stairs and elevators are presented in Figure 2.5. Stairs and elevators are critical for providing vertical transportation routes through the building. The stairs represented in the fault tree are emergency stairs used for egress points, and elevators represented in the fault tree are the minimum number of elevators needed to maintain the building's functionality after an earthquake. Two fault trees are presented to distinguish between those buildings that have different functional requirements for stairs and elevators. If the building is low- to mid-rise, both the emergency stairs and elevators are required to fail for the system to fail; see Figure 2.5(a). It is assumed that if only the elevators fail, emergency stairs will be used to provide the basic building function; if only the emergency stairs fail, then elevators will be used to maintain basic building functions. For high-rise buildings, it is assumed that elevators and stairs must both be functional at the same time to provide the basic building function; see Figure 2.5(b). For high-rise buildings, elevators are critical for the mobility of occupants (as well as required for transportation of construction materials and workers), while emergency stairs are required for several avenues of egress for the safety of occupants in case of fire. In the presented fault tree, the set number of stories, x, that separates two presented scenarios must be decided by the user based on the specificities of the considered building.

The level of damage to stairs and elevators that triggers their loss of function is associated with the unsafe condition. For example, damage to stairs that causes loss of their live load capacity results in loss of their function. Any damage to elevators that are beyond cosmetic damage and pose a safety hazard to users would require that the elevator be shut down [Joshua Cichuniec, Personal Communication, January 22, 2019]. If the elevators are functional, the motor control centers (MCC) failure or power supply failure will cause the elevators to be out of operation; however, if the elevators have access to a backup electrical system, they may be functional even in the case of electrical utilities failure [Mahdi Yoozbashizadeh, Personal Communication, February 22, 2019; Predrag Nikolic, Personal Communication, September 10, 2019]. If the backup electrical system is not present or does not feed into the elevator system, it should be turned off from the fault tree.

When there is no damage to the electrical system, but elevators and/or stairs are tagged for partial loss in functionality, then the elevator and stair system are considered as having partial functionality. In the case of low- to mid-rise buildings, where both elevators and stairs are regularly used, the loss in functionality is calculated as the ratio of the number of total stair and elevator units that are no longer functional to the total number of stairs and elevators in the building. For high-rise buildings, where elevators are the primary and dominant way of transportation, the loss in functionality is equal to the percentage of elevators that are no longer functional. If the electrical system has reduced capacity due to damage to MMCs that have insufficient power for running operational elevators, the functionality of the elevator/stair system will be further reduced. In this case, the total loss in functionality of the elevator/stair system will depend on the emergency plan for the building because the available power has to be distributed among all building equipment.

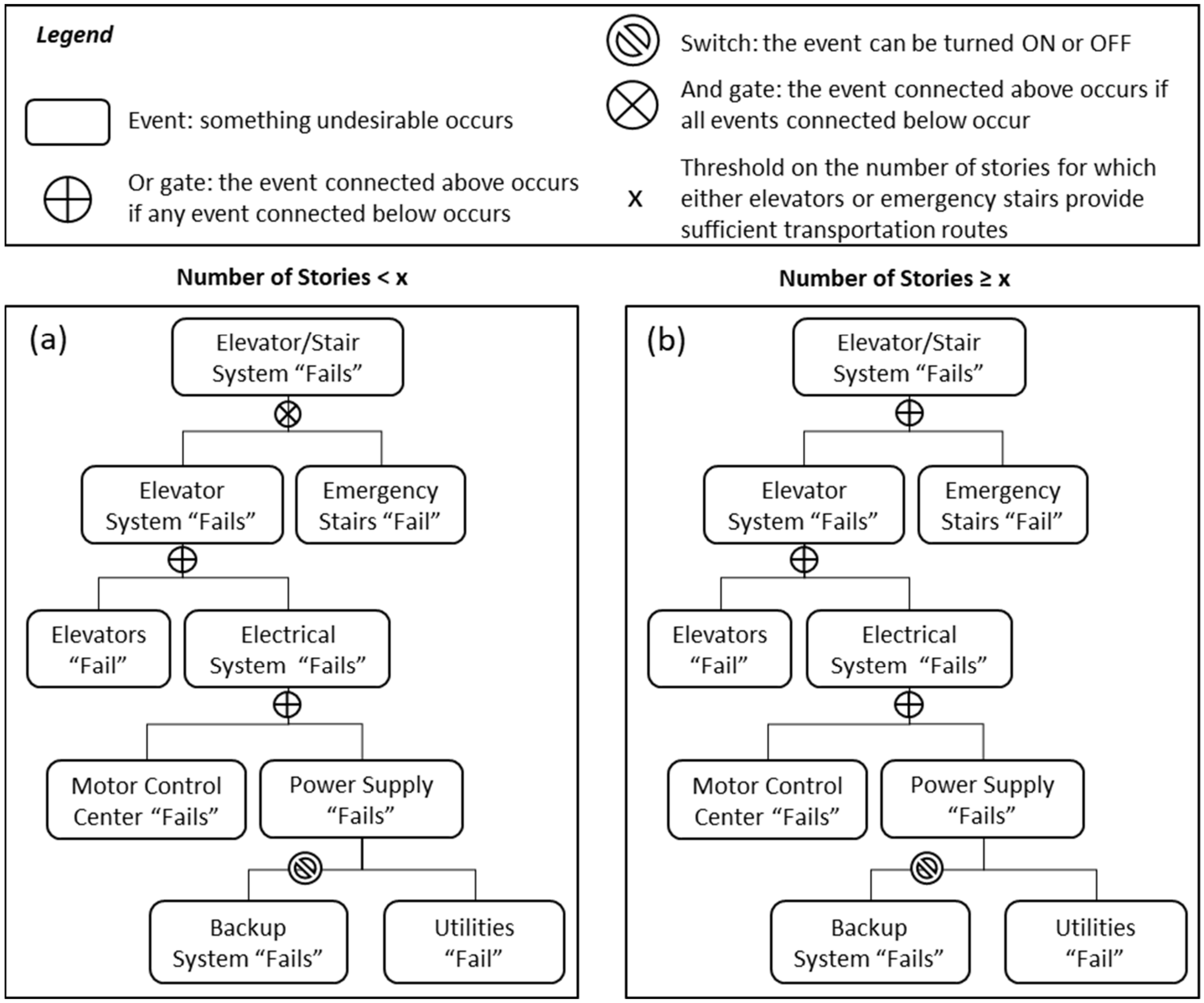

Figure 2.5 Elevator and stair system fault tree (after Terzic and Villanueva [2021]).

Plumbing and Piping Systems. The fault tree for plumbing and piping systems consists of the components presented in Figure 2.6. The purpose of the plumbing and piping system is to distribute water and other required fluids to specific parts of the building. Cold and hot potable piping typically service restrooms and sinks, heating hot water and chilled water piping distribute water from heating and chilling systems to HVAC systems or sinks and fountains, sanitary waste piping distributes waste from restrooms or sinks to sewage systems, steam piping distributes steam typically for laboratory spaces or hospitals, and fire sprinkler piping and fire sprinkler drops provide and dispense water as a fire safety system.

Components critical to the system are cold or hot potable piping, heating hot water piping, chilled water piping, sanitary waste piping, and steam piping (when present within a building). Major leakage from any of these pipes that cannot be contained or isolated can result in overall system failure and building shutdown by facilities manager or other building officials [Joshua Cichuniec, Personal Communication, February 4, 2019].

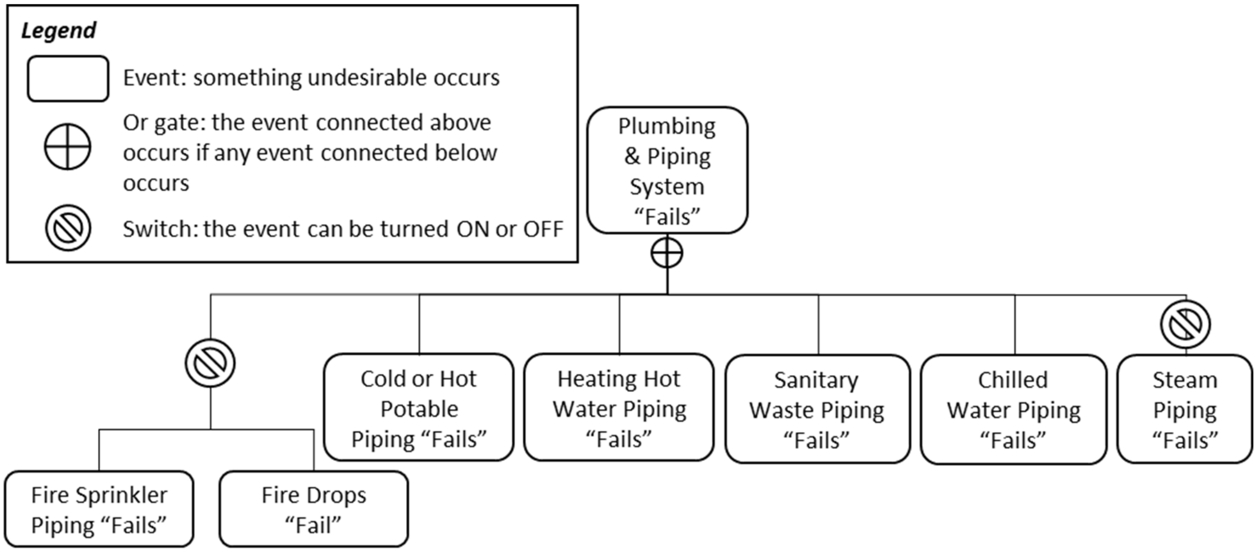

Figure 2.6 Plumbing and piping system fault tree (after Terzic and Villanueva [2021]).

Noncritical components include fire sprinkler piping and fire sprinkler drops. These components are part of a building's fire safety system, but if damaged do not necessarily stop fire safety systems from operating [Joshua Cichuniec, Personal Communication, February 4, 2019]. If fire sprinklers and drops are out of function but the rest of a building is functional, it is possible for facilities staff to conduct "fire watch" by regular building inspection for fires while fire sprinkler systems are undergoing repair. If facility managers have the aforementioned protocol in place, the fire sprinkler system can be turned off from the fault tree, otherwise it will be turned on.

Partial functionality can occur with the piping system if the effects of the piping damage can be contained within an area of the building. Minor leakage and brace failure can occur with any critical piping, resulting in a local shutdown of the affected space in the building, including the area where the leakage occurs and in rooms serviced by these piping systems. The percentage of piping that is no longer functional represents a partial loss in functionality for the piping system.

Special instances and considerations in the piping system include automatic shut off sensors and battery backup systems. There can be cases where specific piping is supported by earthquake valves that shut down at an entry point in the system [Joshua Cichuniec, Personal Communication, February 4, 2019]. Leak detection systems can also support piping but may not have the capability to shut down leaking pipes, only to alert building operators of leaks.

HVAC Systems. The fault tree for HVAC systems consists of the components presented in Figure 2.7. The primary purpose of the HVAC system is to provide ventilation; the secondary purpose is to provide air conditioning and heating if needed or desired. Air handling units (AHUs) supply air and exhaust, cooling towers support chillers in providing cool air to AHUs, boilers provide warm air to AHUs, HVAC ducting supplies air to the building's zones or designated spaces, and the electrical system consisting of motor control centers (MCCs) and power supply system provides power to the HVAC equipment [Joshua Cichuniec, Personal Communication, January 22, 2019; Predrag Nikolic, Personal Communication, September 10, 2019]. Note that power supply components are presented earlier as a part of the fault tree of the power system; see Figure 2.4. Once evaluated as a part of the power systems, the generated information about the available power supply is used within the fault tree for the HVAC system. Lastly, while some facility managers may keep the building occupied as long as ventilation is provided, others may also require air conditioning and/or heating. For this reason, heating and cooling systems can be turned on and off from the fault tree to accommodate different conditions.

While cooling is often considered a luxury, in some instances it may be critical for preserving the building's functionality. Some examples include buildings dedicated to telecommunication equipment, laboratory spaces with special chemicals and equipment, and weather conditions that affect the temperature in a building to a level that prevents occupants from using the building. Similarly, the heating system might be necessary for preserving the building function in the case of extreme cold weather. Furthermore, for spaces with critical equipment, HVAC systems are often supported by backup generators to prevent loss of power supply by utilities from shutting down critical equipment in these spaces.

Figure 2.8 shows the flowchart for calculation of the post-earthquake functionality of the HVAC subsystem when the entire building is airconditioned or heated for the case when cooling or heating systems are turned ON. The presented flowchart can be easily extended to account for other scenarios where only portions of the building are airconditioned or heated.

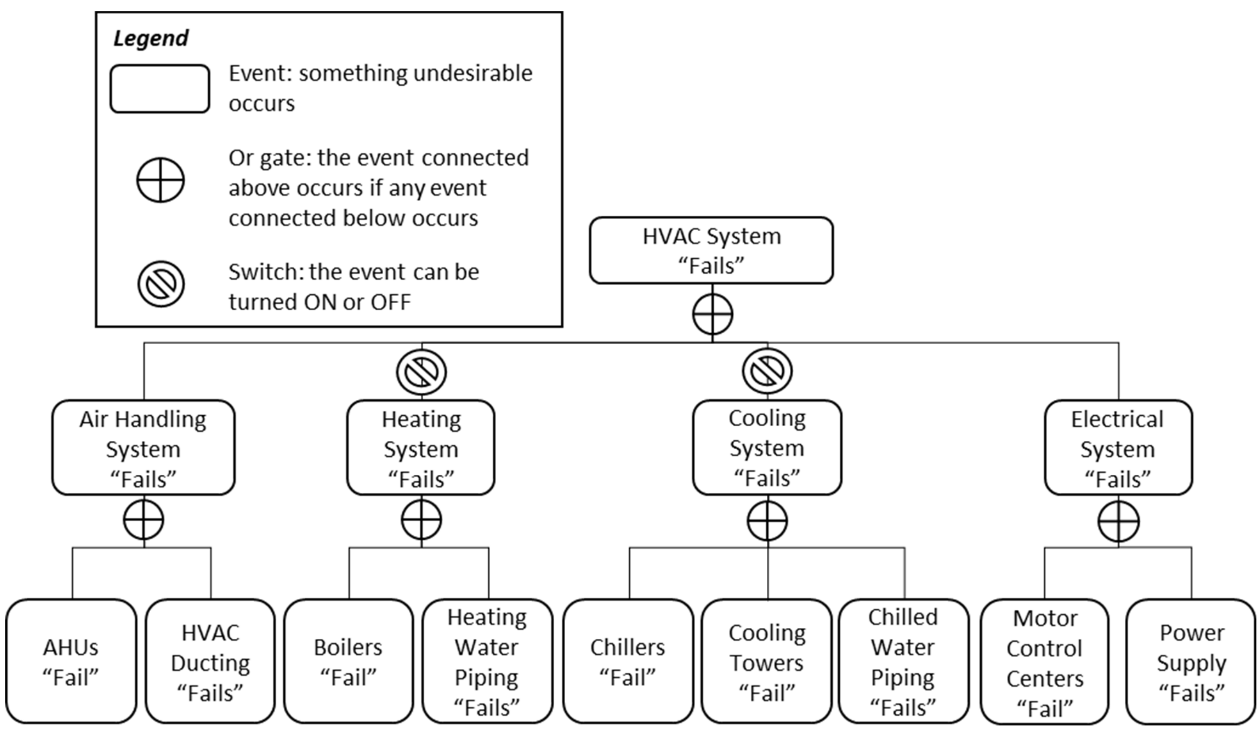

Figure 2.7 HVAC system fault tree (after Terzic and Villanueva [2021]).

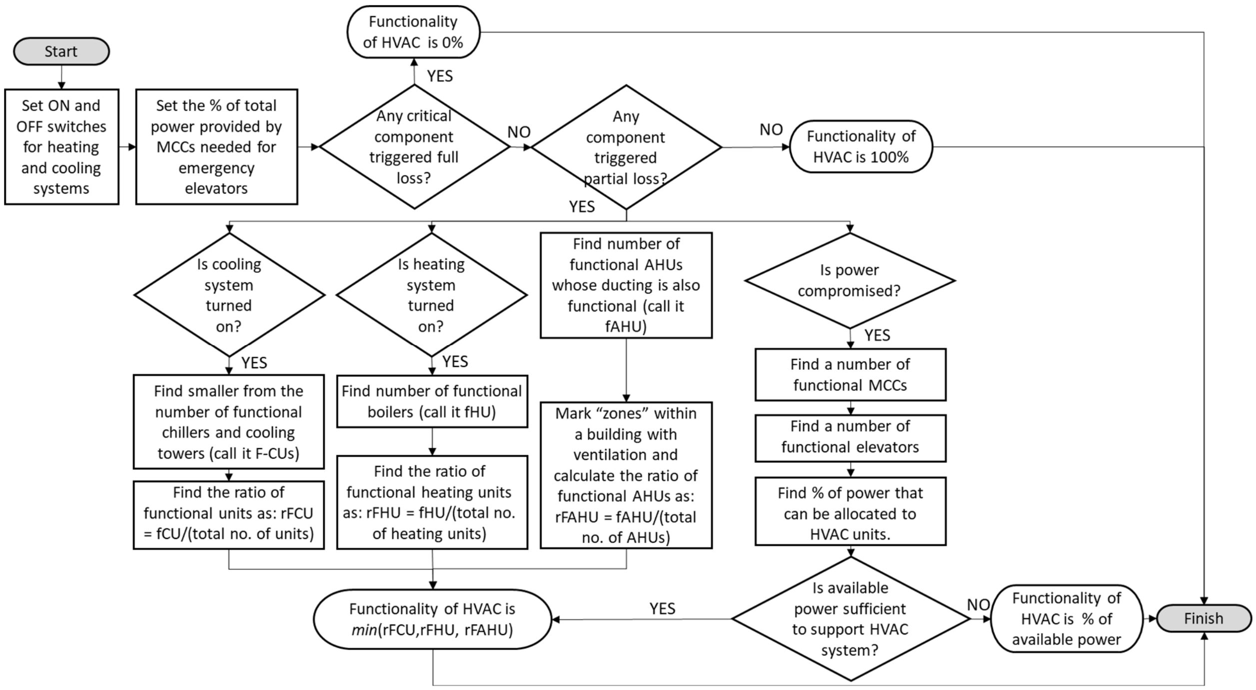

Figure 2.8 Flowchart for calculation of functionality of the HVAC system (after Terzic and Villanueva [2021]).

Following the logic of the HVAC system fault tree (Figure 2.7) and the presented flowchart (Figure 2.8), we see that if any critical component of the HVAC system fails, the entire HVAC system fails. Otherwise, if some components of the HVAC system have compromised functionality, the HVAC system may have partial functionality. This is possible since HVAC components are typically separated by the sections of the building they service or by "zones." Assuming that all "zones" cover an approximately equal amount of space within a building, we can then calculate partial functionality of AHUs as the fraction of the AHUs that are still functional. Furthermore, every functional AHU is checked to determine if the corresponding HVAC ducting is functional. If HVAC ducting of a functional AHU has failed, the corresponding "zone" cannot be ventilated; therefore, the functionality of the air handling system is further reduced.

If the cooling system is necessary for the building functionality and chilled water piping is functional, the cooling system's remaining post-earthquake capacity will be the smaller of the following: the ratio of functional chillers and ratio of functional cooling towers. Similarly, in the case when the heating system is needed to preserve the building's functionality, the heating system's partial functionality is equal to the ratio of functional boilers (assuming functional heating hot water piping). If the electric power is not compromised, the partial functionality of the HVAC system is then smaller of the air handling system functionality and cooling/heating system functionality. In addition to calculating total HVAC system functionality, functional "zones" within a building are identified and used to evaluate the functionality of individual floors.

Next, we will consider the case where the electrical system has reduced functionality. If utilities do not provide power, the HVAC system cannot operate; however, if utilities provide power but MMCs experience damage that reduce the functionality of the electrical system (e.g., 50% of units dysfunctional), the total power they provide must be split between elevators and HVAC units. Depending on the primary building function, building facility managers will have an emergency plan in place to decide how to distribute the power. For instance, their priority may be an emergency elevator that requires 20% of the total power provided by MCC, which is an input for the algorithm presented in Figure 2.8. If there is no damage to mechanical components of the elevator and power is supplied either by utilities or backup system, 20% of the power provided by MCCs is allocated to the elevator. The remaining 30% is then used for the HVAC units based on priorities. However, if the elevator sustains mechanical damage, the full 50% of the remaining power goes to HVAC units. Note that the information about number of functional elevators and the power that they require to maintain their function has been evaluated as a part of stairs and elevator subsystem and utilized when analyzing HVAC system. If the functional HVAC units need less power than what is available, the functionality of the HVAC system is unchanged from what was previously calculated. However, if HVAC units need more power than what is available, the functionality of the HVAC system is equal to the percentage of available power.

Partition Wall Systems. Partition wall systems only consist of partition walls themselves. The purpose of partition wall systems is to provide privacy or separate areas within a building. Generally, partitions are considered cosmetic to the building space except for areas where privacy is essential [Joshua Cichuniec, Personal Communication, February 4, 2019]. If utilities are located in a partition wall and the wall is damaged, such as cracking in a wall exposing piping or electrical conduits, this can pose a hazard to occupants and result in local space being shut down. Significant quantities of partition walls with warping, splitting, or cracking may indicate damage to the structural system, and the building should be shut down until confirmation that no structural damage to the building has occurred or repair of the damage has been completed. Damage to partition walls can result in the partial and full loss of functionality to a building since partition wall damage can allude to potential damage to other subsystems. If the partial loss is triggered, the percent loss in functionality for partition walls is the percent of all partition walls that are severely damaged.

Exterior Wall Systems. The fault tree for the exterior wall system consists of cladding and curtain wall components, as seen in Figure 2.9. The critical purpose of exterior walls is to protect the interior building space and occupants from the outside elements.

Both types of components are critical to the exterior wall system. If a building contains both cladding and curtain walls, both are required to have full functionality for the building to allow any occupancy. Similar to partition walls, extensive damage to cladding and curtain walls can hint of damage of the structural system. If a significant amount of damage such as cracking or warping is observed by facilities management, the building will be shut down until it is confirmed that no structural damage to the building has occurred, or repair of the damage has been completed [Joshua Cichuniec, Personal Communication, February 4, 2019].

The partial functionality of exterior wall systems is possible. The ratio of damaged exterior components is the loss in partial functionality of the system. This would represent the scenario where exterior damage is localized and only those affected areas of the building are closed.

Ceiling Systems. The fault tree for the ceiling system consists only of ceilings themselves. The main purpose of ceiling systems is to hide building infrastructure, including piping, electrical wiring, and ducting. While components of the ceiling system are not critical for maintaining the building function, fallen ceiling tiles can hint of damage to other systems located above the ceiling or rendering the floor unsafe or unoccupiable due to the fallen debris or failure of the ceiling grid system [Joshua Cichuniec, Personal Communication, February 4, 2019]. If significant ceiling damage is found after an earthquake, inspection is required before allowing occupancy, resulting in loss of functionality for the building.

If damage to the ceiling system is localized, the building will have partial loss of functionality, which is calculated as the ratio of the damaged ceiling at a floor, thereby restricting the closure only to the affected building spaces.

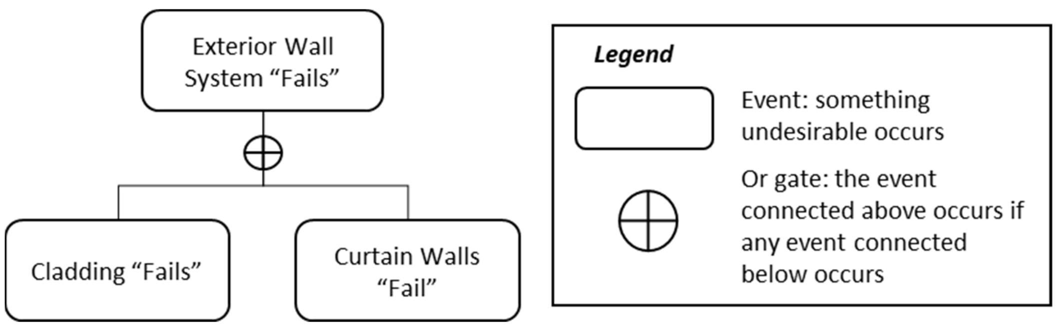

Figure 2.9 Exterior wall system fault tree (after Terzic and Villanueva [2021]).

2.2 REPAIR TIME MODEL

A comprehensive, probabilistic repair time method proposed by Terzic et al. [2016] and Yoo [2016] is based on CPM and was developed in collaboration with general contractors to realistically reflect current construction practices accounting for differences between new construction and repairing earthquake-induced damage. In this section, we will present our model as well as prior repair time models to highlight their differences.

2.2.1 Review of Repair Time Models

From all performance metrics of interest to decision-makers, repair time of the damaged building was studied the most. An overview of four major repair time models (prior to Terzic et al. [2016] and Yoo [2016] model) is presented below, including Mason et al. [2000], Porter et al. [2001], FEMA [2012], and Arup [2013], which addresses their strengths and limitations.

Optimal Strategy for Business Recovery after Earthquakes: Mason et al. [2000] proposed a methodology for choosing the best recovery strategy for a company that owns multiple income-producing properties damaged in an earthquake. The recovery is optimized by identifying recovery actions that will maximize the net asset value of the properties owned by the company. The methodology provides a comprehensive framework that can be effectively used in managing earthquake recovery operations. Given the damage states of structural and nonstructural components of company-owned units, the methodology determines the optimal repair time and optimal expenditure rate assuming the following repair schedule: all rental units are repaired in parallel, and all of the components of a unit are repaired in series. Although there may be situations that follow the repair sequence assumed in the study, the repair scheduling following an earthquake is generally more complex.

For example, suppose that company owns 10 units within the building and all need to be repaired by plumbers and drywall subcontractors. Based on the underlying assumptions of the methodology, the plumbing and drywall subcontractors will each assign 10 crews, one for each unit, with drywall crews following the plumbing crews. In case of an earthquake, there is typically a surge in labor demand, and there is a greater chance that each subcontractor will assign only one crew to do the repair of all 10 units with a drywall crew following the plumbing crew from one unit to another until the repair of all units is completed. In such a situation, the repair sequencing becomes more complex as there is a great chance that each unit will undergo different amount of plumbing and drywall damage, resulting in wait times of the successor crew.

Since the total repair time is an extremely important variable in strategizing business recovery, for the described methodology to provide reliable results, it needs to be based on a realistic repair schedule that provides a more accurate estimation of the total repair time. Without an accurate repair time estimate, the optimal asset value will be inaccurate and may lead to making decisions that will impair the business recovery.

Assembly-Based Vulnerability (ABV) Methodology: In 2001, Porter, Kiremidjian, and LeGrue introduced assembly-based vulnerability (ABV) framework for evaluating the seismic vulnerability and performance of buildings on a building-specific basis [Porter et al. 2001]. The framework is fully probabilistic and addresses damage at a highly detailed level utilizing fragility functions to simulate damage of each structural and nonstructural element in the building, and its contents. Given the damage state of building components, it uses probabilistic construction cost estimation and scheduling to estimate repair cost and "loss-of-use duration" (i.e., a repair time).

The ABV framework proposes a repair time model that is based on dividing the building into individual operational units that independently produce income, such as rental apartments, office suites, or floors. Each operational unit requires a set of critical structural, architectural, mechanical, electrical, and plumbing features to label a unit "functional." For all critical components of a unit, damage states are combined with repair duration and probability distributions to estimate the unit repair time using several simplifying assumptions:

1. Inside an operational unit, crews that are working on the same repair task work in parallel, and crews that are working on different tasks work in series;
2. Repairs are performed in a way that follows Construction Specification Institute (CSI) MasterFormat standard. For example, structural components must be completed before the start of nonstructural components;
3. Tenants cannot occupy the building until critical repairs are completed, and tenant requirements are neglected while critical components remain unrepaired;

4. Only one trade can work at a time in an operational area, which means that the next trade can only begin after that trade finishes its work;
5. A change-of-trade delay can occur depending on the size and complexity of the repair, and its delay must be considered in the duration; and
6. Repairs to different operational units can occur simultaneously if there are enough resources. The contractor has a choice to work several operational units simultaneously or sequentially.

The repair time model of ABV framework is novel as it is fully probabilistic and addresses damage at a highly detailed level. However, the underlying assumptions have several limitations. The first limitation is in the assumption that repairs are performed in an order that follows the MasterFormat divisions. This assumption does not consider the fact that building repairs are different from new construction, and that each building repair is unique. To accommodate the variability in repair schedules, the user must be able to estimate the total repair time of a building by using a flexible repair schedule that allows for an appropriate repair sequencing.

The second limitation is that tenants cannot occupy a building until all critical repairs are finished. The ABV framework does not consider that a building can be functional when there are critical components with minor damage. In such cases, an owner may keep the building as functional and avoid downtime that would result in economic losses. This limitation can be overcome using functionality limit state, as proposed by Terzic et al. [2015], Burton et al. [2015], and Terzic and Villanueava [2021], that establishes if the building is functional or non-functional during repairs.

The third limitation comes from the assumption that only one trade operates at a time in an operational area. Although the scenario can certainly occur, it is rare to see only one trade work at a time because it is neither practical nor economical for subcontractors to operate one at a time. Depending on the size of an operational area, based on repair schedule and resource availability, different subcontractors should be able to work together. While ABV framework provides a solid repair time model, the aforementioned assumptions need to be improved to provide more realistic repair time estimates.

FEMA P-58: Repair Time Estimation: The PBEE methodology has been recently adopted for general use through FEMA P-58 initiative [FEMA 2012; 2018a] by developing a comprehensive library of peer-reviewed fragility curves and associated consequence functions that consider more than 700 structural and nonstructural building components, using standard methods [Porter et al. 2001] and published data. The motivation behind FEMA P-58 was to improve the accuracy and reliability in performance-based seismic design and provide metrics for communicating performances to decision-makers. The methodology is made applicable to engineers by developing the Performance Assessment Computation Tool (PACT) that calculates repair cost, repair time, casualties, and probability of unsafe placards [FEMA 2018b].

To perform the analysis using PACT, first the user creates a performance model of a building in PACT. The performance model consists of types and quantities of all structural/nonstructural components and building contents. In addition, the user needs to provide basic building information, such as replacement cost, occupancy type, footprint, and story height. The user next provides building structural responses (e.g., maximum story drifts, maximum absolute floor horizontal velocity, maximum absolute floor horizontal acceleration, and peak residual story drifts) for earthquake hazard levels or scenarios to perform the loss analysis.

In PACT, each building component and content is associated with a fragility curve that correlates structural response to the probability of that item reaching a particular damage state. The component's damage is then related to a loss (e.g., repair cost, repair time) utilizing consequence functions. The total repair loss at a hazard level or for an earthquake scenario is then estimated by integrating losses over all components of a system. The estimation of the total repair time at a hazard level is more complex and will be described below. To account for the many uncertainties affecting calculation of seismic performance, FEMA P-58 methodology uses the Monte Carlo procedure to perform loss calculations [FEMA 2012; 2018a].

To calculate the total building's repair time, FEMA P-58 considers two bounding cases: (1) repair work on all floors begins simultaneously, i.e., in parallel; see Figure 2.10(a); and (2) repair work of different floors is performed sequentially, i.e., in series; see Figure 2.10(b)]. In addition, each bounding case is further simplified with the following two assumptions: (1) repair sequencing at each floor is assumed to be sequential resulting in a single repair task per floor; and (2) the work force is the same for all repair tasks. FEMA P-58 states: "Neither strategy is likely to represent the actual schedule used to repair a particular building, but the two extremes are expected to represent a reasonable bound to the probable repair time" [FEMA 2012; 2018a]. For the simplified and generic scheduling of repairs of FEMA P-58 repair time model to provide reasonable bounds, the resources or workers used to estimate the total duration of work are to be more realistic, and several repair trades at a floor should be allowed for the parallel repair schedule [Yoo 2016].

FEMA P-58 distributes workers based on worker density, defined as the maximum workers per square foot, recommending 0.1% if the building is occupied during repairs and 0.2% if the building is unoccupied during repairs. For example, if a building floor area is 20,000 ft^2 and worker density is selected to be 0.1%, 20 workers will be assigned to all components to be repaired in a building, regardless of the number of damaged units and their damage state. Consider a building exposed to two ground-motion intensities: (1) low intensity of shaking resulting in a minor damage of one moment connection and moderate damage of partition walls at the first floor; and (2) high-intensity shaking resulting in major damage of 15 moment connections and severe damage of partition walls at the first floor. Per FEMA P-58's repair time model, regardless of the intensity of ground shaking and associated damage, 20 workers will be first assigned to repair moment connections and another crew of 20 workers will be next assigned to repair partition walls. Such resource allocation will result in generous and unrealistic estimates of repair times, especially for systems with minor damage. It is not justifiable to allocate 20 workers to repair only one moment connection and also to allocate the same crew sizes for repair of moment connections and partition walls. The same problem will arise by assigning the same crew to all floor levels as the amount and severity of damage may differ greatly among different floor levels, especially for taller buildings. In reality, construction practices consider resource constraints that are unique to each repair activity given the amount and severity of damage in a building as well as the surge in labor demand.

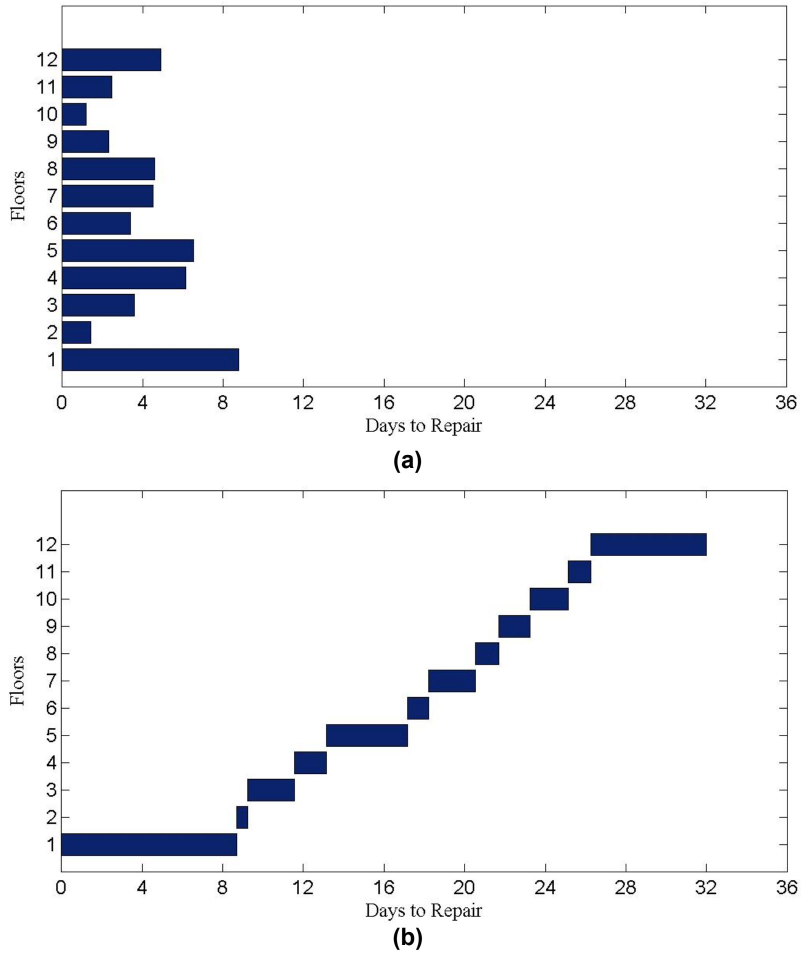

Figure 2.10 Median repair time schedule of a 12-story building: (a) FEMA P-58 parallel schedule; and (b) FEMA P-58 serial schedule (after Yoo [2016]).

In the probabilistic performance analysis, FEMA P-58's repair time model is limited to using a constant density of workers for all realizations of the Monte Carlo simulation process [FEMA 2012; 2018a]. Therefore, their repair time model does not allow for different densities of workers for cases with and without building occupants during the repair. Obviously, for some of the realizations of the Monte Carlo simulation process, there may be only minor damage that can be repaired while the building is still occupied; there also may be some realizations with major damage that will trigger building closure. To distinguish between occupied and non-occupied cases, functionality limit states should be used (e.g., Terzic and Villanueva [2021] and Burton et al. [2015]).

In FEMA P-58's repair time model, the assumption that only one trade operates at one floor level, although possible, is rare to see as it is neither practical nor economical for subcontractors to operate one at a time (e.g., repair of cladding, stairs, and partition walls can occur simultaneously at one floor level). Depending on the size of the floor area, type and amount of damage, and resource availability, different subcontractors should be able to work together.

Arup's REDi™ Rating System: Repair Time Model: Resilience-based Earthquake Design Initiative (REDi™) Rating System [Arup 2013] proposes a framework for owners, architects, and engineers to implement "resilience-based earthquake design." It describes design and planning criteria to enable owners to resume business operations and provide livable conditions quickly after an earthquake, according to their desired resilience objectives. The REDi™ Rating System utilizes downtime as one of the performance metrics in its "resilience-based earthquake design." For that purpose, they have developed a downtime model that complements FEMA P-58 methodology. An integral part of their downtime model is a repair time model that addresses some of the limitations of FEMA P-58 repair time model. However, the REDi™ repair time model still has numerous limitations: fixed repair schedule, unrealistic labor allocation, and erroneous repair time procedure.

REDi™ adapted a new repair sequence by abandoning the FEMA P-58's parallel and serial scheduling. In REDi™, components are organized into seven different groups and the groups are divided into structural, interior repairs, exterior repairs, mechanical equipment, electrical systems, elevators, and stairs, as shown in Table 2.2. Interior repairs consist of pipes, HVAC distributions, partitions, and ceiling tiles. Exterior repairs consist of exterior partitions and cladding or glazing.

Table 2.2 Component subgroups described in Arup's REDi™ [2013].

Repair Sequences	Components	Number of Workers (per ft^2 or damaged units)
Structural	Structure	1 worker/ 500 sf
Sequence A	Pipes/ Sprinkler HVAC distribution Partitions Ceilings	1 worker/ 1000 sf
Sequence B	Exterior Partitions Cladding/Glazing	1 worker/ 1000 sf
Sequence C	Mechanical Equipment	3 workers/damaged unit
Sequence D	Electrical Systems	3 workers/damaged unit
Sequence E	Elevators	2 workers/damaged unit
Sequence F	Stairs	2 workers/damaged unit

The key assumptions in REDi™ methodology are that all structural components within a building need to be finished repairing before the start of nonstructural repair. Repair of both structural and nonstructural repair will be scheduled only one floor at the time starting from the bottom. It is also assumed that temporary elevators are available at the beginning of a project to accommodate materials and equipment during structural repairs of a building. Repair of components within a group are all sequential and the relationships between the established groups are fully fixed with no option of regrouping the repair tasks. Although organizing all components into its groups can be useful, it inhibits flexibility in scheduling. For example, components inside a structural group can never work in parallel. In 1994 Northridge earthquake, moment connections and shear-tab gravity connections of damaged moment frames were typically repaired simultaneously [Yoo 2016]. In the same earthquake, the repair of nonstructural damage would typically start as soon as the structural damage was fixed at the bottom few floors. It was also very common to start the repair of stairs and elevators simultaneously with any other structural repair to provide enough routes for transportation of labor and material. Obviously, every repair work is unique and repair sequencing may vary based on workers availability, labor congestion, and desired recovery speed specified by the decision-makers. To accommodate different situations, it is important that repair tasks are considered independently rather than in groups and that flexible relationships exist between them, both within a floor level and along the building height.

In REDi™, the labor allocation is addressed by introducing labor distributions that are either based on square footage or number of damaged units (Table 2.2), capped by the total number of workers allocated to the project. For repair of structural components, that start first and are the only trade at the time, they use a metric of 1 worker per 500 ft^2. The selected metric aligns with FEMA P-58 recommendation for the workers density of unoccupied building of 0.2%. Nonstructural components that belong to Sequences A and B are based on 1 worker per 1000 ft^2 because the two sequences can occur simultaneously, resulting in the total worker density of 0.2%. Repair of sequences C through F is based on an average number of damaged units.

In comparison to FEMA P-58 labor allocation, structural components, pipes, HVAC distribution, partition, ceiling, cladding, and glazing are treated the same, considering the square footage of a floor area. For example, for the floor area of 20,000 ft^2 regardless of the amount of damage and number of damaged units, 40 workers will be assigned for the repair of every structural component, and 20 workers will be assigned for the repair of every aforementioned nonstructural component (Sequences A and B). In reality, contractors assess the amount of building damage and allocate labor based on a number of damaged units and their damage states, expected deadline set by the stakeholders, and resource limitations. Therefore, a building with a slight damage will utilize significantly smaller work force than a building with an extensive amount of damage. Furthermore, in REDi, the labor allocation for damaged equipment is based on the number of damaged units; e.g., mechanical equipment requires three workers for every damaged unit (Table 2.2). For example, while REDi model would assign 12 workers for a repair of four damaged air handling unit, in reality one crew of two or three workers will be sent to repair all four units.

Finally, per REDi™ document, the median repair time is calculated based on the following procedure:

1. Add direction 1 and 2 repair time values for each drift-sensitive component for each realization;
2. Obtain median (or desired probability of non-exceedance) loss for each component at each floor level;

3. At this point, the data has been filtered such that repair times are displayed for each component at each floor level only; and
4. The total repair time estimates are computed by dividing the total number of "worker-days" per floor by the number of workers allocated to each floor and then repairs across all floors are assumed to occur either simultaneously or only once the repairs on another floor are completed, starting from the lowest level.

The repair time calculated following this procedure is erroneously labeled as a median repair time. The reason is that the median repair times of each component at each floor level are combined using the repair schedule, generating a result where each component outcome is associated with a different realization of the Monte Carlo simulation process as demonstrated in Figure 2.11 Filtering of data in REDi™ procedure. Median values (repair times) of components A, B, C belong to different realizations of the Monte Carlo simulation process (after Yoo [2016]). The correct procedure in calculating the median repair time requires a generation of cumulative distribution functions (CDF) for repair times by utilizing the repair scheduling method for each realization of the Monte Carlo simulation procedure and the usage of the CDF to calculate the median repair time.

	Repair Times in days		
	Realization 1	Realization 2	Realization 3
Component A	1	6	3
Component B	1	2	4
Component C	4	3	6

Figure 2.11 Filtering of data in REDi™ procedure. Median values (repair times) of components A, B, C belong to different realizations of the Monte Carlo simulation process (after Yoo [2016]).

Summary about Existing Repair Time Models: It is obvious from studies by Mason et al. [2000] and Cimellaro et al. [2010] that the estimation of the repair time is crucial in measuring the resiliency of a building. In addition, an accurate estimation can facilitate the stakeholders by providing reliable data for optimal business decisions. The repair time models of ABV framework, FEMA P-58, and REDi™ are all based on sets of simplifying assumptions that are not in agreement with the current construction practice. There is an obvious need for a robust repair time model applicable to different building sizes and occupancies that will allow for realistic repair and resource scheduling.

2.2.2 Proposed Repair Time Model

A comprehensive, probabilistic repair time model by Terzic et al. [2016] and Yoo [2016], which is one of the constituents of the recovery model, was developed in collaboration with general contractors to realistically reflect current construction practices accounting for differences between new construction and repairing earthquake-induced damage. While the repair activities and amount of resources in new building construction are likely to remain constant throughout the building, the repair tasks and resources assigned to each repair activity are likely to be different for each floor of the damaged building. This disparity in damage is due to the sporadic nature of earthquake-induced destruction. Additionally, in such situations, the available repair space is typically limited thus slowing down the construction process and reducing productivity. If an earthquake impacts a large urban area, the number of available workers may be reduced due to a surge in construction demand.

Unlike the currently available repair time models that are based on fixed repair schedules [Mason et. al. 2000; FEMA 2018a; and Arup 2013] and predetermined work-force irrespective of the amount and severity of damage [FEMA 2018a; Arup 2013], Terzic et al.'s [2016] and Yoo's [2016] model is highly flexible and has the following capabilities: (1) it is applicable to any building size, occupancy type, and ground shaking intensity; (2) it can accommodate any repair schedule; (3) it optimizes the work-force based on the amount and severity of damage on building components; and (4) it allows for resource scheduling that meets resource limitations that can either come from labor congestions or from a surge in demand following a disaster. Our repair time model is schematically presented in Figure 2.12 and consists of two components: (1) Repair Scheduling and (2) Resource Scheduling. Repair scheduling can accommodate any repair sequencing and considers realistic labor allocations; whereas resource scheduling provides an efficient way of reducing workers during labor congestions while minimizing its prolonging effect on the project duration.

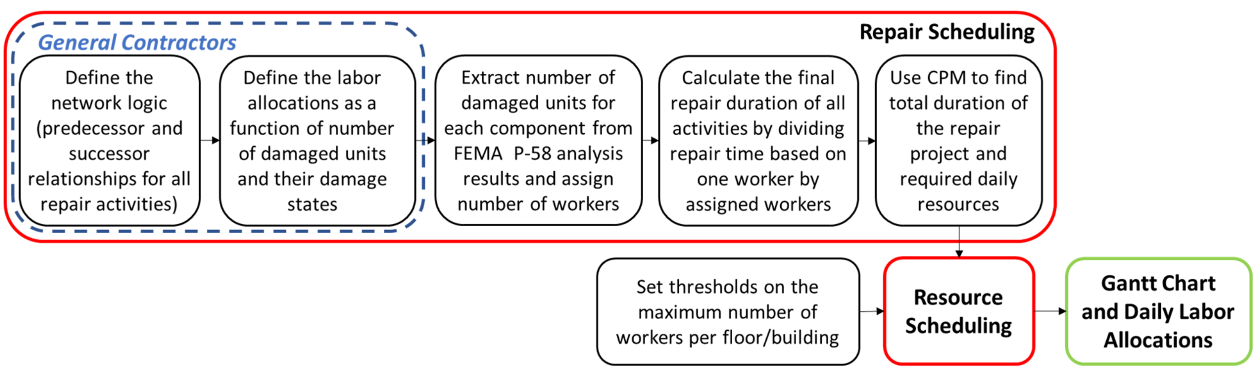

Figure 2.12 Schematics of repair time model for one realization of the Monte Carlo simulation process of FEMA P-58 assessment (after Terzic et al. [2021]).

The Terzic et al. [2016] repair time model uses as its inputs the logic network for repair project and labor allocations for different repair activities. The logic network for repair project is set by defining predecessor and successor relationships for all repair activities and by defining the number of floors repaired simultaneously for each repair activity; hence allowing for great flexibility in scheduling repair. Labor allocations are defined based on the severity and extent of damage to building components. For every building component, the number of damaged units and its damage state are extracted from FEMA P-58 analysis results and used to allocate realistic labor. These labor allocations are used to calculate repair durations of repair activities as repair times extracted from FEMA P-58 analysis results are based on one worker per repair activity. Repair times of all damaged components are next utilized within CPM to find the total duration of the repair project and required daily labor resources (as presented in Section 2.2.2.1). If required daily resources exceed daily resource limits that may arise from labor congestion issues and/or resource-limited conditions, the proposed resource scheduling method would "stretch" the repair durations of congested activities by iteratively reducing the number of workers until resource limits are met (as presented in Section 2.2.2.2). To minimize the impact of activity-stretching on the project duration, this method identifies and prioritizes activities based on their repair durations. An activity with the shortest repair time and the longest free float will be the first in line to which resource reduction will be applied. When reducing demand on resources, a minimum threshold is set for each activity to ensure that the number of workers is not below the smallest size of the crew required for the repair. An example of a generic 3-story building (provided Section 2.2.2.3) fully demonstrates the application of described methods for repair scheduling and resource scheduling. The main outcomes of the method are a repair time fragility function, Gantt chart for a selected realization, and daily resource allocations. Importantly, the Gantt chart can convey a multitude of useful information including the total repair time of the project, repair path, and repair activities that dominate the repair process. Examples of logic networks and labor allocations as a function of the severity of damage to building components are generated in collaboration with general contractors and presented and used in several case studies [Yoo 2016; Terzic and Mahin 2017; Terzic et al 2018; Kolozvari et al. 2018; Garza et al. 2018; and Terzic et al. 2021].

The proposed repair time model can be used in two ways: (1) to find the total repair time associated with all damaged components (stand-alone); and (2) to find the repair time and repair path associated with damaged components that can impair building operation (in conjunction with FLS). While its first application provides a complete picture of the repair process, the second application focuses on the functional recovery process. The case study presented in Section 3, is an application of the proposed repair time model in conjunction with FLS to find the repair time and repair path associated with damaged components that impair building operation.

2.2.2.1 Repair Scheduling Method

Our new repair scheduling method for earthquake-damaged buildings is based on the Critical Path Method (CPM) and requires input from general contractors. This scheduling method is based on several assumptions common for construction scheduling:

- The repair activities are time-continuous, thus once started they cannot be interrupted;
- The resource assignments for each repair activity are assumed constant throughout the duration of the activity;
- The project’s logic network is constant throughout all floors; and
- All activities are based on the Finish to Start (FS) relationship.

This new method was developed to complement the probabilistic seismic performance assessment methodology of FEMA P-58. Therefore, the repair scheduling method requires the user to: (1) create a performance model of a building by specifying the types and quantities of all structural and non-structural components, and building contents; (2) provide building structural responses (e.g., maximum story drifts, maximum absolute floor horizontal velocities, maximum absolute floor horizontal accelerations, peak residual story drifts) for earthquake hazard levels or scenarios for which the loss analysis is to be performed, and (3) execute performance analyses to generate necessary input data for repair time estimation including repair time durations, number of damage units, and damage states for all building components. Currently there are two available tools for performance assessment of buildings: Performance Assessment Computation Tool (PACT) [FEMA 2018b] and NHERI-SimCenter PBE tool [2019]. Repair time durations in these performance assessment tools are based on the metric of 1 day per 1 worker. Depending on the severity and amount of damage, the repair time durations generated by the tools are to be modified using realistic labor allocations. For each building component, the labor allocation is determined based on the severity of damage considering the average damage state of a component and the amount of damage reflected by the number of damaged units.

The repair scheduling method employed for calculation of the repair time of an earthquake-damaged building is presented below; see Figure 2.12 for the flow chart:

Step 1: Set the logic network for repair by defining predecessor and successor relationships for all repair activities and defining the number of floors repaired simultaneously for each repair activity.

Step 2: Import the following information from PACT or PBE tool: repair time durations, number of damaged units (NDU), and corresponding damage states (DM) for all components at every floor for all realizations of the Monte Carlo simulation process within FEMA P-58 loss assessment methodology.

Step 3: Calculate the average damage states (ADS) of all repair activities at each floor for all realizations. An average damage state of a building component is calculated as follows:

$$\text{ADS} = \frac{\sum_1^k n_i DM_i}{n} \tag{1}$$

where n is the total number of units associated with a particular component of one floor level, k is the total number of damage states of that component, and n_i is the number of units in the damage state i.

Step 4: For each component at every floor level and all realizations, allocate the number of required workers commensurate to the average damage state (ADS) and the number of damaged units (NDU). The ADS establishes the size of each crew, while NDU establishes the number of required crews. The total number of workers is then determined as a multiple of the number of crews and the number of workers within each crew. Table 2.3 shows an example of a possible work allocation scenario for building component A. In this example, if the ADS is less than 1, two workers are assigned; if the ADS is greater than 1, three workers are assigned for each crew. Then, the number of crews is determined based on NDU. Consider the following scenarios: (1) if there are 20 damaged units with ADS < 1, two crews of two workers each will result in total of four workers; and (2) if there are 21 or more damaged units with ADS > 1, three crews of three workers each will result in a total of nine workers. For a realistic labor allocation, it is recommended that the user populate Table 2.3 in consultation with a general contractor.

Table 2.3 Sample of worker allocations.

Component Names	Workers per Crew (Based on ADS)			Total workers based on NDU and ADS		
				# of damaged units in a floor		
	ADS < 1	1 < ADS < 2	2< ADS < 3	1 - 10	11 - 20	21 - 30
Component A	2	3	3	1 Crew	2 Crews	3 Crews

Step 5: Calculate the final repair durations of all activities by dividing the total repair durations by the number of workers assigned in Step 4.

Step 6: For each realization of the Monte Carlo simulation procedure, use the repair logic network along with the final repair times of all activities to calculate the duration of building repairs based on the following procedure. First, use the predecessor relationships and the repair time durations to calculate the starting and finish dates of all activities. When there are multiple predecessors, a predecessor with a greater finish date is set as the start date of an activity. Start dates and finish dates of a component *N* are calculated as follows:

$$\text{Start Date}_{N,floor\#} = \max(\text{Finish Date}_{Predecessor,N}) \tag{2}$$

$$\text{Finish Date}_{N,floor\#} = \text{Start Date}_{N,floor\#} + \text{Duration}_{N,floor\#} \tag{3}$$

Second, calculate Free Float (FF) of each activity using successor relationships and a forward pass. Free float of a component is calculated as:

$$\text{FF}_{N,floor\#} = \text{Start Time}_{Earliest\ Successor,N} - \text{Finish Time}_{N,floor\#} \tag{4}$$

Third, begin resource scheduling (to be described in a separate section). Finally, determine the critical path and the total duration of the repair project.

Step 7: Generate cumulative distribution functions (CDF) associated with the duration of the repair project, i.e., repair time.

Step 8: For a selected realization (e.g., median, mean) plot the start dates and finish dates for all activities at all floors including roof level to determine the repair path.

2.2.2.2 Resource Scheduling Method

The resource scheduling method presented herein is designed to address labor congestion issues and/or resource-limited conditions that may arise during repair of earthquake-induced damage of an occupied or non-occupied building. These repair constraints arise either from a limited available space or a surge in labor demand after a disaster. In cases involving limited available space, the maximum worker density can be determined by following FEMA P-58 recommendations and by utilizing the building's functionality limit state (e.g., Terzic and Villanueva [2021]; Burton et. al. [2015]).

This resource scheduling method utilizes the aggregation approach to determine daily resources or labor allocations throughout project duration by aggregating the daily resources used in all activities. If required daily resources exceed daily resource limit, the proposed method would "stretch" the repair durations of congested activities by iteratively reducing the number of workers until resource limits are met. To minimize the impact of activity-stretching on the project duration, this method identifies and prioritizes activities based on their repair durations. An activity with the shortest repair time and the longest free float will be the first in line for consideration of resource reduction. When reducing demand on resources, a minimum threshold is set for each activity to ensure that the number of workers is not below the smallest size of the crew required for the repair.

The resource scheduling method is based on the assumptions adopted from Packing Method for Resource Leveling (PACK) by Harris [1978], commonly used by construction managers; however, these assumptions have been modified according to the requirements of repair construction:

- Resources applied to each activity at each floor are assumed to remain constant throughout the duration of each activity. If the resource constraints are not met, resources are changed in an iterative manner;
- Duration of each activity is assumed to remain constant. If a daily sum of resources exceeds the daily total resource limit, durations are revised in an iterative manner; and
- The project's terminal date is assumed fixed. If the resource constraints cannot be met by keeping the terminal date fixed, the project's terminal date is changed accordingly.

Implementation of the resource scheduling method at any one time applies to one floor and one realization of the Monte Carlo simulation process. This implementation should follow the steps described below as depicted in the flow chart of Figure 2.13:

Step 1: Aggregate a total number of daily resources (workers) associated with each activity during the lifetime of a project.

Step 2: If the daily resources throughout a project never exceed the daily resource limit, the resource scheduling method is terminated. Otherwise, proceed to Step 3.

Step 3: If there are any instances in which the daily resources exceed the daily resource limit, find all the intervals in which such excesses occur. In each interval where the limit of resources is exceeded, identify the activities that contribute to this excess.

Step 4: For each interval that exceeds the threshold, prioritize and sort the identified activities based on their repair durations in ascending order.

Step 5: From this sorted list of repair activities, eliminate all activities that operate with only one crew, since such activities cannot be reduced any further.

Step 6: The first activity in the list of the remaining activities will have the shortest repair time (or the longest float) and will be the activity to which resource reduction will apply by reducing its work force by one crew.

Step 7: Following the resource reduction, total daily resources will be reassessed and compared to the daily resource limit. If there are still extra resources that cause congestion, return to Step 4 using the revised repair time of the activity with reduced resources and the revised list of activities per Step 5. Continue Steps 4 through 7 until the resource limit is satisfied.

Step 8: Stretch repair durations of contributing activities by using reduced workers to estimate the final repair time utilizing the CPM.

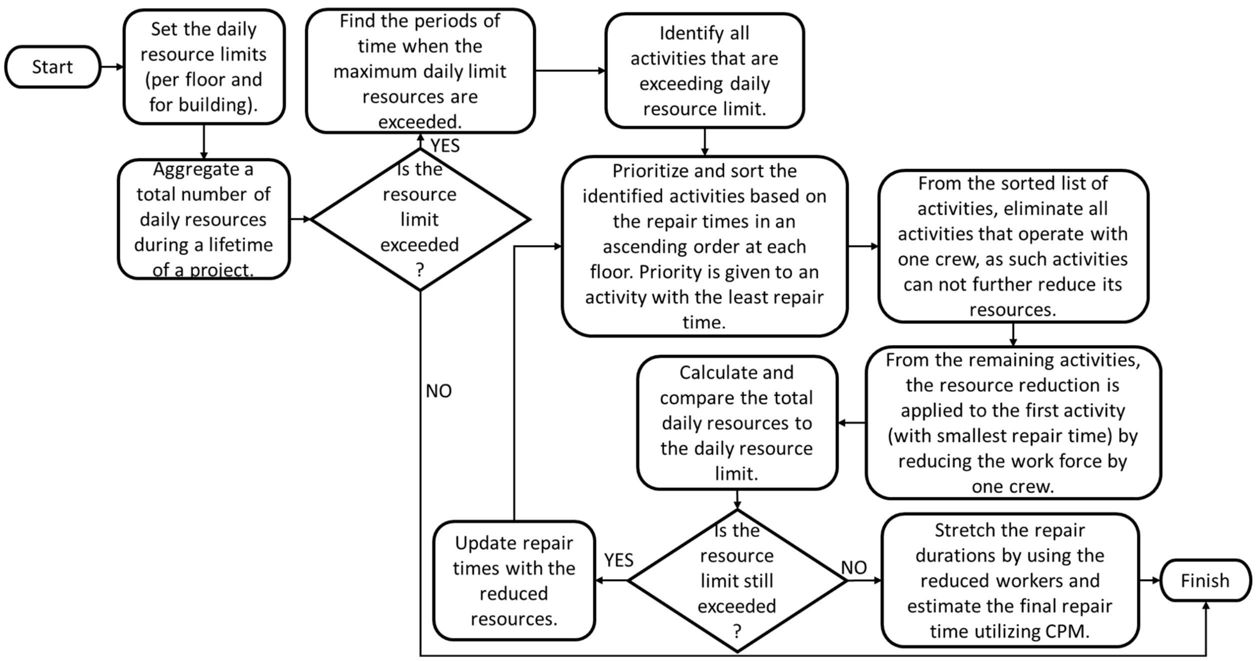

Figure 2.13 **Flowchart for resource scheduling for one realization of the Monte Carlo simulation process of FEMA P-58 assessment (after Terzic et al. [2021]).**

2.2.2.3 Repair Time of a Generic 3-Story Building

To demonstrate the versatility of our repair time method, a generic three-story building with three structural and seven nonstructural components is presented. The repair durations and resources are arbitrarily assigned to avoid a building-specific discussion. Repair Activities A, B, and C are associated with structural components, while Activities D through J are related to nonstructural components (Figure 2.14), with Activity J being the only nonstructural component at the roof level. Structural components are repaired simultaneously at all three floors, and nonstructural components are repaired sequentially one floor at a time. It is assumed that nonstructural repair at a floor level can start following the completion of structural repair at that floor level. The dependencies and inter-relationships among all activities throughout the building are shown in Figure 2.15 in the form of an activity-on-node diagram. The initial parameters of repair scheduling, including the predecessors, successors, and a number of floors being repaired simultaneously for each activity are presented in Table 2.4.

To use the repair scheduling method in conjunction with FEMA P-58, repair durations (work day/(1 worker)), damage states (DM), and the number of damaged units (NDU) need to be extracted from PACT. Then, the average damage states (ADS) are calculated for each activity at each floor, as the number of workers for all activities is assigned based on ADS and NDU. In this generic example, NDU and DM are not available and, consequently, the number of workers cannot be assigned in this manner. To demonstrate the flexibility of the repair scheduling method, repair durations and resources are assigned arbitrarily for all activities; see Table 2.5. For example, structural Activities A, B, and C require a constant number of workers per crew, and all three floors are repaired simultaneously. In contrast, for the nonstructural activities, each crew consists of varying number of workers and only one crew is assigned to repair each floor sequentially.

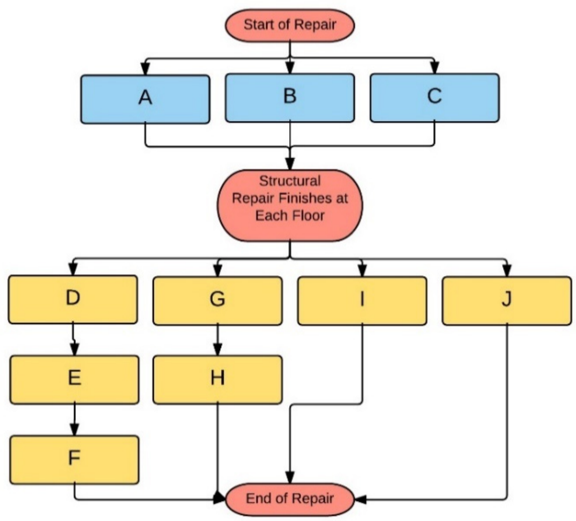

Figure 2.14 Repair schedule of a generic 3-story building (after Terzic et al. [2016]).

Table 2.4 Initial parameters of all repair activates (after Terzic et al. [2016]).

Activity ID	Activity name	Predecessors	Successors	Floors repaired simultaneously
1	A	-	4, 7, 9, 10	3
2	B	-	4, 7, 9, 10	3
3	C	-	4, 7, 9, 10	3
4	D	1, 2, 3	5	1
5	E	4	6	1
6	F	5	-	1
7	G	1, 2, 3	8	1
8	H	7	-	1
9	I	1, 2, 3	-	1
10	J	1, 2, 3	-	1

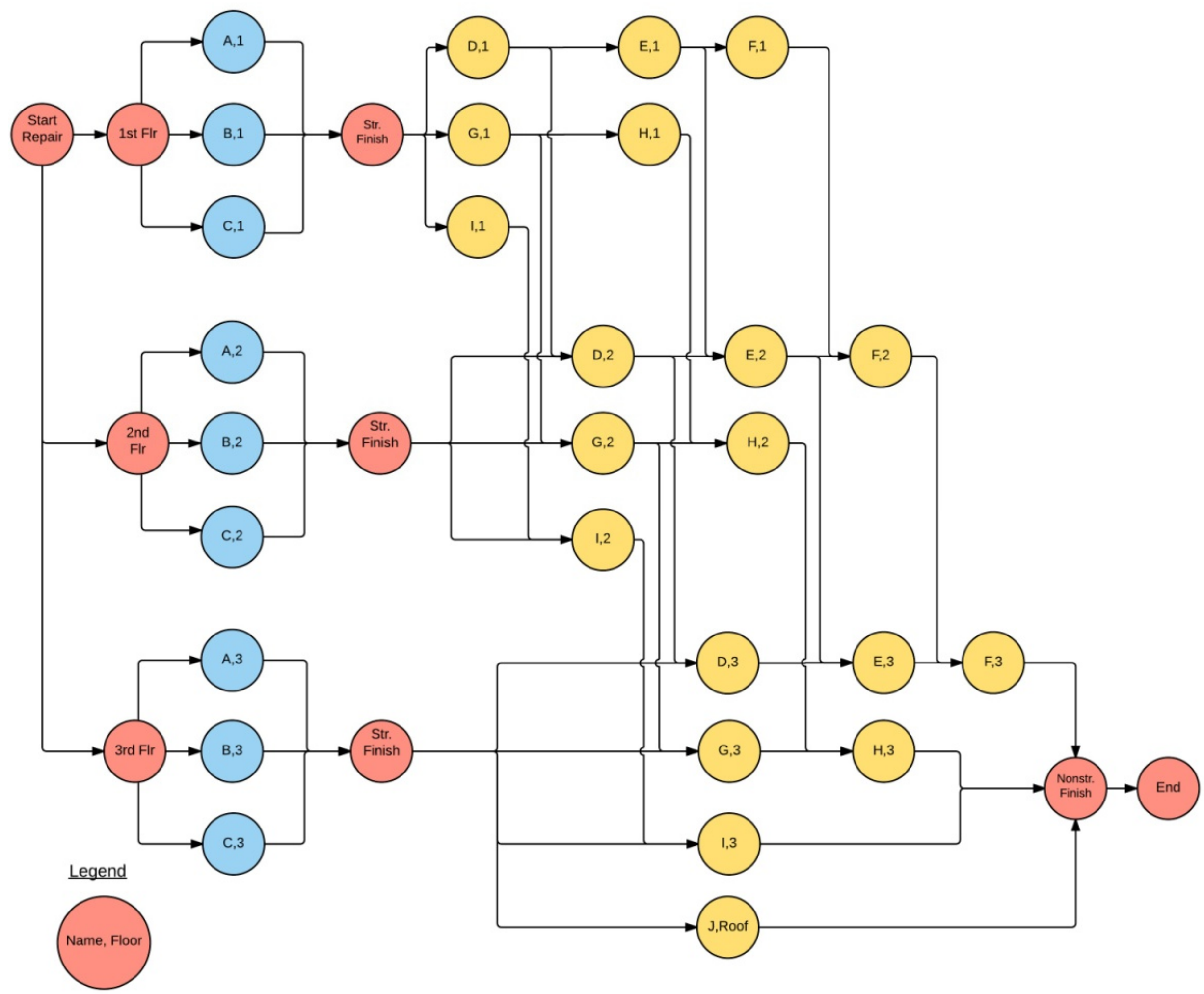

Figure 2.15 Activity-on-node diagram of a generic 3-story building (after Terzic et al. [2016]).

The initial parameters listed in Table 2.4 and the repair duration and resources of Table 2.5 are fed into the CPM to establish start dates, finish dates, and floats of all repair activities. Final durations of all activities are shown in Table 2.6; the start dates, finish dates, and floats are shown in Table 2.7. For example, structural Activities A, B, and C occur simultaneously at all three floors with a start date of 0 days. Duration of Activity A at the first floor is (160 days)/(4 workers) = 40 days, thus its finish date is 0+40=40 days. Similar calculations are performed for Activities B and C. The start date of nonstructural repair activities is governed by the larger of the two following dates: (1) the finish date of the same activity on the floor below, and (2) the finish date of the predecessor activity on the same floor. Activity D is the first nonstructural component that follows the repair of structural components. The start date of Activity D on the first floor is the date of the last structural repair on that floor. Since Activity A is the last one to be completed after 40 days, the start date of Activity D on the first floor is 40 days. Duration of Activity D on the first floor is (18 days)/(1 worker) = 18 days, thus its finish date is 40+18=58 days.

As shown in Table 2.7, the start of Activity D on the second floor is determined either by the finish of structural components on the second floor or the finish of Activity D on the first floor. In this case, the start date of Activity D on the second floor is governed by the finish of Activity D on the first floor at 58 days. Duration of Activity D on the second floor is (20 days)/(1 worker) = 20 days, producing the finish date of 58+20=78 days. Activity E is a successor of Activity D, with its start date on the first floor being governed by the finish date of Activity D at 58 days. Duration of Activity E on the first floor is (40 days)/(2 worker) = 20 days, providing a finish date of 58+20=78 days. The start date of Activity E on the second floor is governed either by the finish date of Activity E on the first floor or the finish date of Activity D on the second floor. In this particular example, the finish dates of these two activities are the same. Therefore, the start date of Activity E on the second floor is 78 days. Using the CPM, the user can quickly calculate the start and finish dates of all activities.

The repair schedule of this generic 3-story building is displayed by a Gantt chart; see Figure 2.16(a). The chart shows that the structural components A, B, and C occur simultaneously at the beginning of the project for all floors. As soon as the repair of the governing structural component (Activity A) is finished on the first floor, the repair activities of nonstructural components D, G, and I begin simultaneously on the first floor. Repair Activity J located on the roof starts upon completion of all structural repairs within the building. The critical path of this repair is associated with activities A, D, E, and F. Components B, C, and H have free floats (FF) available to extend or stretch if the labor congestion requires the use of the resource scheduling method.

Table 2.5 Repair duration and resources (number of workers) of each repair activity (after Terzic et al. 2016).

Activity ID	Activity Name	Repair Duration (work days / 1 worker)			Resources (workers) (Based on ADS and NDU)		
		Floor 1	Floor 2	Floor 3	Floor 1	Floor 2	Floor 3
1	A	160	92	120	4 (1 crew)	4 (1 crew)	4 (1 crew)
2	B	150	100	136	4 (1 crew)	4 (1 crew)	4 (1 crew)
3	C	200	112	140	8 (2 crews)	4 (1 crew)	4 (1 crew)
4	D	18	20	10	1 (1 crew)	1 (1 crew)	1 (1 crew)
5	E	40	10	20	2 (1 crew)	2 (1 crew)	2 (1 crew)
6	F	90	20	57	3 (1 crew)	3 (1 crew)	3 (1 crew)
7	G	40	80	68	7 (1 crew)	7 (1 crew)	7 (1 crew)
8	H	60	16	20	3 (1 crew)	3 (1 crew)	3 (1 crew)
9	I	38	18	20	2 (1 crew)	2 (1 crew)	2 (1 crew)
10	J	0	0	26	2 (1 crew)	2 (1 crew)	2 (1 crew)

Table 2.6 **Repair durations, resources (number of workers), and final durations (after Terzic et al. [2016]).**

Activity ID	Activity name	Repair durations (Days / 1 worker)			Resources			Final repair duration		
		Floor 1	Floor 2	Floor 3	Floor 1	Floor 2	Floor 3	Floor 1	Floor 2	Floor 3
1	A	160	92	120	4	4	4	40	23	30
2	B	150	100	136	4	4	4	38	25	34
3	C	200	112	140	8	4	4	25	28	35
4	D	18	20	10	1	1	1	18	20	10
5	E	40	10	20	2	2	2	20	5	10
6	F	90	20	57	3	3	3	30	7	19
7	G	40	80	68	7	7	7	6	12	10
8	H	60	16	20	3	3	3	20	6	7
9	I	38	18	20	2	2	2	19	9	10
10	J	0	0	26	2	2	2	0	0	13

Table 2.7 **Strat dates, finish dates, and free floats of all repair activities (after Terzic et al. [2016]).**

Activity ID	Activity name	Start Ddate			Finish date			Free float		
		Floor 1	Floor 2	Floor 3	Floor 1	Floor 2	Floor 3	Floor 1	Floor 2	Floor 3
1	A	0	0	0	40	23	30	0	17	10
2	B	0	0	0	38	25	34	2	15	6
3	C	0	0	0	25	28	35	15	12	5
4	D	40	58	78	58	78	88	0	0	0
5	E	58	78	88	78	83	98	0	5	17
6	F	78	108	115	108	115	134	0	0	0
7	G	40	46	58	46	58	68	0	0	4
8	H	46	66	72	66	72	79	0	0	55
9	I	40	59	68	59	68	78	0	0	56
10	J	NA	NA	40	NA	NA	53	0	0	81

The resource histogram of the repair schedule is presented in Figure 2.16(b) using the aggregation method. To demonstrate the use of the proposed resource scheduling method, the daily resource limit is arbitrarily set to 12 workers. It is evident from the resource histogram that the daily limit is only exceeded on the first floor during the first 25 days of repair, while repair Activities A, B, and C were operating at that time. Once the above activities are identified, they are prioritized from shortest to longest duration, with Activity C being recognized as the one having the shortest repair time, followed in ascending order by Activities B and A.

In the next step, activities are eliminated if any of the sorted activities operates with one crew. In this example, structural components A and B are operating with only one crew, consisting of four workers; therefore, they are eliminated from the resource reduction process because such resources cannot be reduced any further. Among the three activities under consideration, the only activity to which the resource reduction can be applied is Activity C.

To remain below the desired resource limit, resource reduction is applied to activity C by reducing the work force by one crew (four workers), resulting in daily resources of 12 workers, which is within the resource limit. In this way, the stretching of repair activities is completed, thus enabling the determination of a final repair time utilizing CPM. Figure 2.17(a) shows the modified repair schedule due to resource scheduling, which depicts the extended duration of repair Activity C on the first floor due to a reduction of workers from 8 to 4. A resource histogram of Figure 2.17(b) graphically demonstrates resource reduction of Activity C by one crew, which was sufficient to meet the resource limit of 12 workers. The reduction of workers in Activity C prolonged the completion date of the project from 134 days to 145 days.

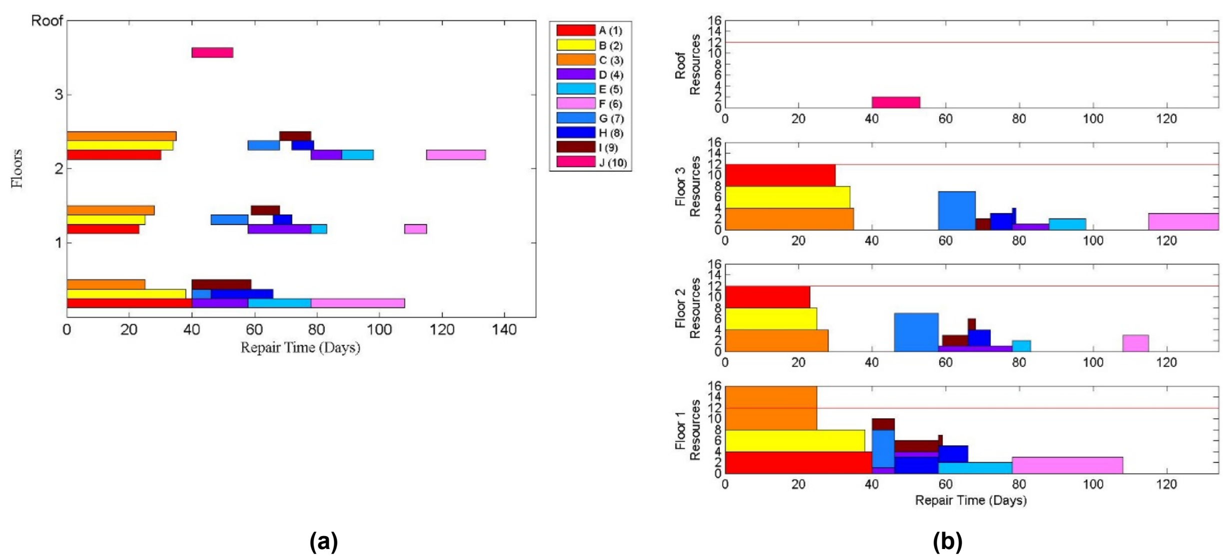

Figure 2.16 Repair schedule and labor allocations before resource scheduling: (a) Gantt chart showing the repair schedule; and (b) resource histogram before resource scheduling (after Terzic et al. 2016).

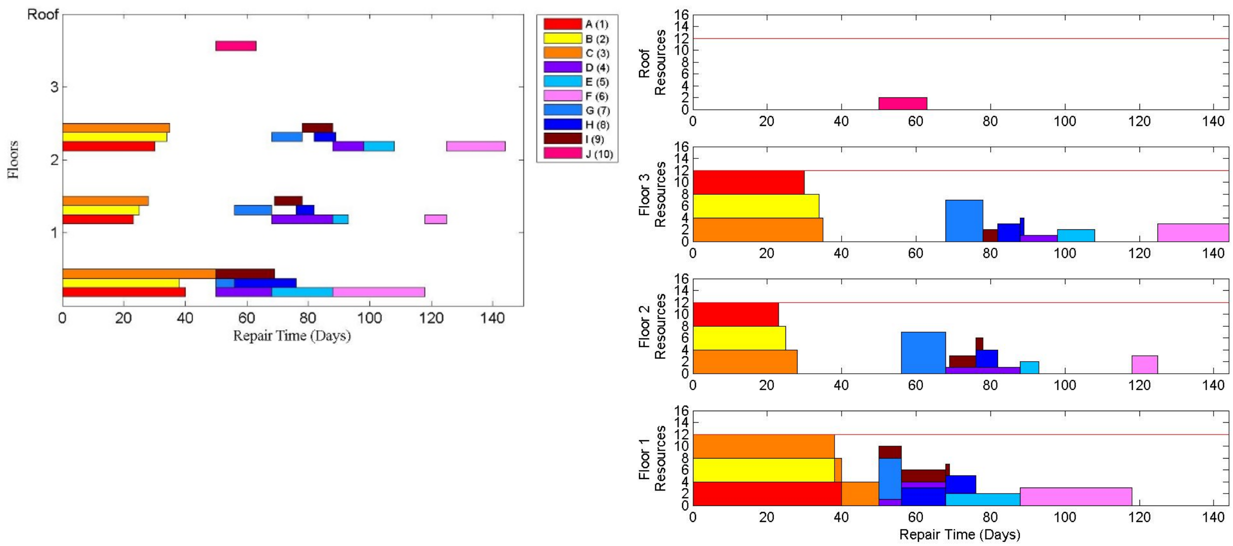

(a) **(b)**

Figure 2.17 **Repair schedule and labor allocations following the resource scheduling: (a) Gantt chart showing the repair schedule after resource scheduling and activity stretching; and (b) resource histogram following the resource scheduling (after Terzic et al. [2016]).**

2.3 MOBILIZATION TIME MODEL

Experience in recent disasters suggests that there is often a large time gap between the closure of a facility and the beginning of repairs. Comerio [2006] has named this period “the mobilization time” and was the first one to provide a simplified downtime assessment methodology that includes both mobilization and repair time. The methodology relates the severity of damage and size of the building to downtime based on the collective experience of engineering and architectural practitioners. Mitrani-Reiser [2007] has adopted the methodology proposed by Comerio [2006] within the PEER PBEE framework, where mobilization time is defined in a simple form by mapping the damage state of the building into a safety tag (e.g., green, yellow, or red), based on which mobilization time is conditioned using collective experience. Following the release of the first set of FEMA P-58 reports in 2012, ARUP adopted the FEMA P-58 methodology and published a REDi™ report [2013] that proposed a new downtime model where mobilization time is estimated based on the damage state of the most severely damaged component within a building, irrespective of the number of components with such damage. The model provides very conservative estimates of the mobilization time, and consequently downtime.

This report describes Terzic et al.’s [2021] mobilization time model which is an extension of an earlier model proposed by Terzic et al. [2015]. The model is based on Comerio’s study [2006], complemented by FEMA 352 [FEMA 2000] post-earthquake inspection strategies and information collected by interviewing general contractors, building inspectors, structural engineers, and facility managers that were greatly involved in the recovery of Los Angeles following the 1994 Northridge earthquake.

The mobilization time model is schematically presented with the flowchart shown in Figure 2.18. The flowchart shows mobilization activities that contribute to functional recovery time and their relationships based on the damage state of the building. Immediately following an earthquake, preliminary (rapid) evaluation of the building may be necessary to determine whether a building has sustained either structural or nonstructural damage, resulting in hazardous conditions [FEMA 2000]. Typically, based on the findings of this evaluation, a building is posted with a placard indicating whether or not the building is safe and repairable. If the building is not repairable as a result of large residual drifts, collapse, and/or significant structural and nonstructural damage—such that the loss ratio is greater than 50% rendering it uneconomical to repair the building [FEMA 2018a]—recovery time is equal to the time required to replace the building. If the building is repairable but there is extensive nonstructural damage and/or major structural damage, a detailed inspection is needed. Site preparation and clean up can occur simultaneously with the inspection. Following the inspection, the owner can simultaneously begin securing necessary funding and hiring architectural and engineering companies to prepare the necessary architectural and engineering drawings and calculations. With the completed drawings, while waiting for the approval for repair by local building authorities the owner can start mobilizing a general contractor and acquiring needed materials. If only nonstructural damage has occurred within the building to the extent that it does not require detailed inspection but affects the building's functionality (non-structural subsystems have only partial loss of functionality), before initiation of repair the owner can simultaneously begin site preparation, building clean up, mobilizing a general contractor, and securing the necessary funding. Finally, if the building is repairable but the damage is minor and to the extent that does not affect the operability (functionality loss is 0%), recovery time is 0.

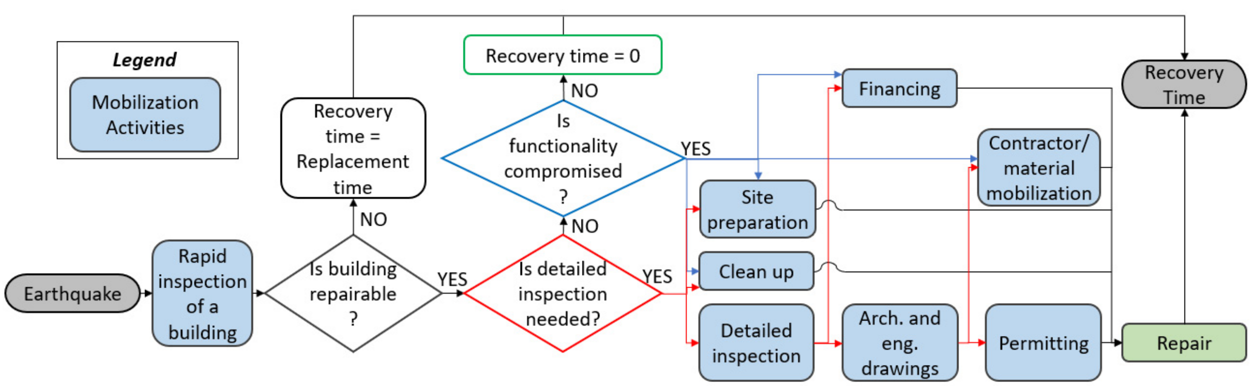

Figure 2.18 **Schematic representation of the mobilization time model highlighting mobilization activities and their relationships based on the damage state of the building (after Terzic et al. [2021]).**

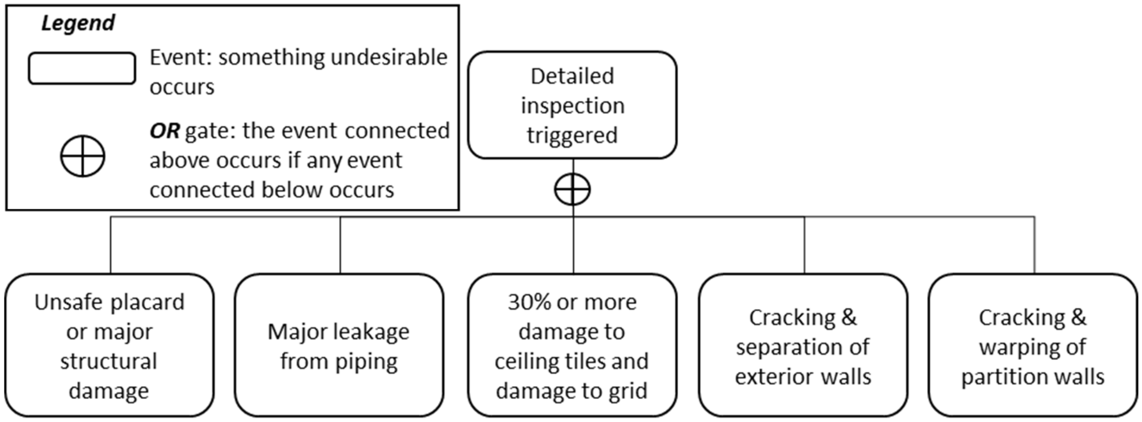

Figure 2.19 Fault tree for the limit state for detailed inspection.

To support the calculation of mobilization time as presented in Figure 2.18, it is necessary to evaluate three probabilistic limit state functions: repairability limit state (RLS), detailed inspection limit state (DILS), and functionality limit state (FLS). While FEMA P-58 provides a methodology for evaluation of RLS, this research presents the procedure for evaluation of the FLS (in Section 2) and DILS (described herein). Consistently, DILS is developed by fault-tree analysis, which utilizes information on structural and nonstructural damage of building components to evaluate if a detailed inspection is needed. The fault tree for the detailed inspection is derived by interviewing with facility managers and building inspectors; see Figure 2.19. Typically, a detailed inspection by structural engineers is requested if a building has significant structural damage that would result in unsafe placard or if there is severe damage to nonstructural subsystems (e.g., piping, ceiling, exterior walls, and partition walls) that can hint of the presence of structural damage. Table 2.8 provides damage state descriptions of nonstructural components (per FEMA P-58) that can trigger a detailed inspection. To enable calculation of the DILS, the model utilizes probabilistic user-defined LSFs to define the damage thresholds for triggering a detailed inspection. For example, 10% of severely damaged partition walls (tearing or bending of the top track, tearing at corners with transverse walls, large gap openings, walls displaced) can hint of the presence of structural damage and might be set as a median of LSF to trigger the detailed inspection.

Note: there is great uncertainty associated with the mobilization times of different mobilization activities when considered in a general sense, as they greatly depend on socio-political factors, the economy of the affected area, and the size and importance of the affected region. To account for this uncertainty, the mobilization activity times (highlighted blue in Figure 2.18) shall be modeled as lognormal functions and shall be selected considering many parameters including the following: the severity of building damage, relative contributions of structural and nonstructural damaged components to the overall damage, the building's loss ratio, local economy, and importance and size of the building. Furthermore, to reduce the uncertainty associated with the estimate of mobilization time for a particular project, median estimates of mobilization activity times for different damage states of the building must be acquired from the building developers and their teams. An example of damage states of a building that could be considered to properly evaluate mobilization time is presented in Section 3.4.

In summary, the presented framework for modeling functional recovery is developed within the probabilistic PEER PBEE/FEMA P-58 framework and is applicable to individual building systems. The model has great flexibility and broad application as it can capture unique features of each building system and construction/repair practices at the location of the building. To reduce the uncertainty of the functional recovery estimates, the model shall be populated with inputs acquired from the building developer, general contractor, facility manager, and engineers involved in the construction of the building. These inputs can be systematically collected at the beginning of the project in a fairly short time. Finally, note that the presented framework can account for the effects of externalities (e.g., utilities) on functional recovery of a building if their fragility functions are available.

Table 2.8 Damage states of nonstructural components (per FEMA P-58) that can trigger a detailed inspection (after Terzic et al. [2021]).

Component	Damage State Description
Piping	Large Leakage with major repair – 1 leak per 1000 feet (304.8 meter) of pipe.
Ceilings	30% of ceiling grid and tile damage.
	30% of tiles dislodge and fall and T-bar grid damage.
	50% of ceiling grid and tile damage.
Glazing/Curtain Walls	The glass falls out from the frame.
Cladding	Cladding unit damaged by out of plane anchorage failure. The unit requires replacement.
Cold-Formed Steel Exterior Walls	Failure of structural panels.
	Failure of the wall.
	Failure of many framing members and collapse.
	Buckling of steel sheathing. Buckling of framing members.
Partition Walls	Buckling of studs and tearing of tracks. Tearing or bending of the top track, tearing at corners with transverse walls, large gap openings, walls displaced.

3 Demonstration of the F-Rec Framework: A Case Study

The efficiency of F-Rec framework for the evaluation of functional recovery is demonstrated on an existing 13-story building located at a site of high seismicity. To provide content to the data, this section includes the building description, structural analysis responses relevant for recovery analysis, description of building performance model per FEMA P-58, and definition of all user-defined inputs for recovery analysis. Finally, the results of the recovery analysis are presented and interpreted; see Terzic and Kolozvari [2021] for another case study that evaluates functional recovery of a tall RC core wall building.

3.1 BUILDING DESCRIPTION

The building selected for evaluation of functional recovery is a 13-story steel-framed building with one underground level located in downtown Los Angeles, California, built circa 1956. A study by Garza et al. [2018] provides a detailed description of the building and presents a performance assessment of the building in terms of repair loss and total repair time considering three levels of earthquake hazard: 50% in 50 years, 10% in 50 years, and 2% in 50 years.

The selected building has a typical column layout of 20 ft–23 ft-3 in. on center within a building footprint of 86 ft-8 in. × 160 ft. It is framed with wide-flanged columns in each direction, and wide flanged beams typically spaced 6 ft-8 in. on center, supporting a 1½-in.-deep metal deck with concrete fill for a total slab thickness of 3¾ in. Unlike typical steel moment frames, this building used relatively shallow beam sections that constitute a moment connection at every beam-to-column joint in both directions; see Figure 3.1 and Figure 3.2. Hence there are many weak-axis moment-connections in this building that do not conform to the current building code requirements.

Typical beam sections in the building's long direction (X-direction) range from W14 × 34 to W16 × 71, and in the short direction (Y-direction) from W12 × 22 and W14 × 48. The columns change size every three floors with sizes ranging from W14 × 158 to W14 × 34, with column splices on the 2nd, 5th, 8th, and 11th floor. The orientation of the column changes at alternate locations. According to the typical detail for column splices, the flanges are welded with CJP welds, while the web is bolted using erection angles; see Figure 3.3. ASTM A7 steel (F_y = 30 ksi) was specified for all structural steel.

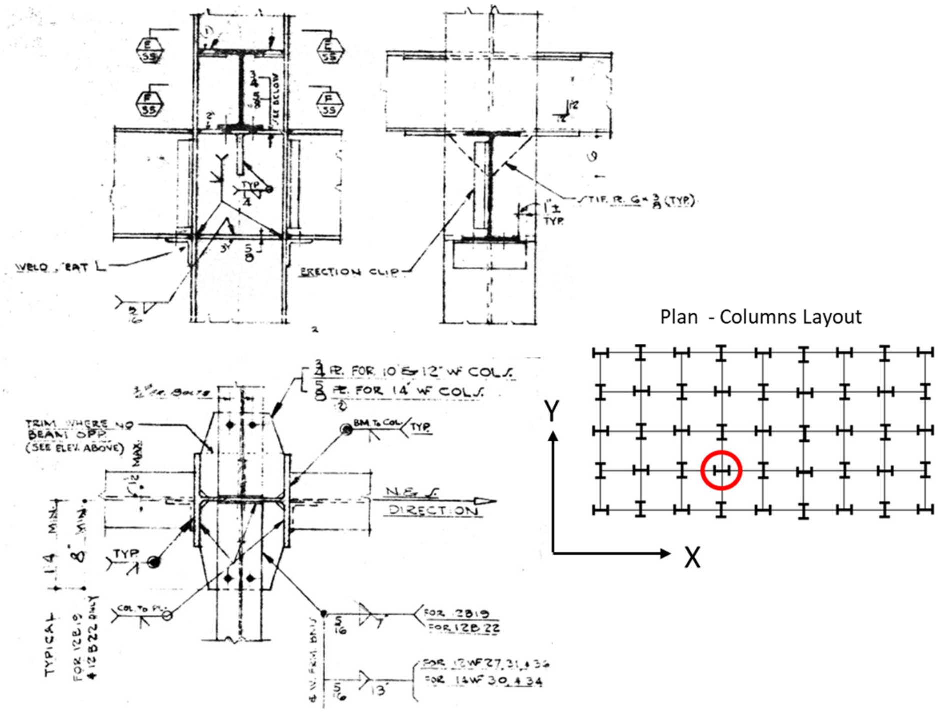

Figure 3.1 **Detail of the moment connection for the case when strong column axis is along *X*-axis.**

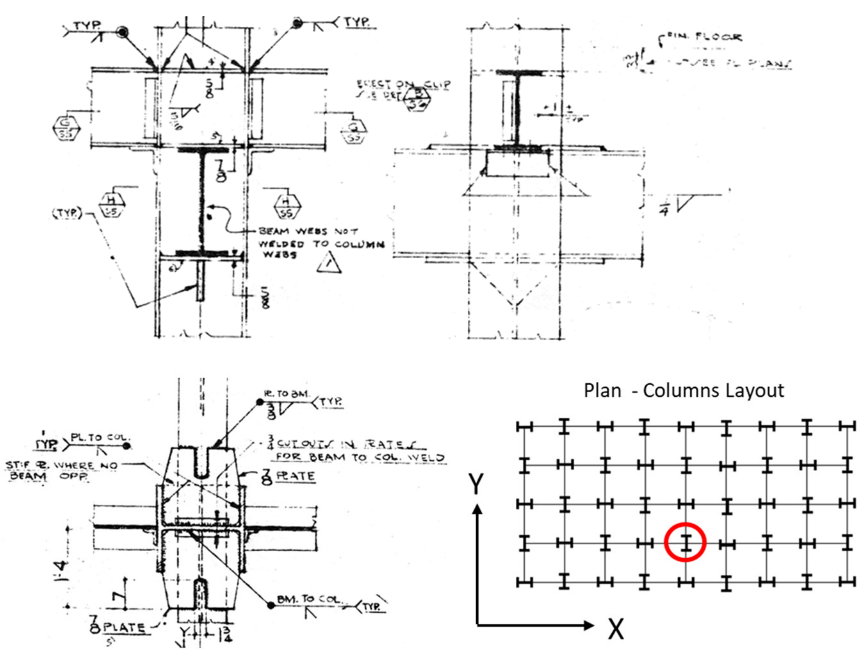

Figure 3.2 **Detail of the moment connection for the case when strong column axis is along *Y*-axis.**

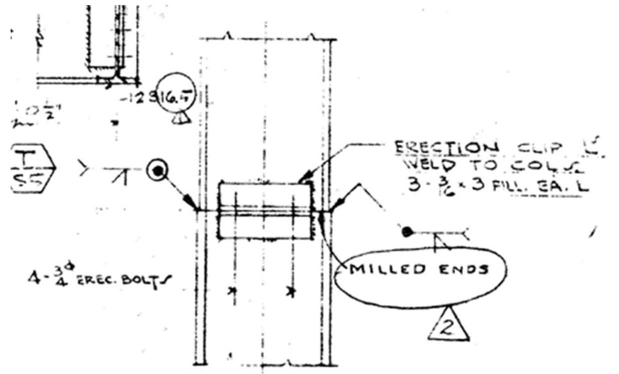

Figure 3.3 Typical detail of column splices.

3.2 STRUCTURAL ANALYSIS RESPONSES RELEVANT FOR PERFORMANCE ANALYSIS

3.2.1 Numerical Model of the Building

To simulate earthquake responses of the building, a comprehensive 3D nonlinear model of the building was developed in OpenSees [McKenna and Fenves 2004]. Assumptions and the procedure used in developing a nonlinear model of the building are as follows:

1. The penthouse and canopies were not explicitly modeled but were included as additional mass;
2. The basement walls were not explicitly modeled but were included as relatively rigid co-rotational trusses;
3. The base of all columns was assumed to be pinned (with no moment resistance);
4. The out-of-plane directions of the building were braced at the ground level;
5. Beams were modeled with elastic beam–column element with two zero-length rotational hinges at each end. The backbone curves assigned to the hinges were calculated per ASCE 41-17 recommendations for Welded Unreinforced Flange (WUF) connection with modifications for panel zone strength, clear span-to-depth ratio, and section compactness. While no specific guidelines regarding the strong and weak axis moment connections exist in ASCE 14-17, experimental tests conducted by Popov and Tsai [1989] showed that the weak axis moment connections with shallow beams and good detailing demonstrated satisfactory ductility. Therefore, the weak axis moment connections were also modeled with backbone curves for WUF connections per ASCE 14-17. An example of a backbone curve for beams W16 × 45 is shown in Figure 3.4. The stiffness of the rotational hinges was modified by a factor of 10 according to Ibarra et al. [2005] to capture the correct overall beam stiffness;

6. Columns were modeled with force-based beam–column elements with fiber sections using 16 × 2 fibers and 16 × 1 fibers for the flange and web, respectively. Five Gauss points were used along the element length. A section wrapper was used to include elastic springs in the torsion and both shear directions. *Steel02* was used to define the material behavior of the fibers;
7. Column splices were modeled with zero-length sections with a section wrapper to consider the shear and torsional stiffness. To capture the behavior of the column splices (Figure 3.3), the column splice zero-length section was assumed to have weak web fibers (*Steel02* material with F_y = 10 ksi), and typical *Steel02* with the expected F_y = 33 ksi for flange fibers (note that analysis is using 10% larger yield strength than its nominal value);
8. Panel zones were not explicitly modeled but panel zone offset elements with twice the stiffness of the incoming beam-column elements were included;
9. Diaphragms were assumed to be rigid;
10. The effects of large deformation were included by using *P*-delta nonlinear geometric transformation of the columns;
11. For the purpose of FEMA P-58 performance evaluations, 20 ground motions were selected at three hazard levels: 50% in 50 years, 10% in 50 years, and 2% in 50 years;
12. Damping was modeled using a Rayleigh damping model that was proportional to mass and committed (i.e., tangent) stiffness and was based on the first and the third period of vibration. A damping ratio of 2% was used for 2% in 50 years hazard and 10% in 50 years hazard, while damping ratio of 5% was used for 50% in 50 years hazard. Rayleigh damping was not assigned to zero-length elements to avoid spurious damping forces and unbalanced joint moments in those elements; and
13. To obtain residual interstory drifts, each response history analysis was followed by free vibrations to bring the building to "rest".

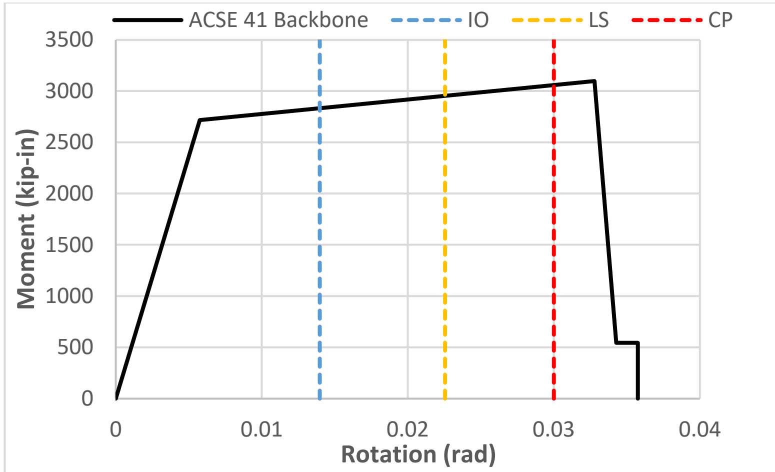

Figure 3.4 Backbone curve for WUF connection W16 × 45 (per ASCE 41-17).

3.2.2 Ground-Motion Selection and Scaling

Ground motions used to evaluate the structural response were selected following FEMA P-58 recommendations. Sets of twenty pairs of horizontal ground-motion records were selected for the building seismic hazard at each of the three levels: 50%, 10%, and 2% probabilities of exceedance in 50 years. These ground motions were selected and scaled using PEER ground motion NGA-West2 database tool [PEER 2013] such that arithmetic mean of the ground-motion suite matches the target acceleration response spectrum over a period range from $0.2T_s$ to $2T_1$, where T_s is smaller and T_1 is larger of the two fundamental translational periods along orthogonal axes of the building. Additionally, ground-motion pairs were selected such that their geomean spectral shapes were similar to the target spectrum over the established period range (i.e., $0.2T_s$ to $2T_1$). The period range of interest was determined to be 0.5 sec–6.2 sec.

The Conditional Mean Spectra (CMS) are used as target spectra. The CMS was chosen over Uniform Hazard Spectra as it provides a more realistic "scenario spectra" for a particular intensity at a period of interest and therefore provides more accurate estimates of median interstory drift and floor acceleration responses [FEMA 2018a]. The CMS were derived using Baker's [2011] method and are associated with the causal events for the location close to downtown Los Angeles. The CMS are the composite of four ground-motion prediction models (GMPM); namely Abrahamson-Silva-Kamai (2014), Chiou-Youngs (2014), Campbell-Bozorgnia (2014), and Boore-Stewart-Seyhan-Atkinson (2014). The composite of these GMPMs was attained utilizing PEER NGA-West2 Flatfiles [PEER 2015] whose input data (e.g., moment magnitude of earthquake, the closest distance to the rupture) were collected using USGS's unified hazard deaggregation tool [USGS 2014]. The CMS were developed utilizing the spectral acceleration associated with the selected hazard at period, T_{avg}, that is an average of fundamental translational periods along two orthogonal axes of the building (i.e., $T_{avg} = 2.77$ sec for the considered building). Damping ratios used to derive CMS for the three hazard levels were adopted from LATBSDC guidelines [Naiem et al. 2015] and are 2.5% for 50% in 50 years hazard level, and 5% for 10% and 2% in 50 years hazard levels.

In addition to the aforementioned procedure for ground-motion selection and scaling, the following requirements were considered:

- Both horizontal components of a ground motion were scaled by the same factor to match their target spectrum as closely as possible through minimizing the sum of squared differences between the logarithm of the scaled ground motion's geometric mean spectrum and the logarithm of the target spectrum over the established period range;
- The scaling factors were restricted to be smaller than 4 and larger than 0.25;
- A maximum of three ground motions were selected from the same earthquake.
- The lowest usable frequency was set to $1/(2T_1)$;
- Records with the peak ground velocity (PGV) similar to the PGV for the controlling event at the site was used as a metric to capture the records that have appropriate velocity pulses due to proximity of the site to the local sources;
- Ground motions were selected to have moment magnitudes between 5.5 and 7.9 to approximately match the magnitudes of causal earthquakes identified through hazard deaggregation;
- Ground motions were selected to have closest distances to the fault rupture between 5 km and 50 km for 50% in 50 years hazard, 5 km and 35 km for 10% in 50 years hazard, and 5 km and 25 km for 2% in 50 years hazard;
- Ground motions were selected to originate from the either strike-slip fault, reverse fault, or reverse-oblique fault; and
- Given that the hazard curves and deaggreagations generated with the USGS unified hazard tool provide spectral accelerations and seismic source characterizations for a hazard level at the discrete building periods (e.g., 0.5 sec, 1 sec, 2 sec, and 3 sec), that information was collected for the periods nearest to the fundamental period of the building under investigation (i.e., 2 sec and 3 sec for the considered buildings) and the required information were generated by interpolation.

Figure 3.5 shows the CMS and the geometric mean of the 20 selected ground motions for the three selected hazard levels. For the established range of interest, the average of the selected suite of ground motions closely matches the target spectrum. The geometric mean of individual earthquakes has some variability around the target spectra due to the inherent "bumpiness" of real ground motions.

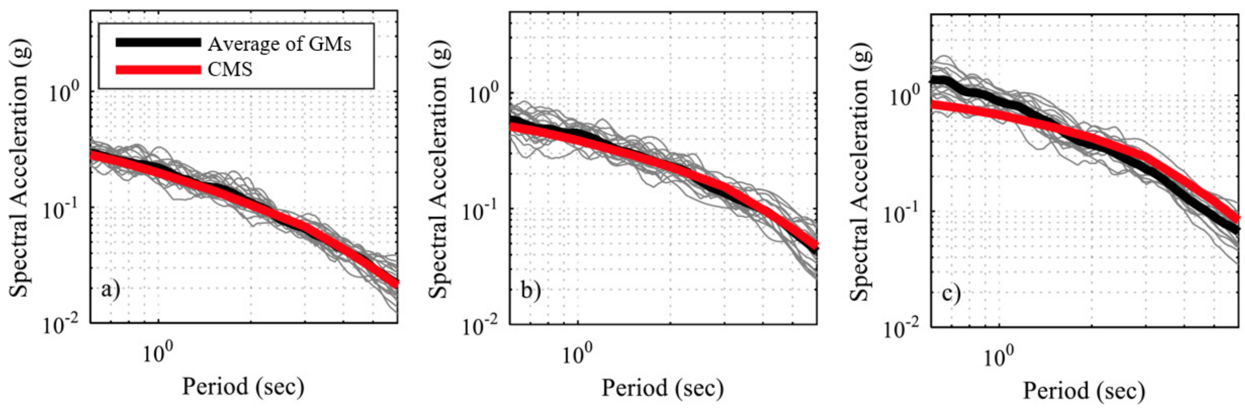

Figure 3.5 Conditional mean spectrum (CMS) and the arithmetic mean of the selected ground motions for each of three hazard levels: a) 50% in 50 years, b) 10% in 50 years, and c) 2% in 50 years.

3.2.3 Structural Analysis Responses

To perform the recovery evaluation of the building, its structural responses were evaluated at the three considered hazard levels; 50% in 50 years, 10% in 50 years, and 2% in 50 years. Figure 3.6 shows profiles of peak interstory drifts, residual drifts, and floor accelerations at the three considered hazard levels. At frequent earthquakes (50% in 50 years), structural response profiles are stable and fairly constant, attaining interstory drifts of 0.5% and floor accelerations of 0.2*g*, accompanied by negligible residual drifts. In contrast, for rare and very rare earthquakes (10% in 50 years and 2% in 50 years), interstory drifts and residual drifts start to concentrate at the bottom half of the building, resulting in excessive structural response. For example, at very rare earthquakes, interstory drifts might exceed 3% and residual drifts might reach 2%, suggesting substantial building damage. Furthermore, at 2% in 50 years hazard level, seven ground motions (out of twenty) caused building collapse and therefore are excluded from the results presented in Figure 3.6.

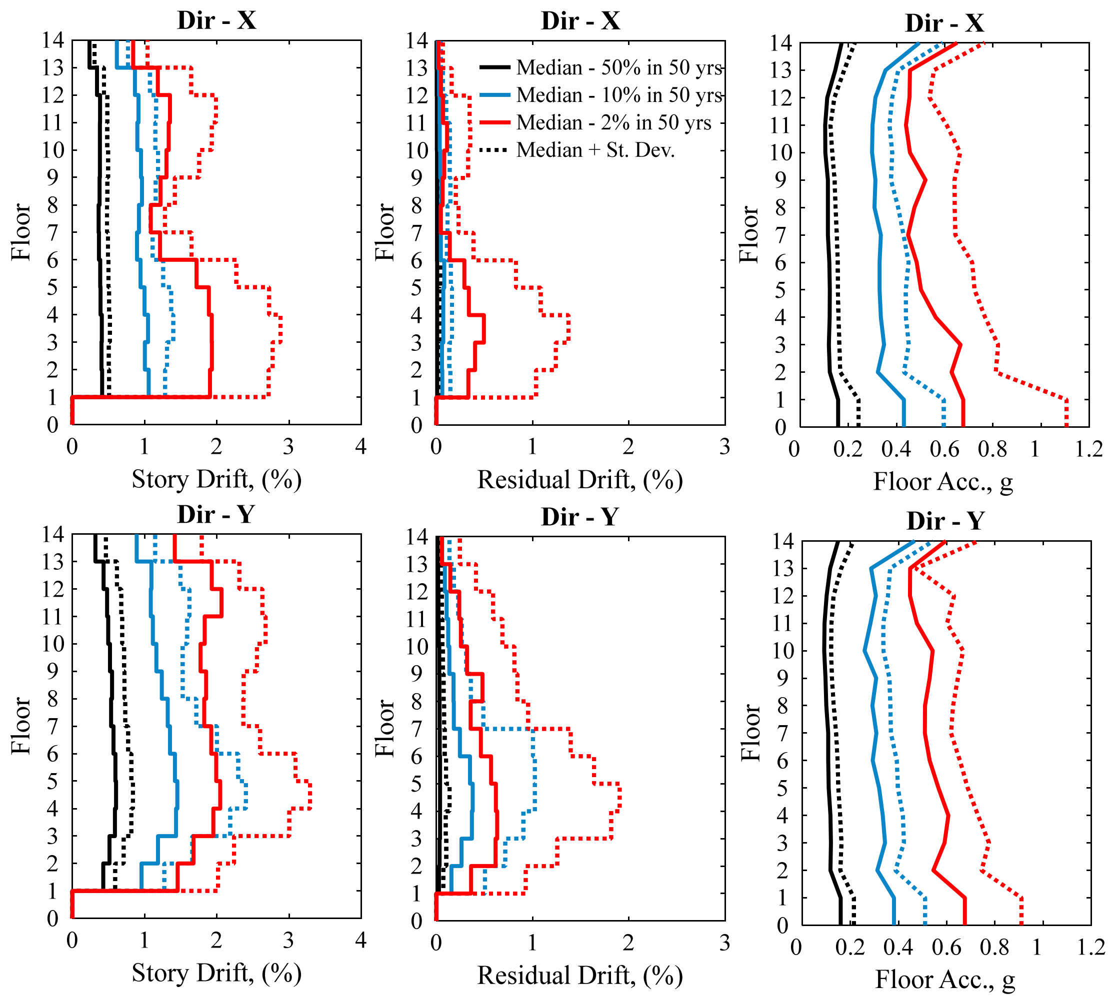

Figure 3.6 **Profiles of peak interstory drifts, residual drifts, and floor accelerations in both building directions (*X* and *Y*) for three hazard levels: 50% in 50 years, 10% in 50 years, and 2% in 50 years.**

3.3 PERFORMANCE MODELING PER FEMA P-58

The structural analysis results were incorporated into the performance model of the building, developed in PACT [FEMA 2018b], which included appropriate fragilities for all structural, architectural, mechanical, electrical, and plumbing components of the building. A Monte Carlo simulation process, implemented in PACT, utilized 2000 realizations for each hazard level to probabilistically simulate the possible range of building damage. This study utilizes information on building damage to evaluate the functional recovery times at different hazard levels.

The types and quantities of structural components were extracted from the drawings of the building. The types of structural components included in the performance model are pre-Northridge beam–column connections and column splices. Base plates were not included in the model as they are located at the underground level of the building that does not experience any interstory drift during earthquake shaking.

The types of nonstructural components for the original building are selected based on the following assumptions:

- Median displacement that causes the glass in exterior walls to fall out is assumed to be 1 in., which represents their original condition;
- Piping and ducting are laterally unbraced (original);
- All elevators are assumed to be original;
- Mechanical and electrical equipment are assumed to be unanchored;
- 50% of the ceiling is assumed to be unbraced (original), and 50% is remodeled (i.e., laterally braced/supported); and
- Partition walls are assumed to be fully remodeled (i.e., laterally braced).

The quantities of non-structural components for this commercial building were determined using the normative quantities for office occupancy recommended by FEMA P-58 and are shown in Table 3.1.

In PACT, each building component is associated with a fragility curve that correlates EDPs to the probability of that item reaching a particular damage state. Furthermore, PACT uses residual drifts to determine the feasibility of repairing a building by introducing a fragility curve that relates the peak story residual drift to the probability that the structure will be demolished. This curve has a lognormal distribution with a median residual drift value of 1.0% and a dispersion of 0.3 (per FEMA P-58). The excessive residual drifts of an analyzed building trigger its demolition (e.g., full replacement costs).

Table 3.1 Fragilities and their quantities per FEMA P-58 (after Terzic and Villanueva [2021]).

Fragility ID	Component Description per FEMA P-58	Units	Location (Floor)	Quantity per Direction			EDP
				L	T	ND	
B1035.041	Pre-Northridge WUF-B beam-column joint, beam one side of column, beam depth <= W27	EA	1,2	12	18		SDR
			3-14	10	18		
B1035.051	Pre-Northridge WUF-B beam-column joint, beam both sides of column, beam depth <= W27	EA	1,2	42	36		SDR
			3-14	35	27		
B1031.021a	Welded column splices, Column W < 150 plf	EA	3	18	18		SDR
			6,9,12	23	22		
B1031.021b	Welded column splices, Column 150 plf < W < 300 plf	EA	3	5	4		SDR
C1011.001b	Wall Partition, Type: Gypsum with metal studs, Partial Height, Fixed Below, Lateral Braced Above	100 LF (30.48 m)	2	6.436	4.66		SDR
			3-14	7.212	3.884		
C1011.001a	Wall Partition, Type: Gypsum with metal studs, Full Height, Fixed Below, Slip Track Above with returns	100 LF (30.48 m)	2	1.609	1.165		SDR
			3-14	1.803	0.971		
C3011.001b	Wall Partition, Type: Gypsum + Wallpaper, Partial Height, Fixed Below, Lateral Braced Above	100 LF (30.48 m)	2-14	0.525	0.525		SDR
B2022.033	Midrise stick-built curtain wall, Config: Monolithic, Lamination: Not laminated, Glass Type: Annealed, Details: 1/4 in. (6 mm) AN monolithic; glass-frame clearance = 0.13 in. (3 mm); aspect ratio = 6:5	30 SF (2.79 m^2)	2	164.4	119.9		SDR
			3	58.67	31.78		
			4-14	61.33	33.22		
B2022.035	Midrise stick-built curtain wall, Config: Monolithic, Lamination: Not laminated, Glass Type: Annealed	30 (SF) (2.79 m^2)	3	29.33	15.88		SDR
			4-14	30.67	16.61		
B2011.021a	Exterior Wall - Cold formed steel walls with 22 or 31 mil steel sheathing, interior - gypsum board	100 SF (9.29 m^2)	3	8.8	4.766		SDR
			4-14	9.2	4.983		
C2011.001b	Prefabricated steel stair with steel treads and landings with no seismic joint	EA	All floors	1	1		SDR
C3032.002a	Suspended Ceiling, SDC A,B,C, Area (A): A < 250, Vert. support only	250 SF (23.22 m^2)	3,5,7,9,11,13			12.48	PFA
C3032.002b	Suspended Ceiling, SDC A,B,C, Area (A): 250 < A < 1000, Vert. support only	600 SF (55.74 m^2)	3,5,7,9,11,13			5.2	PFA
C3032.002c	Suspended Ceiling, SDC A,B,C, Area (A): 1000 < A < 2500, Vert. support only	1800 SF (167.2 m^2)	3,5,7,9,11,13			3.47	PFA
C3032.003a	Suspended ceiling, SDC D, E Area (A): A < 250, Vert. & lat. supports	250 SF (23.22 m^2)	2			16.8	PFA
			4,6,8,10,12,14			12.48	
C3032.003b	Suspended ceiling, SDC D, E Area (A): 250 < A < 1000, Vert. & lat. supports	600 SF (55.74 m^2)	2			7	PFA
			4,6,8,10,12,14			5.2	
C3032.003c	Suspended ceiling, SDC D, E Area (A): 1000 < A < 2500, Vert. & lat. supports	1800 SF (167.2 m^2)	2			4.67	PFA
			4,6,8,10,12,14			3.47	
D2021.021a	Cold or Hot Potable Water Piping (dia > 2.5 inches),SDC A & B, PIPING FRAGILITY	1000 LF (304.8 m)	1,2			0.28	PFA
			3-14			0.21	
D2022.011a	Heating hot Water Piping - Small Diameter Threaded Steel - (2.5 inches in diameter or less), SDC A & B, PIPING FRAGILITY	1000 LF (304.8 m)	1,2			1.568	PFA
			3-14			1.16	
D2022.021a	Heating hot Water Piping - Large Diameter Welded Steel - (greater than 2.5 inches in diameter), SDC A & B, PIPING FRAGILITY	1000 LF (304.8 m)	1,2			0.56	PFA
			3-14			0.42	
D2031.011b	Sanitary Waste Piping - Cast Iron w/flexible couplings, SDC A & B, PIPING FRAGILITY	1000 LF (304.8 m)	1,2			0.56	PFA
			3-14			0.42	
D3041.011a	HVAC Galvanized Sheet Metal Ducting (A < 6 sf.) SDC A &B	1000 LF (304.8 m)	1,2			1.4	PFA
			3-14			1.04	
D3041.012a	HVAC Galvanized Sheet Metal Ducting (A > 6 sf.) SDC A & B	1000 LF (304.8 m)	1,2			0.37	PFA
			3-14			0.28	
D4011.021a	Fire Sprinkler Water Piping - Horizontal Mains and Branches - Old Style Victaulic - Thin Wall Steel - No bracing, SDC A &B, PIPING	100 LF (30.48 m)	1,2			3.73	PFA
			3-14			2.77	
D4011.071a	Fire Sprinkler Drop Standard Threaded Steel - No Ceiling - SDC A or B	1000 LF (304.8 m)	1			1.68	PFA
D4011.031a	Fire Sprinkler Drop Standard Threaded Steel - Dropping into unbraced lay-in tile SOFT ceiling - 6 ft. long drop maximum, SDC A,B	1000 LF (304.8 m)	2			1.68	PFA
			3-14			1.25	
D1014.012	Traction Elevator, prior to 1976	EA	1			5	PFA
D3031.011b	Chiller (100 < Tons < 350) Unanchored equipment that is not vibration isolated	EA	1,Roof			1	PFA
D3031.021b	Cooling Tower - Capacity: 100 to <350 Ton - Unanchored equipment that is not vibration isolated - Equipment fragility only	EA	1,Roof			1	PFA
D3052.011c	Air Handling Unit - Capacity: 10000 to <25000 CFM - Unanchored equipment that is not vibration isolated - Equipment fragility only	EA	1,Roof			3	PFA
D5012.013a	Motor Control Center - Capacity: all - Unanchored equipment that is not vibration isolated - Equipment fragility only	EA	1,Roof			4	PFA
D5012.021a	Low Voltage Switchgear - Capacity: 100 to <350 Amp - Unanchored equipment that is not vibration isolated - Equipment fragility only	EA	1,2			3	PFA
			3-14			2	

EA = each; LF = linear foot; SF = square feet; m = meter; SDR = story drift ratio (unitless); PFA = peak floor acceleration (g);
L = Longitudinal; T = Transversal; ND = Nondirectional;

3.4 MODELING OF FUNCTIONAL RECOVERY

Input data necessary for evaluation of functional recovery of the considered building using the F-Rec framework are provided for all of its internal moduli: FLS, repair time, and mobilization time.

As explained earlier, the three main constituents necessary for the calculation of FLS are damage assessment results from FEMA-58 analysis, fault trees of the building and its subsystems, and limit state functions of building components that probabilistically define damage thresholds to impair building function (partially and fully). This example utilizes fault trees defined in Section 2.1.3, damage assessment results from FEMA P-58 analysis of the 13-story building, and limit state ratios (user-defined input) of building components as specified in Table 3.2. The tabulated data present the specific components of the building subsystems along with their functionally impairing damage states, and corresponding medians of their LSFs for the purpose of the building-based and floor-based analysis; all LSFs have a dispersion of 0.3. It is important to note that these LSFs are selected only for the purpose of demonstrating the proposed method for evaluating post-earthquake functionality (presented in Section 2.1). To provide the content to the case study, LSFs were selected based on recommendations from facility managers and structural engineers. However, this selection is based on a limited set of collected information and is not intended for wide application until verified.

Table 3.2 Limit State Functions for the Component Damage States for the 13-Story Building (after Terzic and Villanueva [2021]).

Component Type	DS #	DS description	Median ratios of damaged components to trigger interruption of function					
			Builidng-based LSFs		Floor-based LSF			
					Partial loss		Full loss	
			Partial loss	Full loss	LSF	No. of stories	LSF	No. of stories
Structural Subsystem								
Column Splices	2	DS1 followed by complete failure of the web splice plate and dislocation of the two column segments on either side of the splice.	0.01	0.02	0.01	1	0.02	1
Pre-Northridge Moment Connections	1	Fracture of upper or lower beam flange weld.	0.20	0.50	0.30	4	0.75	2
	2	Similar to DS1, except fracture propagates into column flanges.	0.20	0.50	0.30	4	0.75	2
	3	Fracture initiating at weld access hole and propagating through beam flange, possibly accompanied by local buckling deformations of web and flange.	0.10	0.25	0.15	4	0.35	2
Exterior Wall Subsystem								
Curtain Walls	2,3	Glass falls from frame	0.05	0.5	0.1	7	0.75	5
Cold Form Exterior Walls	2	Buckling of steel sheathing. Buckling of framing members.	0.05	0.5	0.1	7	0.75	5
Partition Wall Subsystem								
Partition Walls	3	Buckling of studs and tearing of tracks. Tearing or bending of top track, tearing at corners with transverse walls, large gap openings, walls displaced.	0.05	0.7	0.1	7	0.85	5
Stair & Elevator Subsystems								
Stairs	3	Loss of live load capacity. Connection and or weld fracture	0.2	0.75	0.25	4	0.85	2
Traction Elevators	1-1	Controller anchorage failed, and or machine anchorage failed, and or motor generator anchorage failed, and or governor anchorage failed, and or rope guard failures.	0.01	1	n/a	n/a	n/a	n/a
	1-2	Rail distortion, and or intermediate bracket separate and spread, and or counterweight bracket break or bend, and/or car bracket break or bend, and or car guide shoes damaged, and or counterweight guide shoes damaged, and or counterweight frame distortion, and or tail sheave dislodged and/or twisted.	0.01	1	n/a	n/a	n/a	n/a
	1-3	Cab stabilizers bent, or cab walls damaged, or cab doors damaged.	0.01	1	n/a	n/a	n/a	n/a
Motor Control Center	1	Damaged, inoperative	0.01	1	n/a	n/a	n/a	n/a
Ceiling Subsystem								
Suspended Ceilings	2	30% of ceiling damage	0.1	0.75	0.15	7	0.85	5
	3	50% of ceiling damage	0.05	0.5	0.1	7	0.75	5
Piping Subsystem								
All piping (w/o sanitary)	2	Large Leakage w/ major repair - 1 leak per 1000 feet of pipe	0.05	0.1	0.075	4	0.15	2
Sanitary piping	2	Large Leakage w/ major repair - 1 leak per 1000 feet of pipe	0.02	0.05	0.02	4	0.05	2
Electrical Subsystem								
Low Voltage Switchgear	1	Damaged, inoperative.	0.1	0.75	0.15	7	0.9	5
HVAC Subsystem								
AHU	1-1	Equipment does not function. Damage to attached ducting or piping.	0.01	1.0	n/a	n/a	n/a	n/a
HVAC Ducting	2	Several adjacent supports fail and sections of ducting fall - 60 feet of ducting fail and fall per 1000 foot of ducting.	0.1	0.75	0.15	7	0.95	5
Motor Control Center	1	Damaged, inoperative	0.01	1.0	n/a	n/a	n/a	n/a

DS: damage state; LSF: limit state function

To properly model repair time it is necessary to use a realistic logic network of repair activities along with the appropriate labor allocations. This research uses a realistic repair schedule and labor allocations, recommended by contractors greatly involved in the recovery of the greater Los Angeles area following the 1994 Northridge earthquake [Yoo 2016]. The presented repair schedule highlights basic inter-relationships among different groups of components on one floor. The repair of the building starts with the simultaneous repair of structural elements and vertical transportation routes (stairs and elevators) to ensure overall structural integrity and to provide transportation of labor and materials; repair of stairs and elevators does not interfere with the overall repair progress because typical repair construction utilizes external elevators when needed. The repair of structural components starts from the bottom of the building and is executed by simultaneous repair across three floors at a time. Nonstructural components are repaired sequentially two floors at a time where the repair of a nonstructural component is conditioned by the completion of structural repairs at respective floors and the same nonstructural repair activity on the floors below (so that the corresponding crews can move to the next two floors). At each floor level, a simultaneous repair was permitted for the following components: (1) interior finishes and piping (i.e., water/steam piping, HVAC ducts/drops, fire pipes/drops, ceiling, and partitions), (2) exterior enclosure (i.e., curtain walls); and (3) electrical units (i.e., switchgear). Equipment located at the base and roof level, including chillers, cooling towers, air handling units, and motor control centers (MCCs) are all repaired simultaneously, one floor at a time. In case of excessive structural damage that creates an unsafe condition for the occupants (e.g., unsafe placard), equipment repair follows the completion of structural repair throughout the building. Otherwise, the repair of building equipment is initiated at the beginning of the repair project. Labor allocations for building components that commensurate to the amount of damage that impairs building functionality are provided in Table 3.3.

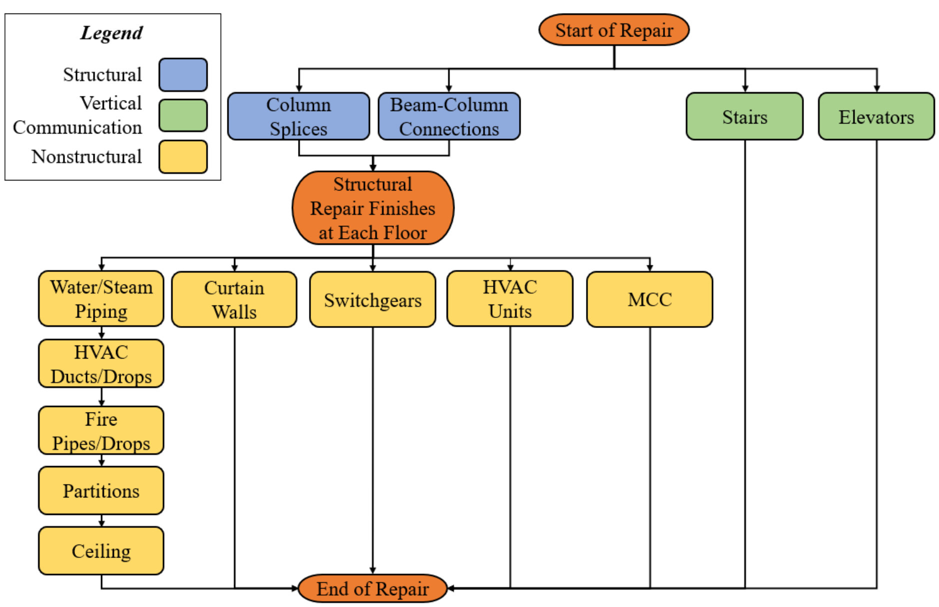

Figure 3.7 Flowchart of a realistic repair schedule for the 13-story building (after Terzic et al. [2021]).

To properly evaluate the mobilization time, two types of inputs are necessary: (1) LSFs of nonstructural components (piping, ceiling, exterior walls, and partition walls) that define the damage thresholds for triggering detailed inspection, and (2) time allocations for different mobilization activities. For this study, the medians of LSFs for all nonstructural components are set to 10%, meaning that if 10% of a component type (e.g., ceiling) experiences severe damage, this would trigger a detailed inspection. Time allocations of mobilization activities for this project are provided in Table 3.4. They are based on types of damaged components that impair functionality (e.g., equipment, nonstructural, structural), functionality tag of components (full, partial, or no loss), the overall building functionality state (full, partial, no loss), detailed inspection state (e.g., yes or no), and repair cost ratio as a percentage of the replacement cost.

Table 3.3 Labor allocations based on Average Damage State (ADS) and Number of Functionally Impairing Damaged Units (NFIDU) for the repair of structural components, stairs, and curtain walls; based on Ratio of Functionally Impairing Damaged Units (RFIDU) for the repair of interior nonstructural components; based on presence of damage to equipment that impairs function (after Terzic et al. [2021]).

Workforce per crew based on ADS				Number of crews based on NFIDU per floor				
ADS =	0 - 1	1 - 2	2 - 3	NFIDU =	1 - 10	11 - 20	21 - 30	> 31
Beam/Column Con.	4	6	6	Beam/Column Con.	1	2	3	4
Column Splices	4	6	6	Column Splices	1	2	3	4
Stairs	2	3	4	Stairs	1 crew			
Curtain Walls	5	5	N/A	Curtain Walls	If NFIDU< 20, 1 crew If NFIDU>20 , 2 crews			
Total workforce based on RFIDU				Total workforce for equipment that impairs function				
RFIDU =	0-0.1	0.1-0.5	0.5-1.0					
Partitions	2	5	11	Switchgear	2			
Ceiling Tiles	1	3	5	Elevator	2			
HVAC Ducting	1	3	5	AHU	3			
Fire Drops	1	2	3	MCC	3			
Water Piping	1	2	3					

Table 3.4 Median time allocations for the mobilization activities based on types of damaged components that impair functionality and the functionality state of the building (after Terzic et al. [2021]).

Mobilization Activity	Type of damaged components that impair functionality	Functionality State	Median Time Allocation
Detailed Inspection (DI)	Nonstructural only	Partial or full loss	3 days
	Structural	Partial loss	2 weeks
		Full loss	4 weeks
Architectural and Engineering Drawings	Nonstructural only	Full Loss + DI triggered	2 weeks
	Structural	Partial loss + DI triggered	3 weeks
		Full loss + DI triggered	6 weeks
Permitting	Nonstructural only	Full Loss + DI triggered	1 week
	Structural	Partial loss + DI triggered	2 weeks
		Full loss + DI triggered	4 weeks
Contractor and Material Mobilization	Equipment only	Partial loss & BF is partial loss	3 days
	Nonstructural only or with equipment	Partial loss & BF is partial loss	3 days
	Structural	Partial loss & BF is partial loss	1 weeks
	Equipment only	Full loss & BF is full loss	3 days
	Nonstructural only or with equipment	Full loss & BF is full loss	1 weeks
	Structural	Full loss & BF is full loss	2 weeks
Clean-up	Exterior walls, ceilings, partitions	Partial loss	3 days
		Full loss	1 weeks
Site Preparation	Equipment only	Full loss	0 days
	Structural and/or nonstructural	Full loss	1 weeks
Financing	Structural	Full loss & RCR>0.2	6 weeks
	Structural and/or nonstructural	Partial or full loss & RCR<0.2	1 week
	Equipment only	Partial or full loss	3 days

BF: building functionality; RCR: repair cost ratio as a percentage of replacement cost
Note: Dispersion of 0.2 is used for all activities

3.5 EVALUATION OF FUNCTIONAL RECOVERY

The structural analysis responses are incorporated in the performance model to evaluate damage states of all building components and associated repair times. This information is then utilized within the presented framework for modeling functional recovery. Analysis of the building's post-earthquake functionality is conducted first, and its results are used in conjunction with repair time and mobilization time models to evaluate the entire recovery process.

For each subsystem and the entire building, Figure 3.8 presents probabilities of each of the functionality states (no loss, partial loss, and full loss of functionality) for the three considered hazard levels (50% in 50 years, 10% in 50 years, and 2% in 50 years). The results suggest a high probability of attaining the partial loss of functionality for a building experiencing frequent earthquakes (50% in 50 years). For rare and very rare earthquakes (10% in 50 years, and 2% in 50 years), the building will most certainly have a full loss of functionality. When the functionality of the core subsystems is studied, it is obvious that the HVAC subsystem has the strongest influence on the building's functionality. It is accompanied by stair/elevator, piping, and structural subsystems, especially at higher hazard levels. The results further show that there is a high certainty that the partition walls, exterior walls, ceiling, and electrical subsystem, will be fully functional for frequent earthquakes, with compromised function for rare and very rare earthquakes.

Figure 3.9 shows functionality limit states for every subsystem and the entire building, which show probability that "x" percent loss in subsystem/building functionality will be reached for each of the three considered hazard levels. For example, the median value of functionality loss (reduction of the usable area) for a building experiencing frequent earthquakes is 50%. For rare and very rare earthquakes, the median value of the building's loss of functionality is 100%. Again, we see that the functionality limit states for the building are primarily governed by the HVAC subsystem. Contributions of the building subsystems to its functionality loss are as follows: (1) for frequent earthquakes, median values for loss of functionality are 0% for all subsystems, except for HVAC and stair/elevator subsystems, which are 50% and 20%, respectively; (2) for rare earthquakes, the median values for loss of functionality are 0% for the ceiling, exterior wall, and electrical subsystem, while they are 2% for piping, 13% for partition walls, 27% for the structural system, 80% for stairs and elevators, and 100% for HVAC; and (3) for very rare earthquakes, median values of loss of functionality are 0% for the ceiling, 15% for the electrical subsystem, 35% for exterior and partition walls, and 100% for structural, piping, HVAC, and stairs/elevator subsystems.

These functionality limit states (as presented in Figure 3.9) can be compared to functionality-based performance objectives (i.e., acceptance criteria) set by decision-makers to check whether the building's performance is acceptable. For example, for a frequent earthquake, the analyzed building with its median functionality loss of 50% greatly exceeds a typical performance objective of close to full functionality, indicating a need for a building retrofit.

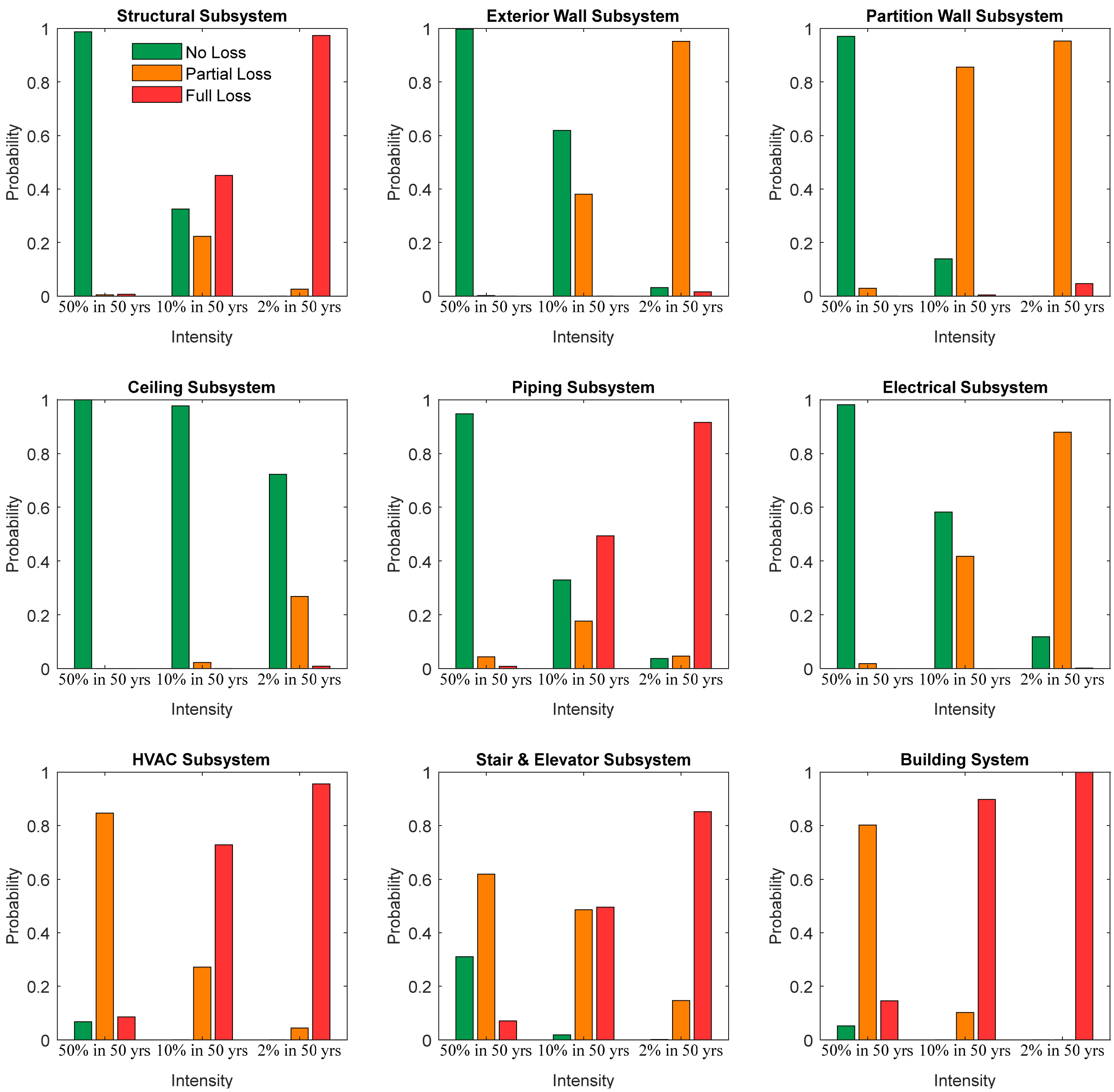

Figure 3.8 Probability of functionality states (no loss, partial loss, and full loss of functionality) for the building system and its subsystems at three considered hazard levels (after Terzic and Villanueva [2021]).

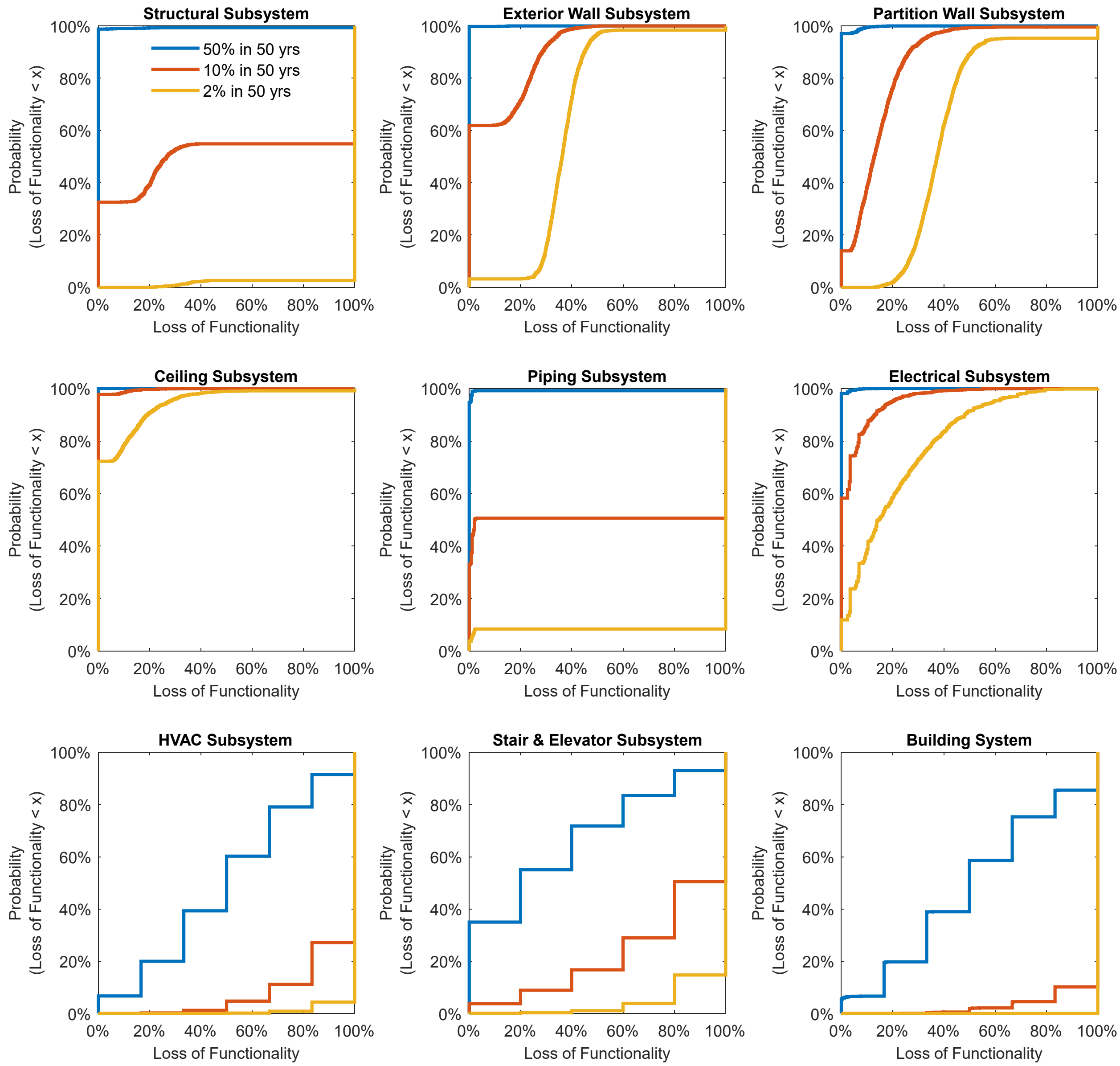

Figure 3.9 **Functionality limit states for the building system and its subsystems at three considered hazard levels (after Terzic and Villanueva [2021]).**

Next, Figure 3.10 shows the cumulative distribution functions of functional recovery time for the three considered hazard levels along with the median and 90th percentile outcomes. In line with the structural analysis responses (Figure 3.6) and functionality limit state analysis (Figure 3.8 and Figure 3.9), the building is expected to fully regain its function in a few weeks for frequent earthquakes, it takes several months to two years (the assumed time for the building replacement) for rare earthquakes, and almost certainly two years for very rare earthquakes. Note: the building replacement is triggered by excessive residual drifts.

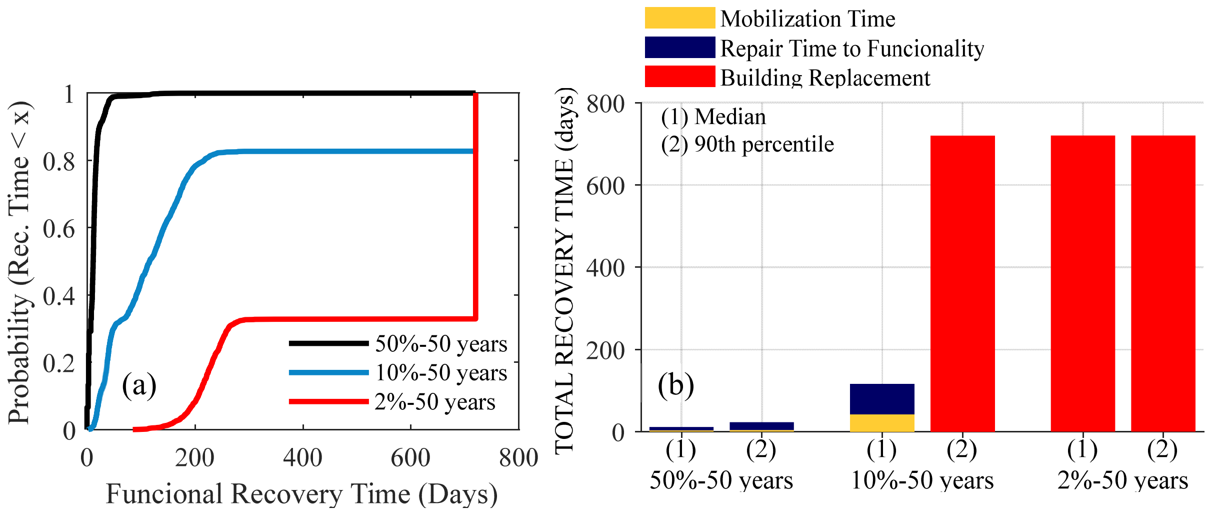

Figure 3.10 Functional recovery evaluation results at three considered hazard levels: (a) functional recovery time fragilities, (b) median and 90th percentile functional recovery times (after Terzic et al. [2021]).

Moreover, Figure 3.11 and Figure 3.12 provide detailed information for the median outcomes at frequent and rare earthquakes; additional information is not provided for very rare earthquakes as the median outcome requires a building replacement. Selected results of the building recovery analyses presented in Figure 3.11 and Figure 3.12 include: (1) functional recovery curve, which shows the change in building's capacity to function from the occurrence of the earthquake (time = 0) until the building fully recovers its function; (2) duration of all mobilization activities that occur in parallel to prepare the building for repairs; and (3) median repair schedule considering all components that impair building's functionality. Median outcome at frequent earthquakes shows that the building preserves 50% of its functionality and fully recovers within 11 days; see Figure 3.11(a). The functionality is compromised due to the damage to the HVAC subsystem, where it takes three days to mobilize a contractor and 8 days to perform the repair; see Figure 3.11(b) and (c). The median outcome at rare earthquakes shows that the building experiences full loss of its functionality, taking 70 days to recover 50% of its functionality and 115 days to achieve full recovery; see Figure 3.12(a). The functionality is primarily lost due to damage to beam–column connections, elevators, glazing, and HVAC units; see Figure 3.12(c). In this case, it takes 47 days to prepare for the repair and 68 days to perform the actual repair; see Figure 3.12(b) and (c).

As illustrated by the results, the F-Rec framework for modeling functional recovery produces unique and detailed information about the recovery process that considers all building components. This information can be used to guide the development of a retrofit solution that would improve the seismic performance of the building system. In case of the considered building, it is clear that the structure, HVAC system, elevators, and piping need to be retrofitted to improve building's post-earthquake recovery across all hazard levels. For example, the employment of dampers within the building, along with the equipment anchorage and replacement of elevators and piping, could greatly improve the post-earthquake recovery of the building. Note that the recovery curve shown in Figure 3.12(a) resembles the idealized recovery curve shown in Figure

1.1, demonstrating that the general concept for evaluation of recovery and associated resilience can be implemented using the F-Rec framework.

In sum, the presented framework is readily applicable to individual buildings, as user-defined data (e.g., LSFs and mobilization activities time allocations) can be uniquely defined for every project by collecting the appropriate data from the building developer and their teams. To provide broad research application of the presented method, efforts towards creating generic sets of probabilistic LSFs (where applicable) and mobilization activities time allocations with the goal of evaluating not only the functional recovery of individual buildings but rather clusters of buildings and their effects on community resilience are critical.

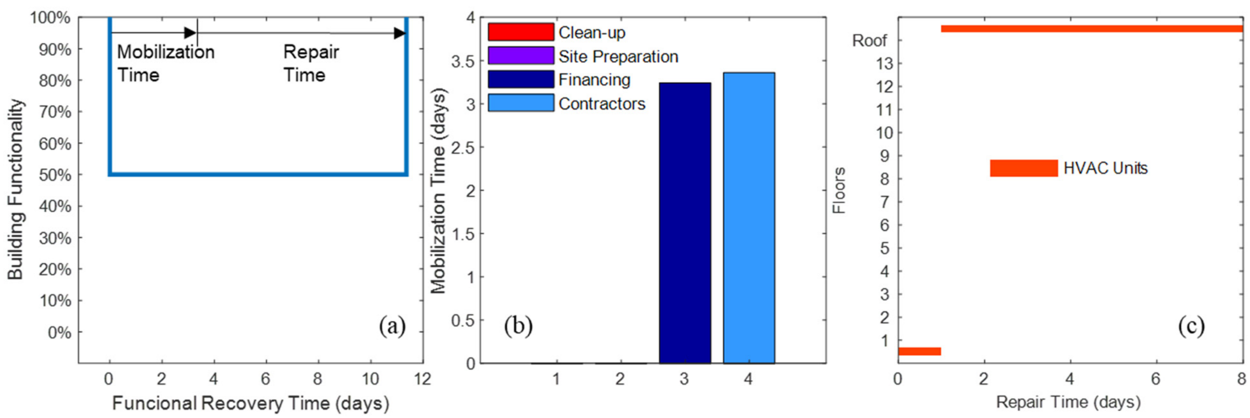

Figure 3.11 Median functional recovery evaluation results for 50% in 50 years hazard levels: (a) functional recovery curve, (b) time allocations of mobilization activities, and (c) repair schedule (after Terzic et al. [2021]).

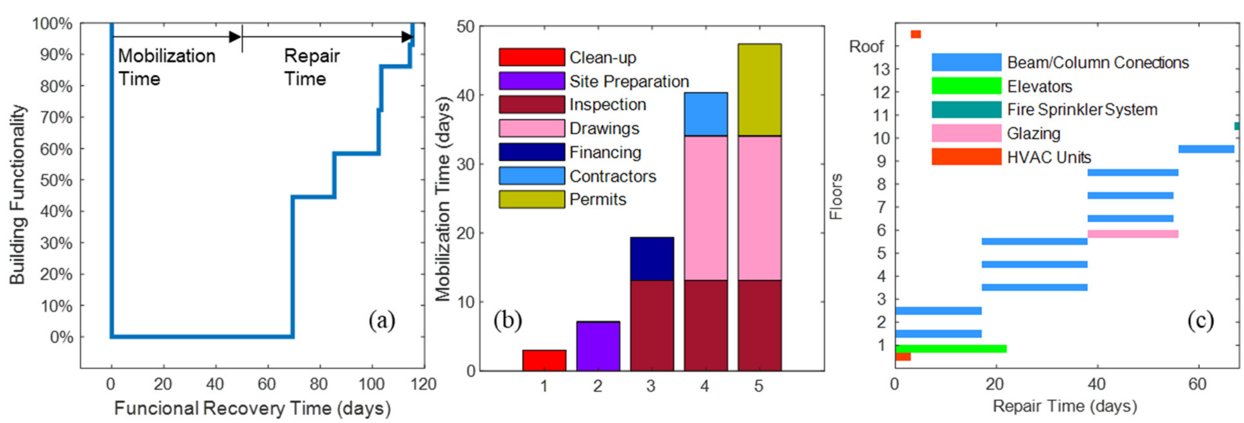

Figure 3.12 Median functional recovery evaluation results for 10% in 50 years hazard levels: (a) functional recovery curve, (b) time allocations of mobilization activities, and (c) repair schedule (after Terzic et al. [2021]).

4 Summary and Conclusions

This study proposes a novel, building-level framework for the probabilistic evaluation of the recovery process of building systems (F-Rec Framework). The F-Rec framework is in line with probabilistic PBEE methodology and uses FEMA P-58 damage/performance assessment results to evaluate recovery process. The unique features of the F-Rec framework are its capability to generate a functional recovery curve and to highlight the main contributors to interrupted building function along with the repair and mobilization activities that dominate the recovery process. The outcomes of the case study of an existing 13-story office building demonstrate how these unique recovery-based results can be effectively used as a guide for the development of earthquake mitigation strategies and design/retrofit solutions to improve seismic performance.

The main developments of this research are the sets of flowcharts and fault trees that are integrated and used to first calculate functionality and detailed inspection limit states (FLS and DILS). Next, mobilization and repair times associated with the building damage that impairs functionality are derived, so that the entire recovery process of the building; building's post-earthquake functionality (the percent of the inaccessible functional area within a building), duration, and path of functional recovery can be evaluated. The proposed framework for modeling functional recovery provides:

1. flexibility—branches in the fault trees can be easily turned ON and OFF;
2. robustness—the framework has a modular structure allowing for effortless extension and additions of new features; and
3. rapid evaluation—workflows between structural analysis, damage analysis, post-earthquake FLS and DILS analysis, and repair and mobilization time analysis can be created to allow for rapid evaluation of building's recovery process.

The F-Rec framework is readily applicable to individual buildings, as user-defined data can be uniquely defined for every project by collecting the appropriate data from the building developer and their contractors. To provide a broader application of the presented framework, efforts towards creating generic sets of user-defined inputs to evaluate not only the recovery of individual buildings but rather clusters of buildings and their effects on community resilience are critical.

Considering all of its features and potential for integration with the existing tools, methodologies, and datasets, the F-Rec framework presented herein provides numerous opportunities for its application: (1) it can be used for the development of design requirements for improving the post-earthquake functionality of new buildings; (2) it can be used for the development of retrofit solutions that will accelerate the recovery process: (3) it can be used for rapid post-earthquake evaluation of recovery time using building instrumentation; and (4) it can facilitate the evaluation of community resilience.

REFERENCES

Abrahamson N.A., Silva W.J., Kamai R. (2014). Summary of the ASK14 ground motion relation for active crustal regions, *Earthq. Spectra*: 30(3):1025–1055, https://doi.org/10.1193/070913EQS198M.

ASCE (2017). *Seismic Evaluation and Retrofit of Existing Buildings, ASCE 41-17*, American Society of Civil Engineering, Reston, VA, https://doi.org/10.1061/978078441485.

Arup (2013). Resilience-based earthquake design initiative for the next generation of buildings: REDi™ rating system, San Francisco, CA, https://www.arup.com/perspectives/publications/research/section/redi-rating-system.

Baker J.W. (2011). Conditional Mean Spectrum: Tool for ground motion selection, *J. Struct. Eng*. 137(3):708–723, tttps://doi.org/10.1061/(ASCE)ST.1943-541X.0000215.

Boore D.M., Stewart J.P., Seyhan E., Atkinson G.M. (2014). NGA-West 2 equations for predicting PGA, PGV, and 5%-damped PSA for shallow crustal earthquakes, *Earthq. Spectra*, 30(3):1057–1085, https://doi.org/10.1193/070113EQS184M.

Burton H.V., Deierlein G.G., Lallemant D., Lin T. (2015). Framework for incorporating probabilistic building performance in the assessment of community seismic resilience, *J. Struct. Eng*., 142(8), https://doi.org/10.1061/(ASCE)ST.1943-541X.0001321.

Campbell K.W., Bozorgnia Y. (2014). Campbell-Bozorgnia NGA-West2 horizontal ground motion model for active tectonic domains, *Proceedings, 10th U.S. National Conference in Earthquake Engineering*, Anchorage, AL.

Chiou B.S-J., Youngs R.R. (2014). Update of the Chiou and Youngs NGA model for the average horizontal component of peak ground motion and response spectra, *Earthq. Spectra*, 30(3):1117–1153, https://doi.org/10.1193/1.2894832.

Cimellaro G.P., Reinhorn A.M., Bruneau M. (2010), Framework for analytical quantification of disaster resilience, *Eng. Struct.*, 32(11):3639–3649, https://doi.org/10.1016/j.engstruct.2010.08.008.

Comerio MC (2006). “Estimating downtime in loss modeling.” Earthquake Spectra, Vol. 22, No. 2, pp. 349–365.

EERI (2010). *The 27 February 2010 Central South Chile Earthquake: Emerging Research Needs and Opportunities*, Earthquake Engineering Research Institute, Oakland, CA.

FEMA (2000). *Recommended Post-Earthquake Evaluation and Repair Criteria for Welded Steel Moment-Frame Buildings*, *FEMA 352*, Federal Emergency Management Agency Washington, D.C.

FEMA (2012). *Seismic Performance Assessment of Buildings, Volume 1–Methodology, FEMA P-58-1*, 1st ed., Federal Emergency Management Agency, Washington, DC.

FEMA (2018a). *Seismic Performance Assessment of Buildings, Volume 1–Methodology, FEMA P-58-1*, 2nd ed., Federal Emergency Management Agency, Washington, DC.

FEMA (2018b). *SPerformance Assessment Calculation Tool (PACT), FEMA P-58-2*, Federal Emergency Management Agency, Washington, DC.

FEMA/NIST (2021). *Recommended Options for Improving the Built Environment for Post-Earthquake Reoccupancy and Functional Recovery Time*, *FEMA P-2090/ NIST SP-1245*, Federal Emergency Management Agency, National Institute of Standards and Technology, Washington, D.C.

Garza J., Terzic V., Qian X., Saldana D., Ball S.C. (2018). Should we rely on existing building lateral systems when retrofitting buildings?, *Proceedings, SEAOC Convention*, Palm Desert, CA.

Gordin E. (2010). *Performance-Based Decision-Making in Post-Earthquake Highway Bridge Repair*, Department of Civil and Environmental Engineering, PhD thesis, UC Berkeley.

Harris R.B. (1978). *Precedence and Arrow Networking Techniques for Construction*, John Wiley @ Sons, New York, NY.

Haselton C.B., DeBock D.J., Almeter E, Wade K. (2019). *Resilient Design for Functional Recovery – Expectations for Current California Buildings and Approaches to Resilient Design*, Haselton Baker Risk Group, LLC, Chico, CA.

Ibarra L.F., Medina R.A., Krawinkler H. (2005). Hysteretic models that incorporate strength and stiffness deterioration, *Earthq. Eng. Struct. Dyn.*, 34(12):1489–1511, https://doi.org/10.1002/eqe.495.

Jacques C., McIntosh J.K., Giovinazzi S., Kirsch T.D., Wilson T.M., Mitrani-Reiser J. (2014). Resilience of the Canterbury health care system to the 2011 Christchurch (Mw=6.2) earthquake, NZ, *Earthq. Spectra*, 30(1):533–554, https://doi.org/10.1193/032013EQS074M.

Johnson G.S., Sheppard R.E., Quilici M.D., Eder S.J., Scawthorn C.R. (1999). Seismic reliability assessment of critical facilities: a handbook, supporting documentation, and model code provisions, *MCEER-99-0008*, University of at Buffalo, Buffalo, NY.

Kolozvari K., Terzic V., Miller R., Saldana D. (2018). Assessment of dynamic behavior and seismic performance of a high-rise RC coupled wall building, *Eng. Struct.*, 176(1):606–620, https://doi.org/10.1016/j.engstruct.2018.08.100.

Naiem F., Carpenter D., Ghodsi T., Hart G.C., Lew M., Mehrain M., Sabol T.A., Wallace J.W. (2015). An Alternative Procedure for Seismic Analysis and Design of Tall Buildings Located in the Los Angeles Region, Los Angeles Tall Buildings Structural Design Council, Los Angeles, CA.

Mason A.B., Beck J.L., Achkire Y., Wilkie S., Irfanoglu A., (2000). Optimal strategy for business recovery after earthquakes, *Proceedings, 12th World Conference on Earthquake Engineering*, New Zealand Society for Earthquake Engineering, Paper-1497, Wellington, NZ.

McKenna F., Fenves G.L. (2004). *Open System for Earthquake Engineering Simulation* (*OpenSees*), Pacific Earthquake Engineering Research Center, University of California, Berkeley, CA.

Mieler M.W., Mitrani-Reiser J. 2018. Review of the state of the art in assessing earthquake-induced loss of functionality in buildings, *J. Struct. Eng.*, 144(3), https://doi.org/10.1061/(ASCE)ST.1943-541X.0001959.

Miranda E., Aslani H. (2003). Probabilistic response assessment for building specific loss estimation, *PEER Report No. 2003/03*, Pacific Earthquake Engineering Research Center, University of California, Berkeley, CA.

Miranda E., Mosqueda G., Retamales R., Pekcan G. (2012). Performance of nonstructural components during the 27 February 2010 Chile earthquake, *Earthq. Spectra*, 28(S1)S453-S471, https://doi.org/10.1193/1.4000032.

Mitrani-Reiser J. (2007). *An Ounce of Prevention: Probabilistic Loss Estimation or Performance-Based Earthquake Engineering*" PhD thesis, California Institute of Technology, Pasadena, CA.

Pate-Cornell E.M. (1984). Fault trees vs. event trees in reliability analysis, *Risk Anal.*; 4(3):177–186, https://doi.org/10.1111/j.1539-6924.1984.tb00137.x.

PEER (2013). PEER NGA-West2 strong ground motion database, Pacific Earthquake Engineering Research Center, http://ngawest2.berkeley.edu (accessed Dec. 9, 2016).

PEER (2015). PEER NGA-West2 Flatfile, Pacific Earthquake Engineering Research Center, https://peer.berkeley.edu/thrust-areas/data-sciences/databases (accessed Dec. 23, 2017).

Poland C. (2009). *The Resilient City: Defining what San Francisco Needs from Its Seismic Mitigation Polices*, San Francisco Planning and Urban Research Association (SPUR), http://www.spur.org/initiative/resilient-city, (accessed Feb. 1, 2009).

Popov E.P., Tsai K.C. (1989). Performance of large seismic steel moment connections under cyclic loads, *Eng. J.*, 26(2):51–60.

Porter K.A., Kiremidjian A.S., LeGrue J.S. (2001). Assembly-based vulnerability of buildings and its use in performance evaluation, *Earthq. Spectra*, 17(2):291–312, https://doi.org/10.1193/1.1586176.

Porter K.A., Ramer K. (2012). Estimating earthquake-induced failure probability and downtime of critical facilities, *J. Bus. Cont. Emerg. Plann.,* 5(4):352–364.

Prassinos P.G., Ravindra M.K., Savy J.B. (1986). Recommendations to the nuclear regulatory commission on trial guidelines for seismic margin reviews of nuclear power plants, *NUREG/CR-4482*, U.S. Nuclear Regulatory Commission, Washington, D.C.

Sun L., Stojadinovic B., Sansavini G. (2019), Resilience evaluation framework for integrated civil infrastructure–community systems under seismic hazard, *J. Infrastruc. Syst.*, Vol. 25(2), https://doi.org/10.1061/(ASCE)IS.1943-555X.0000492.

Terzic V., Kolozvari K. (2021). Probabilistic evaluation of post-earthquake functional recovery for a tall RC core wall building, *Eng. Struct.* (in review).

Terzic V., Mahin S.A. (2017). Using PBEE to assess and improve performance of different structural systems for low-rise steel buildings, *Int. J. Safety Secur. Eng.*, 7(4):532–544, https://doi.org/10.2495/SAFE-V7-N4-532-544.

Terzic V., Villanueva P.K. (2021). Method for probabilistic evaluation of post-earthquake functionality of building systems, *Eng. Struct.,* 241(15), https://doi.org/10.1016/j.engstruct.2021.112370.

Terzic V., Kolozvari K., Saldana D. (2018). Seismic performance assessment of low- and mid-rise office and hospital shear wall buildings, *Proceedings, 16th European Conference in Earthquake Engineering*, Paper I.D. 10773, Thessaloniki, Greece.

Terzic V., Mahin S.A., Comerio M.C. (2015). Using PBEE to assess and improve performance of different structural systems for low-rise steel buildings, Oral presentation, *2nd ATC-SEI Conference on Improving the Seismic Performance of Existing Buildings and Other Structures*, San Francisco, CA.

Terzic V., Villanueva P.K., Saldana D., Dong D.Y. (2021). Framework for modelling post-earthquake functional recovery of buildings, *Eng. Struct.,* 246(8), https://doi.org/10.1016/j.engstruct.2021.113074.

Terzic V., Yoo D., Aryan A.H. (2016). Repair time model for buildings considering the earthquake hazard, *Proceedings*, *SEAOC Convention*, Maui, HI.

Toyoda T. (2008). Economic impacts of Kobe earthquake: A quantitative evaluation after 13 years, *Proceedings, 5th International Information Systems for Crisis Response and Management Conference*, ISCRAM, Washington, DC, pp. 606–617.

U.S. Geological Survey (2014). Unified hazard tool, https://earthquake.usgs.gov/hazards/interactive/, (accessed June 03, 2018).

Vesely W.E., Goldberg F.F., Roberts N.H., Haasl D.F. (1981). Fault three handbook, *NUREG-0492*, U.S. Nuclear Regulatory Commission, Washington, D.C.

Yoo D.Y. (2016). *Repair Time Model for Different Building Sizes Considering the Earthquake Hazard*, Master's Thesis, California State University, Long Beach, CA.

Zsarnóczay A., McKenna F., Wang C., Elhaddad W., Gardner M. (2019). NHERI-SimCenter/PBE: Release v2.0.0 (Version v2.0.0). https://doi.org/10.5281/zenodo.3491145.

The Pacifi c Earthquake Engineering Research Center (PEER) is a multi-institutional research and education center with headquarters at the University of California, Berkeley. Investigators from over 20 universities, several consulting companies, and researchers at various state and federal government agencies contribute to research programs focused on performance-based earthquake engineering.

These research programs aim to identify and reduce the risks from major earthquakes to life safety and to the economy by including research in a wide variety of disciplines including structural and geotechnical engineering, geology/seismology, lifelines, transportation, architecture, economics, risk management, and public policy.

PEER is supported by federal, state, local, and regional agencies, together with industry partners.

PEER Core Institutions

University of California, Berkeley (Lead Institution)
California Institute of Technology
Oregon State University
Stanford University
University of California, Davis
University of California, Irvine
University of California, Los Angeles
University of California, San Diego
University of Nevada, Reno
University of Southern California
University of Washington

PEER reports can be ordered at https://peer.berkeley.edu/peer-reports or by contacting

Pacific Earthquake Engineering Research Center
University of California, Berkeley
325 Davis Hall, Mail Code 1792
Berkeley, CA 94720-1792
Tel: 510-642-3437
Email: peer_center@berkeley.edu

ISSN 2770-8314
https://doi.org/10.55461/DPBD8076